uOttawa

L'Université canadienne
Canada's university

FACULTÉ DES ÉTUDES SUPÉRIEURES ET POSTOCTORALES

uOttawa

L'Université canadienne
Canada's university

FACULTY OF GRADUATE AND POSDOCTORAL STUDIES

Marsha Saldanha
AUTEUR DE LA THÈSE / AUTHOR OF THESIS

M.Sc. (Microbiology and Immunology)
GRADE / DEGREE

Department of Biochemistry, Microbiology and Immunology
FACULTÉ, ÉCOLE, DÉPARTEMENT / FACULTY, SCHOOL, DEPARTMENT

Influence of the potency of antigen presentation on CD8+ T cell differentiation and memory

TITRE DE LA THÈSE / TITLE OF THESIS

Dr. Subash Sad
DIRECTEUR (DIRECTRICE) DE LA THÈSE / THESIS SUPERVISOR

Dr. Lionel Filion
CO-DIRECTEUR (CO-DIRECTRICE) DE LA THÈSE / THESIS CO-SUPERVISOR

EXAMINATEURS (EXAMINATRICES) DE LA THÈSE / THESIS EXAMINERS

Dr. Karen Copeland

Dr. Marko Kryworuchko

Gary W. Slater
Le Doyen de la Faculté des études supérieures et postdoctorales / Dean of the Faculty of Graduate and Postdoctoral Studies

Influence of the potency of antigen presentation on $CD8^+$ T cell differentiation and memory

A Thesis Submitted to The

School of Graduate Studies

University of Ottawa

In Partial Fulfillment of the

Requirements for the degree

of

Master of Science

Department of Biochemistry, Microbiology, and Immunology

Faculty of Medicine

By Marsha Saldanha

Your file Votre référence
ISBN: 978-0-494-49274-1
Our file Notre référence
ISBN: 978-0-494-49274-1

Abstract

$CD8^+$ T cells curtail the proliferation of intracellular pathogens. However, the influence of the potency of stimulation on the development of $CD8^+$ T cell memory is not clear. Using recombinant Ovalbumin (OVA) expressing intracellular bacteria, *Mycobacterium bovis* (BCG) which induces muted T cell activation, and *Listeria monocytogenes* (LM) which induces massive T cell activation, the influence of T cell stimulation on memory development was discerned. It was hypothesized that muted activation of $CD8^+$ T cells by BCG might result in impaired development of memory. It was found that in contrast to LM naïve as well as memory $CD8^+$ T cells undergo delayed and muted expansion and contraction during BCG infection. Memory $CD8^+$ T cells remained functional as they expressed cytokines, killed targets and proliferated in response to antigen. Furthermore, inflammatory cytokines and T cells curtail antigen-presentation during BCG infection which curbs T cell stimulation and favors the development of functional memory.

Acknowledgements

First and foremost I would like to thank Dr Subash Sad for giving me the opportunity to conduct research in his laboratory. He is a dedicated and enthusiastic supervisor who was always available for scientific advice and guidance in this research. I would like to thank him for his patience and for taking a chance on a student with no immunology background and that has never worked with animals. He has taught me so much over these two years and I am indebted to him.

I would like to thank my co-supervisor Dr. Lionel Filion for his guidance in my research and in writing this thesis. I would like to also extend my gratitude to my committee members Dr. Lakshmi Krishnan and Dr. Ashok Kumar for their guidance in this project.

I am indebted to Renu Dudani and Henk Van Faassen for their technical support and guidance in this research. Their patience and encouragement has been invaluable to me throughout these two years. They have both spent a great deal of time and energy into helping me with my research and teaching me the various techniques that I needed to make this research succeed. From the first day I came to Dr. Sad's lab they have both taken the time to answer any questions I may have had and made me feel like I was part of the lab. I am forever grateful to them both.

I would also like to thank to Dr. John Nash and his technician Oksana Mykytczuk for their help in the mRNA quantification. Dr Nash has given me advice and direction in aspects of the research as well as access to necessary equipment in his lab. Oksana displayed untiring patience in teaching me the techniques involved and answering any questions I may have had no matter how trivial.

I would like to thank the animal care staff at the National Research Council Institute for Biological Sciences for their assistance with maintaining the facility and assisting with various experiments. Every morning they greeted me with a smile and started my days off right. Their dedication ensured this research progressed smoothly.

I would like to thank the Canadian Institute for Health Research (CIHR) for funding this research project. I would also like to thank the National Research Council for granting me the Graduate Student Scholarship Supplement Program (GSSSP) scholarship and the Ontario Government for granting me the Ontario Graduate Scholarship in Science and Technology (OGSST) scholarship. This financial support has greatly assisted me in funding my research.

Last but certainly not least I would like to thank my family. My husband Matthew Russell has been a constant unwavering source of support for me both financially and emotionally. He has kept me sane and forced me to enjoy life outside research. He is my best friend and I am eternally grateful to him for everything he has given me. My parents Richard and Doreen Saldanha have been beacons in my life long before I entered into science. Their dedication to my education and their unconditional love and support has helped me to succeed in every facet of my life. They have supported me both financially and emotionally throughout my education and they never once faltered. I thank them for giving me the opportunity to recognize my goals and aspirations. They have sacrificed a lot to get me to where I am today and I will be forever indebted to them! Mom, Dad and Matt, you are truly giants in my life!

~ "If I have seen farther, it is by standing on the shoulders of giants". ~
(Sir Isaac Newton)

Table of contents

Content	Page
Abstract	ii
Acknowledgements	iii
Table of Contents	v
List of Abbreviations	vii
List of Figures	viii
1.0 – General Introduction: The Immune System	1
1.1 – Antigen processing and presentation	3
1.2 - T cell Priming and the establishment of memory	5
1.3 – *Listeria monocytogenes*	7
1.4 – *Mycobacterium Bovis*	9
1.5 – Antigen Presentation in Acute Versus Chronic Infections: A Comparison Between LM and BCG	9
2.0 - Material and Methods	11
2.1 - Mice and Infections	11
2.2 – Media, Bacterial Strains, Bacterial Immunizations, Antibiotic Treatments, Antibodies, and Other Reagents	11
2.3 – Lymphocyte Extraction From Spleen and Other Organs	13
2.4 – Assessment of Bacterial Burden in Organs	14
2.5 – ELISPOT Assay	15
2.6 – The Adoptive Transfer Model	16
2.7 – Cell Cycling	16
2.8 – Assessment of Phenotype of Antigen Specific $CD8^+$ T cells	18
2.9 – Assessment of Intracellular IFN-γ Production	19
2.10 – In vivo CTL	19
2.11 – T cell Purifications	20
2.12 – In vivo Antigen Presentation	21
2.13 – Quantification of Bacterial Gene Expression in Infected Spleens	21
3.0 – Results	24
3.1.0 – Bacterial Burden in the Spleens of Mice Infected With LM-Ova and BCG-Ova	24
3.2.0 – Characterization of the $CD8^+$ T cell Response to LM-Ova and BCG-Ova	26
3.2.1 – Evaluating the Frequency of $CD8^+$ T cells Against $Ova_{257-264}$ by ELISPOT Assay	26
3.2.2 – Tracking Antigen Specific $CD8^+$ T cell Response During LM-Ova and BCG-Ova Infections	26
3.2.2.1 – Has the $CD8^+$ T cell population Responding to BCG-Ova Arisen as a result of Clonal Burst or a Gradual Accumulation of Cells Over Time?	31
3.2.3 – Cycling Status of Antigen Specific $CD8^+$ T cells During LM-Ova and BCG-Ova Infections.	33
3.3.0 – Evaluating the Activation and Differentiation Status of the $CD8^+$ T cells Generated During BCG-Ova Infection	35
3.3.1 – Evaluation of Activation Markers on Antigen Specific $CD8^+$ T cells During LM-Ova and BCG-Ova Infections	36

3.3.2 – Evaluation of the Differentiation Profile of $CD8^+$ T cells During LM-Ova and BCG-Ova Infections ____ 38
3.4.0 – Maintenance of Antigen Specific $CD8^+$ T cells During BCG-Ova Infection ____ 40
3.4.1 – Evaluation of the Effects of Inflammation on CD127 Expression in $CD8^+$ T cells ____ 40
3.4.2 – Evaluation of the Effects of the Presence of Antigen on the Cell Surface Expression of CD127 on Antigen Specific $CD8^+$ T cells Responding to BCG-Ova ____ 42
3.5.0 – Evaluation of the Functionality of the $CD8^+$ T cells Responding to a BCG-Ova Infection ____ 47
3.5.1 – Evaluation of IFN-γ Production by $CD8^+$ T cells Responding to LM-Ova or BCG-Ova Infections ____ 47
3.5.2 – Evaluation of In vivo Lytic Activity of Antigen Specific $CD8^+$ T cells Responding to LM-Ova or BCG-Ova ____ 50
3.5.3 – Memory Recall Ability of Antigen Specific Memory $CD8^+$ T cells Generated During LM-Ova and BCG-Ova Infections ____ 53
3.6.0 – Evaluation of In vivo Antigen Presentation ____ 59
3.6.1 – Evaluation of In vivo Antigen Presentation During LM-Ova and BCG-Ova Infections ____ 59
3.6.2 – Evaluation of in vivo antigen presentation during BCG-Ova infection when increased response time for donor OT-1 cells is provided ____ 62
3.6.3 – Evaluation of the Mechanisms That Contribute to the Curtailment in Antigen-presentation During the Later Time Intervals of BCG-Ova Infection ____ 64
3.6.4 – Contribution of $CD4^+$ and $CD8^+$ T cells to the Delay and Curtailment of Antigen-presentation During BCG-Ova Infection ____ 67
3.6.5 – Effects of Early Inflammation on the Delayed $CD8^+$ T cell Response to BCG-Ova ____ 69
3.7.0 – Influence of Antigenic Dose on the Delay in $CD8^+$ T cell Priming During BCG-Ova Infection ____ 73
3.7.1 – The Influence of Initial Amount of Pathogen Burden on $CD8^+$ T cell Activation ____ 73
3.7.2 – The Influence of Initial Amount of Pathogen Burden on Antigen-presentation During BCG-Ova Infection ____ 75
3.7.3 – Quantification of the mRNA Expression of Ova in Spleens of Mice Infected with BCG-Ova ____ 77
4.0 – Discussion ____ 80
5.0 – Concluding Remarks ____ 91
6.0 – Reference List ____ 94
Appendix I ____ 114
Curriculum vitae ____ 115

List of Abbreviations

APC	Antigen presenting cell
BCG	*Mycobacterium Bovis* BCG Pasteur strain
BCR	B cell receptor
BHI	Brain Heart Infusion
BrdU	5-bromo-2-deoxyuridine
CD	Cluster of Differentiation
CFSE	Carboxyfluorescein succinimidyl ester
CFU	Colony Forming Units
FBS	Fetal Bovine Serum
HBSS	Hank's Balanced Salt Solution
IFN-γ	Interferon Gamma
IL	Interleukin
i.p.	Intraperitoneal Cavity Injection
i.v.	Lateral Tail Vein Injection
LCMV	Lymphocytic choriomeningitis Virus
LM	*Listeria monocytogens*
MHC	Major Histocompatibility Complex
NK	Natural Killer Cells
OT-1	$OVA_{257-264}$-specific TCR Transgenic Mice
OT-1R	$OVA_{257-264}$-specific TCR Transgenic Mice That Have Been Backcrossed in a Rag-1 Deficient Background
PBS-T80	1x PBS with 0.05% Tween 80
R8-A	RPMI 1640 Containing 8% Fetal Bovine Serum and 50ug/ml Gentamicin
s.c.	Subcutaneous Injection
ST	*Salmonella typhimurium* SL 1344
SIINFEKL	Codons 257-264 of the Chicken Ovalbumin Gene
TCR	T cell Receptor
TNF-α	Tumor Necrosis Factor Alpha
TAP1 and TAP2	Transporters Associated with Antigen Processing-1 and -2

List of Figures

Figure Title **Page**

Figure 1: BCG and LM have different intracellular niches within the antigen presenting cell ____ 8
Figure 2: The adoptive transfer model ____ 17
Figure 3: Bacterial burden in the spleens of mice infected with LM-Ova and BCG-Ova ____ 25
Figure 4: Frequency of endogenous Ova-specific $CD8^+$ T cells during LM-Ova and BCG-Ova infection ____ 27
Figure 5: Using $H2K^bOva_{257-264}$ tetramers to track endogenous Ova-specific $CD8^+$ T cells during LM-Ova and BCG-Ova infection ____ 29
Figure 6: Antigen-specific $CD8^+$ T cell response during LM-Ova and BCG-Ova infections ____ 30
Figure 7: Relative expansion of Ova-specific $CD8^+$ T cells during the different phases of BCG-Ova infection ____ 32
Figure 8: Cycling of antigen specific $CD8^+$ T cells during LM-Ova and BCG-Ova Infections ____ 34
Figure 9: CD69, CD25, and CD127 cell surface expression on antigen specific $CD8^+$ T cells during LM-Ova and BCG-Ova infections ____ 37
Figure 10: Contrasting differentiation of antigen specific $CD8^+$ T cells during LM-Ova and BCG-Ova infections ____ 39
Figure 11: Experimental layout to assess the effects of inflammation on CD127 cell surface expression on $CD8^+$ T cells responding to BCG-Ova ____ 41
Figure 12: The effects of inflammation on CD127 cell surface expression ____ 43
Figure 13: Experimental layout to assess the effects of antigen persistence on CD127 cell surface expression on $CD8^+$ T cells responding to BCG-Ova ____ 44
Figure 14: The effects of antigen persistence on CD127 cell surface expression ____ 46
Figure 15: Experimental layout to evaluate the ability of $CD8^+$ T cells responding to BCG-Ova to produce IFN-γ ____ 48
Figure 16: Intracellular IFN-γ expression of antigen specific $CD8^+$ T cells during LM-Ova and BCG-Ova infections ____ 49
Figure 17: Experimental layout to evaluate the ability of $CD8^+$ T cells responding to BCG-Ova to exhibit lytic activity ____ 51
Figure 18: In vivo lytic activity of antigen specific $CD8^+$ T cells during LM-Ova and BCG-Ova infections ____ 52
Figure 19: Experimental layout to evaluate the response of memory $CD8^+$ T cells to re-challenge ____ 54
Figure 20: Response of memory $CD8^+$ T cells to re-challenge ____ 56
Figure 21: Response of memory $CD8^+$ T cells to re-challenge after homeostatic Equilibration ____ 58
Figure 22: Experimental layout to evaluate the kinetics of antigen presentation to $CD8^+$ T cells infections ____ 60
Figure 23: Kinetics of antigen presentation during LM-Ova and BCG-Ova infections ____ 61
Figure 24: Kinetics of antigen presentation during BCG-Ova infection with

longer parking interval of donor OT-1 cells ____ 63
Figure 25: Kinetics of antigen presentation during BCG-Ova infections in knockout mice ____ 66
Figure 26: Kinetics of antigen presentation during BCG-Ova infections in non-lymphoid organs in knockout mice ____ 68
Figure 27: Kinetics of antigen presentation during BCG-Ova infection in CD4 and CD8 knockout mice ____ 70
Figure 28: Influence of enhancement of early inflammation on the $CD8^+$ T cell response to BCG-Ova ____ 72
Figure 29: Influence of BCG-Ova dose on CD69, CD25, and CD127 cell surface expression on antigen specific $CD8^+$ T cells ____ 74
Figure 30: Influence of BCG-Ova dose on the kinetics of antigen presentation ____ 76
Figure 31: Ova mRNA and 16S mRNA expression in BCG-Ova infected spleens ____ 78
Figure 32: Model of the events that may be contributing to the $CD8^+$ T cell response to BCG ____ 92

1.0 – General Introduction: The immune system

The immune system is composed of many mutually dependent cell types that cooperatively defend the body from bacterial, parasitic, fungal, viral infections and from the growth of tumor cells. These cell types have dedicated functions. Immune system cells can engulf bacteria, kill parasites or tumor cells, or kill viral-infected cells. These cells depend on the T cell subset for activation signals in the form of secretions formally known as cytokines, lymphokines, or more specifically interleukins. The immune system can be divided into two main branches, the innate immune system and the adaptive immune system [rev in 1].

The innate immune system is composed of physical and chemical barriers such as skin, gastric acids, mucus, or tears and it has specialized cells known as phagocytes, and natural killer cells and the complement system. Phagocytes are cells, such as neutrophils, monocytes and macrophages, that have the ability to extend their plasma membranes and engulf a foreign particle or microorganism [rev in 2]. The invading microorganism is constrained inside a vacuole which fuses with lysosomes. These vacuoles are rich in enzymes and acids, which digest the particle or organism. Phagocytic cells respond to cytokines which are highly specialized molecular signals produced by lymphocytes known as T cells or B cells. They also patrol the body surveying for foreign invaders. This form of defense is more important against bacterial infections, because viruses usually have their own means of entering host cells and the majority of parasites are too large to be consumed. Natural killer cells or NK cells are a major component of the innate immune system [3]. They are lymphocytes that attack cells that have been infected by microbes and they show activity against some tumor cells. NK cells destroy cells which are missing "self". "Self" is a term used to describe cells that express low levels of MHC (major histocompatibility complex) class I cell surface marker molecules; a situation that sometimes occurs due to viral infection,

or in tumors under strong selection pressure of killer T cells [rev in 1;4]. The complement system is a biochemical cascade that assists in clearing pathogens from an organism [rev in 5]. It is compsed of many small plasma proteins working together to culminate in cytolysis of the target cell's plasma membrane [rev in 5]. The innate immune response also causes inflammation [rev in 6]. Inflammation is characterised by redness, heat, swelling, pain and dysfunction of the organs involved. Inflammation is stimulated by chemical factors that are released by injured cells. These factors such as histamine sensitize pain receptors and cause vasodilation of the blood vessels at the scene, and also attract phagocytes to the site of infection [rev in 6]. Phagocytosis induces the phagocytes to release other factors that recruit lymphocytes and other phagocytes to the site of infection. The innate immune system drives the adaptive immune response via the secretion of cytokines, chemokines, and antigen presentation [rev in 7].

The basis of the adaptive immune system resides in the ability of immune cells to distinguish between proteins produced by the body's own cells ("self" antigen), and proteins produced by invaders or cells infected with a virus ("non-self" antigen) [rev in 4]. This distinction is made via T-Cell Receptors (TCR) on T lymphocytes or B-Cell Receptors (BCR) on B lymphocytes. For these receptors to be efficient they must be produced in thousands of configurations, thus they are able to differentiate between many different invaders and respond to a repertoire or antigens. The vast majority of lymphocytes never find a protein that its receptor is specific for. Those that do find one are stimulated to clonally expand in response to the stimulation and simultaneous co-stimulation. Activated cells are generated with the specific receptor and these cells eliminate the invader via direct killing in the case of $CD8^+$ T cells or indirect killing through the secretion of antibodies (in the case of B cells) and the secretion of cytokines and chemokines. These cytokines induce the

phagocytes to destroy the invader they have engulfed and the chemokines recruit more lymphocytes and phagocytes to the site of infection. Once the antigen has been cleared from the organism the vast majority of these cells (>90%) undergo apoptosis or programmed cell death. Those that survive this become memory cells. These memory cells are quiescent and they are long lived. The signature feature of these memory cells is that they are capable of identifying this antigen long after it has been eliminated. If the antigen is encountered again these cells will multiply themselves quickly and rapidly respond to the secondary infection [rev in 8;9].

Bacteria on the other hand have adapted and developed ways to evade this immune system so as to enhance their own survival. Some evade the immune system by replicating either too fast (*Vibrio cholerae* or *Salmonella*) [10 rev in 11] or too slow (*Mycobacterium*) [12] for the immune system to respond effectively. Some secrete antigens into the blood stream there by diverting the response away from them. Some manipulate phagocytosis and apoptosis [13]. Some inhibit phago-lysosome fusion [14]. Some also evade the complement cascade [15]. There are many other strategies that pathogens have evolved over the centuries to evade the immune system that have not been mentioned but are still very effective at this task. This thesis delves into the intricate way the immune system of a mammal (*mus musculus*) attempts to contend with an acute (*Listeria monocytogenes*) intracellular bacterium and a chronic (*mycobacterium bovis*) intracellular bacterium.

1.1 – Antigen processing and presentation

Infectious agents are phagocytosed and subsequently processed by APCs and peptides are generated from pathogens present in the cytosol or in the intracellular vesicular compartments (phagosomes) of these specialized cells [rev in 2]. These peptides are loaded onto MHC class I molecules in the case of cytosol derived peptides and MHC class II molecules

in the case of exogenous vesicular derived peptides [16]. The folding and assembly of newly synthesized MHC class I molecules occurs in the endoplasmic reticulum. The cytosolic peptide is degraded by proteosomes in the cytosol and resulting peptide fragments are transported into the lumen of the endoplasmic reticulum via the TAP1 and TAP2 and loaded onto MHC class I molecules [17-19]. A vesicle buds off the end of the endoplasmic reticulum containing the MHC class I/peptide complex and fuses with the cell surface membrane and the MHC class I/peptide complex is displayed on the cell surface. The $CD8^+$ T cells specifically recognize MHC class I bound peptides [20]. While only cytosolic antigens were previously presumed to be presented on MHC class I processing pathway, however, there is a lot of evidence showing that peptides derived from exogenous antigens in some cases do get presented via MHC class I [21-25]. This is referred to as cross-priming and the process by which the exogenous antigen is processed and loaded onto MHC class I is referred to as cross-presentation. How cross-presentation happens exactly is still controversial [rev in 26]. There are many pathways that have been considered. One such pathway is the vacuolar pathway where MHC class I molecules obtain peptides that are generated in phagosomes in a TAP-independent manner[27-30]. Another pathway is the phagosome-to-cytosol-to-phagosome pathway where the phagosome fuses with the ER and thus acquires MHC class I, TAP, Sec61 and other ER molecules and processing occurs in a similar manner to the classical MHC class I peptide loading [31]. Whether or not this fusion occurs is still not clear [32-34] however, phagosomes themselves have been shown to contain the proteins necessary for MHC class I loading [35]. In either case, in the phagosome-to-cytosol-to-phagosome pathway internalized antigen is thought to be exported to the cytosol by Sec61 where it is hydrolyzed by proteasomes and the peptides are re-introduced into phagosomes by TAP, where they subsequently bind MHC class I molecules [36-38]. Another pathway is the phagosome-to-

cytosol pathway in which exogenous antigen internalized into phagosome is thought to be exported into the cytosol, hydrolyzed by proteasomes and the peptides are transported to MHC class I molecules in the ER via TAP [39]. Another pathway is the GAP junction pathway in which APCs obtain peptides from other cells through GAP junctions [40]. A final pathway proposed to be involved in cross-presentation is the endosome-to-ER pathway where antigen in endosomes is thought to be transported into the ER and degraded in the cytosol by the ER associated degradation pathway [41]. The peptides are transported to class I molecules in the ER by TAP. Some of these propositions of how exactly cross-presentation and cross-priming occurs have only been shown in vitro however it is widely accepted that cross-priming most likely occurs in vivo and exogenously derived peptides are presented on MHC class I molecules [10;12].

1.2 - T cell Priming and the establishment of memory

The $CD8^+$ T cell response can be divided into three phases [42]. The first is the priming and expansion phase. $CD8^+$ T cells become activated upon encountering an APC bearing a foreign peptide within its MHC class I molecule. The T cell receptor on the $CD8^+$ T cell recognizes this peptide/MHC class I complex. Upon engagement of the TCR and peptide/MHC class I complex an intracellular signaling cascade occurs within the $CD8^+$ T cell via the TCR. This leads to the production of transcription factors, which translocate to the nucleus and transcribe genes for various growth factors and inflammatory cytokines. These cytokines cause the $CD8^+$ T cell to undergo massive clonal expansion and differentiation into an effector ($CD62L^{low}$, $CD44^{hi}$) or central phenotype ($CD62L^{hi}$, $CD44^{hi}$) [43]. The effector $CD8^+$ T cells now possess the ability to carry out cell mediated cytotoxicity following encounter with any cell expressing an MHC class I molecule containing the same antigen, via the Fas- and perforin-dependent pathways [44-46]. In a typical acute infection this

process occurs around 5-7 days of infection. As naïve T cells, the $CD8^+$ T cells utilize IL-7 as a growth cytokine [47;48] and upon activation the T cells switch to using IL-2 and IL-15 as a growth cytokine [49]. IL-2 is the key growth cytokine produced during the activation stage and is used by rapidly dividing cells [rev in 50]. The alpha chain of the receptor for IL-7 (CD127) is down-regulated upon $CD8^+$ T cell priming and expansion and the alpha chain of the high affinity receptor for the IL-2 cytokine (CD25) is expressed on the cell surface. When the three chains of the IL-2 receptor appear on the surface of the cell it forms a receptor that has a high affinity for the IL-2 cytokine [51]. Upon priming the $CD8^+$ T cell also transiently up-regulates on its cell surface CD69 which is an early antigen activation marker [52;53]. Another signature cytokine produced at this stage is IFN-γ. This is a pro-inflammatory cytokine that is produced by $CD8^+$ T cells. IFN-γ activates macrophages and causes the induction of antimicrobial mechanisms in macrophages namely the production of pro-inflammatory cytokines such as TNF-α and the production of nitrous oxide [54].

The next phase in the $CD8^+$ T cell response is the death phase. Once the antigen has been cleared from the system, the bulk of the $CD8^+$ T cells generated at the peak of the response undergo apoptosis (~90-95%). The $CD8^+$ T cell response is programmed to contract and proceeds despite the continued persistence of antigen and even when $CD8^+$ T cell expansion gets curtailed [55]. This contraction in an acute infection typically occurs within 7-30 days of the response. Those $CD8^+$ T cells that survive the death phase now enter the memory phase. The remaining $CD8^+$ T cells become long-lived memory cells which are capable of responding rapidly and specifically if they encounter the same antigen again [56-58]. These cells rely on the IL-7 and IL-15 for sustained growth and thus the receptor for these cytokines is highly expressed on the surface of these memory cells [47;49]. CD127 expression has been found to be a crucial marker for identifying the activation and differentiation status

of $CD8^+$ T cells [59]. Naïve cells ($CD44^{low}CD62L^{hi}CD127^{hi}$) upon stimulation differentiate into various phenotypic subsets of cells: Effectors ($CD44^{hi}CD62L^{low}CD127^{low}$), effector memory cells ($CD44^{hi}CD62L^{low}CD127^{hi}$) and central memory cells ($CD44^{hi}CD62L^{hi}CD127^{hi}$). In fact up-regulation of CD127 expression is required for $CD8^+$ effector T cells to differentiate into memory cells [60]. Regardless of the antigen dose, the proportion of long-lived memory $CD8^+$ T cells remains constant at around 10% of the maximum number of cells generated during the primary response [61;62]. The manner in which antigen is presented to the immune system can have a profound effect on the phenotype of the resulting $CD8^+$ T cells and subsequent repercussions for long-term protection.

1.3 – *Listeria monocytogenes*

Listeria monocytogens (LM) is a facultative aerobe, gram-positive rod, with an in vitro doubling time of 46 min. [10;12]. LM causes a serious food-borne illness especially in high risk groups such as the elderly, infants, and pregnant women [63]. LM induces phagocytosis, shedding its flagella upon entry, and once inside the phagosome it releases a protein known as listeriolysin, a thiolactivated cytolysin or hemolysin which releases it from the confines of the phagosome (Figure 1B) [64]. LM possesses the ability to polymerize actin into long actin tails and upon escaping the phagosome, it uses these actin tails to propel itself through the cytoplasm spreading from cell to cell [65;66]. LM replicates within the cytosol of both phagocytic and non phagocytic cells [67]. By escaping from the phagosome LM is exposed to the classical MHC Class I presentation pathway. LM is a classical intracellular pathogen used to study T cell memory [68] because of its potent activation of T cells which has been well documented [69-74].

Figure 1: BCG and LM have different intracellular niches within the APC. Once phagocytized, BCG prevents phagosome-lysozome fusion and acidification of the phagosome. BCG actively replicates within the phagosome of the APC. It is not known exactly how antigens produced by BCG enter the MHC Class I pathway for presentation but somehow they do and they do induce a $CD8^+$ T cell response (A). Once phagocytized, LM produces a protein called listeriolysin which causes it to escape from the phagosome and exposes it to the MHC class I pathway of peptide presentation. LM polymerizes actin filaments and uses them to travel from cell to cell (B).

Figure 1

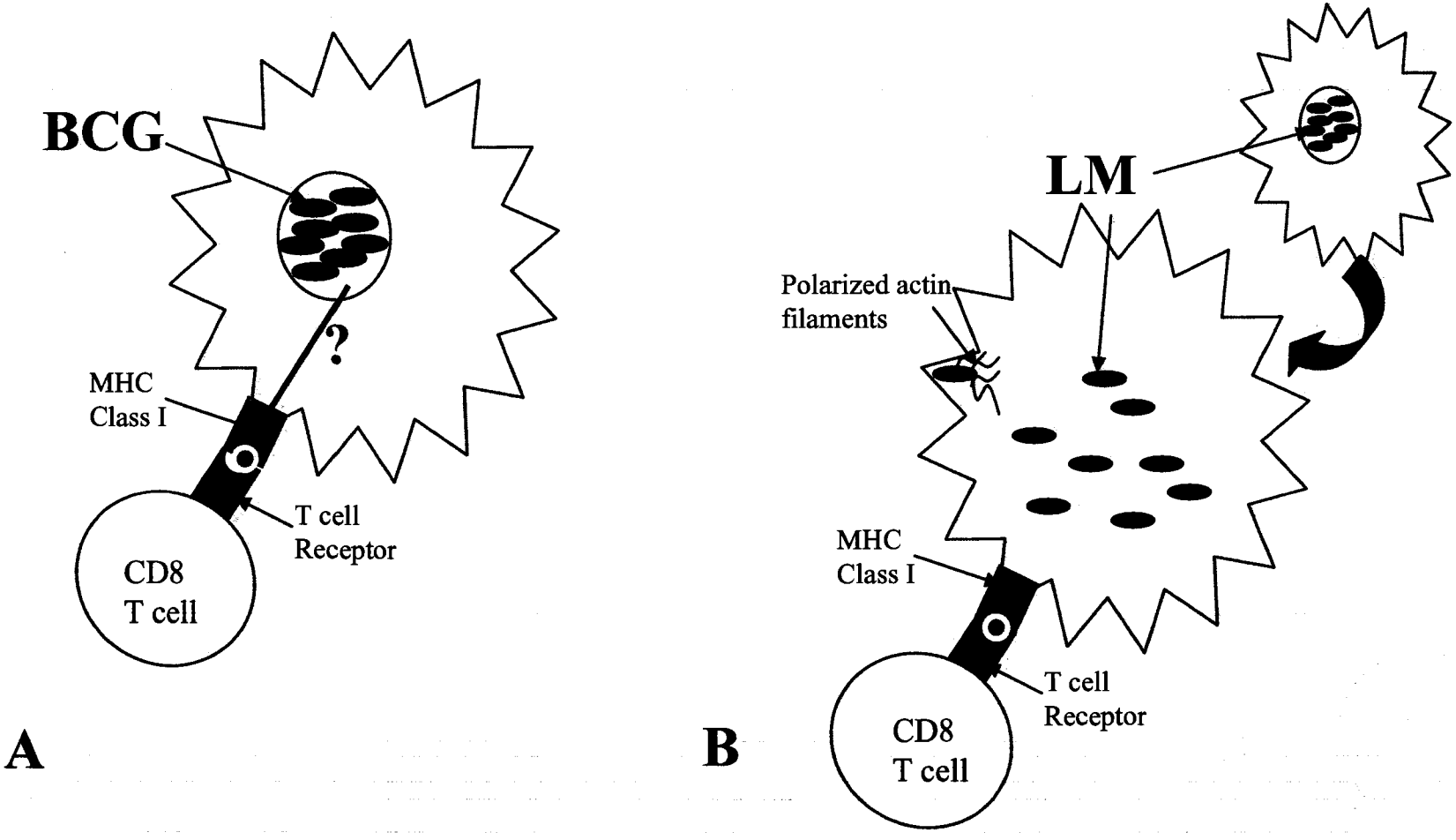
BCG
?
MHC
Class I
T cell
Receptor
CD8
T cell
A
LM
Polarized actin
filaments
MHC
Class I
T cell
Receptor
CD8
T cell
B

1.4 – *Mycobacterium Bovis*

An avirulent strain of *Mycobacterium Bovis*, referred to as BCG Pasture, is currently used as a live vaccine for the human pathogen *Mycobacterium tuberculosis* [75-79]. It is thought that approximately one-third of the world's population (or 2 billion people) are currently asymptomatically infected with *M. tuberculosis* which causes the disease known as tuberculosis and kills about 2 million people annually [80]. *M. bovis* is a facultative aerobe, rod-shaped (slightly curved forming strands and cords) bacterium possessing a gram-positive type cell wall with unusually high lipid content [81]. *M. bovis* is non-spore forming, non-motile, and grows very slow with an in vitro doubling time of 29.5 hrs [12]. *M. bovis* infects macrophages and dendritic cells, both of which are key APCs of the immune system.

Once *M. bovis* has been phagocytosed by the macrophage it appears to de-rail host responses by preventing the fusion of the phagosome with the lysosome [82], inhibiting antigen-presentation [83], and modulates apoptosis by promoting [84] or inhibiting it [85;86]. However, all of these inhibitory effects have mainly been studied in vitro and it is not clear whether these mechanisms operate in vivo as well. Once internalized in the macrophage, Mycobacteria are confined to the phagosome where mycobacterial antigens are secluded from the classical MHC Class I presentation pathway (Figure 1A). There are controversial reports on the activation of $CD8^+$ T cells induced by BCG with some reporting immune suppression and others reporting potent immune activation [87-96]. Memory to mycobacteria is not well defined.

1.5 – Antigen Presentation in Acute versus Chronic infections: A comparison between LM and BCG

LM and BCG are both intracellular pathogens with unique life styles and $CD8^+$ T cells play a crucial role in circumventing the proliferation of these pathogens. Previously,

codons 230-359 containing the $CD8^+$ T cell epitope SIINFEKL ($Ova_{257-264}$) of the Ovalbumin (Ova) gene were cloned into LM and BCG and the recombinant forms were termed LM-Ova and BCG-Ova respectively [95]. LM-Ova caused an acute infection resulting in a ~100 fold increase in bacterial burden in the spleen within the first 24hrs [12,95]. LM-Ova bacterial burden peaked on day 3 and was eliminated by day 7 [12,95]. On the other hand BCG-Ova caused a chronic infection resulting in a ~13 fold increase in bacterial burden in the spleen within the first 3wks [12,95]. BCG-Ova bacterial burden peaked between days 15-30 and was not cleared even at 60 days post-infection [12;95]. It was also found that LM-Ova induced a potent $CD8^+$ T cell response which peaked on day 7 followed by rapid attrition contrastingly; BCG-Ova induced a delayed and muted $CD8^+$ T cell response which peaked from day 15-30 and experienced little attrition [12,95]. It was also noted that antigen-presentation during a BCG infection gets curtailed as host T cell responses develop but is maintained at low levels even at 60 days post-infection, contrasting to LM-Ova infection which terminated around 6-10 days [12].

Antigen presentation is a key event that directly dictates the magnitude of $CD8^+$ T cell memory. During BCG infection it has been observed that there is a delayed and weak response by the $CD8^+$ T cells. Also, the overall numbers of $CD8^+$ T cells generated during a BCG-Ova infection are much lower than what is generated during LM-Ova infection. Based on these findings it is hypothesized that $CD8^+$ T cells generated under these weak stimulation conditions are functionally incompetent.

2.0 - Material and Methods

2.1 - Mice and Infections

Six–to-eight-week-old female C57BL/6 mice and 129X1SvJ mice were obtained from The Jackson Laboratory (Bar Harbor, ME, USA). Six–to-eight-week-old female C57BL/6-Tg (TcraTcrb)1100Mjb mice (OT-1), B6.129S7-*Rag1*^{tm1Mom} mice, B6.129S2-*Cd8a*^{tm1Mak} mice, B6.129S6-*Cd4*^{tm1Knw} mice, B6;129S-*Tnfrsf1a*^{tm1Imx} *Tnfrsf1b*^{tm1Imx} mice, B6.129P2-*Nos2*^{tm1Lau} mice, and B6.129S7-*Ifng*^{tm1Ts} mice were also obtained from the Jackson Laboratory (Bar Harbor, ME, USA). Six–to-eight-week-old female $OVA_{257–264}$-specific TCR transgenic mice that have been backcrossed in a Rag-1 deficient background (OT-1R) were obtained from Taconic Farms (Germantown NY, USA). Female $OVA_{257–264}$-specific TCR transgenic mice (OT-1) were also bred in-house. B6129F1 mice were bred in-house in the animal facilities at the Institute of Biological Sciences of the National Research Council Canada (NRC) (Ottawa, Ontario, Canada) by mating 129XsvJ female mice with C57BL/6 male mice. All the mice used were housed in pathogen-free conditions at the animal facilities at the Institute of Biological Sciences of the National Research Council Canada (Ottawa, Ontario, Canada) in accordance with the guidelines of the Canadian council on Animal Care. Mice were infected with the respective pathogen at 8-12 weeks of age via lateral tail vein injection (i.v).

2.2 – Media, Bacterial Strains, Bacterial Immunizations, Antibiotic Treatments, Antibodies, and Other Reagents

Previously, a strain of *Mycobacterium Bovis* BCG Pasture (BCG) was engineered to express a partial sequence of the ovalbumin gene (Codons 230-359) under the control of the HSP60 promoter (BCG-Ova) [95]. Codons 230-359 contain the $CD8^+$ T cell epitope SIINFEKL ($OVA_{257-264}$). Single colonies were used to inoculate liquid cultures, which were

incubated at 37°C under constant shaking in 7H9 medium (BD biosciences, Franklin Lakes, NJ, USA) containing glycerol (0.2%), Tween 80 (0.05%), and albumin-dextrose supplement 10% (ADC, Difco, Detroit, MI) supplemented with kanamycin (15ug/ml). At mid-log phase ($O.D._{600}$=1.0), bacteria were harvested and frozen at -80°C (in 20% glycerol). Colony forming units (CFU's) were determined by plating serial dilutions in PBS-T80 (PBS containing 0.05% Tween 80), which were spread on 7H10 agar plates (BD biosciences, Franklin Lakes, NJ, USA) containing glycerol (0.5%) and OADC enrichment 10% (Difco Detroit MI) and occasionally supplemented with kanamycin (15ug/ml) when indicated.

Previously, a recombinant strain of *Listeria monocytogenes* (10403S) (LM) expressing the gene for ovalbumin (LM-Ova) was generated [95]. Single colonies were used to inoculate liquid cultures, which were incubated at 37°C under constant shaking in Brain Heart Infusion (BHI) media (BD biosciences, Franklin Lakes, NJ, USA) supplemented with erythromycin (5 μg/ml) (Sigma-Aldrich Canada, Oakville, On, Canada). At mid-log phase ($O.D._{600}$=1.0), bacteria were harvested and frozen at -80°C (in 20% glycerol). CFU's were determined by plating serial dilutions in 0.9% NaCl, which were spread on BHI-streptomycin (50ug/ml) agar plates.

Single colonies of *Salmonella typhimurium* SL 1344 (ST) were used to inoculate liquid cultures which were incubated at 37°C under constant shaking in Brain Heart Infusion (BHI) media (DIFCO Laboratories, Detroit MI). At mid-log phase ($O.D._{600}$=0.8), bacteria were harvested and frozen at –80°C (in 20% glycerol). CFU's were determined by performing serial dilutions in 0.9% NaCl, which were spread on BHI agar plates.

For immunization with BCG or BCG-Ova frozen stocks of BCG, or BCG-Ova were thawed, washed once with PBS-T80 (PBS containing 0.05% Tween-80), and reconstituted in

PBS-T80, and injected into mice via the lateral tail vein. Control mice were injected with PBS-T80. For immunization with LM-Ova frozen stocks of LM-Ova were diluted in 0.9% NaCl and injected via the lateral tail vein. Control mice were injected with PBS. For immunization with S. *typhimurium* frozen stocks of S. *typhimurium* were diluted in 0.9% NaCl and injected via the lateral tail vein. Control mice were injected with PBS.

The antibiotic cocktail for BCG consisted of: Isoniazid (Sigma, Oakville, Ontario, Canada) and Rifampicin (Sigma, Oakville, Ontario, Canada) were obtained from Sigma-Aldrich. The antibiotics were administered in drinking water as a cocktail of 0.1 mg/ml Isoniazid and 0.15 mg/ml of Rifampicin. The antibiotic mixture in the drinking water was changed fresh once a week for 8 weeks.

All antibodies used in this study were monoclonal antibodies. Anti-mouse CD44, anti-mouse CD69, anti-mouse IFN-γ, anti-mouse CD8α, and anti-mouse CD25 were purchased from BD Pharmingen (Mississauga, Ontario, Canada). Anti-mouse CD62L, anti-mouse CD127 and RatIgG 2a isotype control were purchased from eBioscience (San Diego, California, USA). H-2K^b MHC class I $Ova_{257-264}$ murine tetramers were purchased from Beckman Coulter (Mississauga, Ontario, Canada).

The CpG oligonucleotides and controls were obtained from Coley Pharmaceuticals (Ottawa, Ontario, Canada) and diluted in 1x PBS to the desired concentration. *Methanobrevibacter smithii* (*M. Smithii)* archeosomes entrapped with OVA peptide (SIINFEKL $OVA_{257-264}$) was prepared as described previously [97-100] and stored in PBS.

2.3 – Lymphocyte Extraction From Spleen and Other Organs

Spleens were harvested under aseptic conditions and spleen cell suspensions were prepared by tweezing the spleens between the frosted ends of two sterile glass slides in RPMI 1640 (Invitrogen, Burlington, Ontario, Canada). Cells were subsequently passed

through Falcon 2360 cell strainers (BD Labware, Franklin Lake, NJ, USA), centrifuged, and reconstituted in RPMI 1640 containing 8% Fetal Bovine Serum (FBS) (HyClone Laboratories, Logan, UT, USA) and 50 ug/ml Gentamicin (Invitrogen, Burlington, Ontario, Canada), which henceforth will be referred to as R8-A. Cells were passed through a Falcon 2360 cell strainer again. An aliquot was taken for counting. Dead and live cells were distinguished by staining with trypan blue (Invitrogen, Burlington, Ontario, Canada) in a 1:1 volume ratio. Live cells were counted on a hemocytometer.

Lungs and livers were harvested under aseptic conditions following perfusion with PBS and heparin 75-100 i.u. per mouse (LEO Pharma Inc. Thornhill, Ontario, Canada). Lungs or livers were chopped into tiny pieces with sterile scissors and lymphocytes were extracted using 250 ug/ml collagenase type IV (Worthington Biochemicals, Lakewood, NJ, USA) followed by 1mM EDTA. The lung pieces were homogenized using a plunger through a strainer. A 30%/70% percoll gradient (Sigma, Oakville, Ontario, Canada) was used to separate the connective tissue from the lymphocytes. The lymphocytes were collected at the interface and washed with 15ml RPMI.

2.4 – Assessment of bacterial burden in organs

Single spleen cell suspensions from infected mice were prepared as above in 10ml RPMI 1640. With LM-Ova immunized mice, CFU's were determined by plating a 100ul aliquot of the cell suspension and subsequent serial 10-fold dilutions in 0.9% NaCl onto BHI agar plates. Plates were incubated for 24 hours at 37°C and colonies were counted visually. With BCG-Ova immunized mice, CFU's were determined by plating a 100ul aliquot of the cell suspension and subsequent serial 10-fold dilutions in PBST-80 onto 7H10 agar plates supplemented with OADC enrichment. Plates were incubated for 21-30 days at 37°C and colonies were counted visually. With S. *typhimurium* immunized mice, CFU's were

determined by plating a 100ul aliquot of the cell suspension and subsequent serial 10-fold dilutions in 0.9% saline onto BHI agar plates. Plates were incubated for 24 hours at 37°C and colonies were counted visually.

2.5 – ELISPOT assay

Multiscreen IP 96 well 0.45μm hydrophobic filtration plates (Millipore, Cambridge, On, Canada) were moistened with 70% methanol and washed with $NaHCO_3$ buffer. The plates were coated with R46A2 primary anti-IFN-γ antibody at 13ug/ml in $NaHCO_3$ buffer and incubated at room temperature overnight. The following day the wells were washed with RPMI media and blocked with 1.5% skim milk powder in RPMI containing Gentamycin (50ug/ml) for 3-4 hours at 37°C. Spleen cells from infected mice were processed as in section 2.3 and the number of spleen cells from infected mice was varied to achieve a final cell density of $5x10^5$/well using feeder cells from unimmunized mice. Cells were incubated at 37°C for both 24 hours and 48 hours supplemented with IL-2 (0.1ng/ml) and with or without Ova peptide (5ug/ml). After stimulation, the cells were lysed with milli-Q water and the wells were washed with 0.01% PBS-T20. The wells were incubated 2 hours at 37°C with the biotinylated secondary anti-IFN-γ antibody XMG1.2 (0.6ug/ml) in 0.05% PBS-T20. The plate was washed with 0.01% PBS-T20 and the wells were incubated at room temperature for 1 hour with the peroxidase conjugated streptavidin 1ug/ml (MediCorp, Montreal Quebec Canada) in sterile 0.05% PBS-T20. The plate was again washed with 0.01% PBS-T20 followed by washing with 1x PBS. The wells were incubated with the AEC substrate (Sigma, Oakville, Ontario, Canada) prepared according to manufactures instructions for 10-12 mins at room temperature. The reaction was stopped by plunging the plate into cold tap water. The plates were dried overnight and spots were enumerated the next day.

2.6 – The Adoptive Transfer Model

In order to track T cells directly the $CD8^+$ T cell response had to be amplified. Thus, an adoptive transfer model was employed which involved the use of C57BL/6-Tg (TcraTcrb)1100Mjb mice commonly referred to as OT-1 mice. These mice have >90% of the T cell receptors on the entire $CD8^+$ T cell population, specific for the $CD8^+$ T cell epitope $Ova_{257-264}$ (SIINFEKL). Splenocytes from these mice were obtained and processed as in section 2.3 except that these splenocytes were reconstituted in hank's balanced salt solution (HBSS) instead of R8-A. Live and dead cells were determined and the splenocytes were injected via the lateral tail vein (i.v.) into C57BL/6 mice or B6.129F1 mice. These mice would have either previously been injected with LM-Ova or BCG-Ova i.v., or would subsequently be injected with LM-Ova or BCG-Ova i.v., or Ova archeosomes [97-100] subcutaneously (s.c.) as the experiment dictated (Figure 2).

2.7 – Cell Cycling

Cell cycling was enumerated according to the protocol of Tough et al [101] using the BD Biosciences BrdU staining kit. Three days prior to the harvesting of spleens from infected mice, 5-bromo-2-deoxyuridine (BrdU) was provided (80 mg/100ml) in the drinking water every day. Spleens were harvested and processed as in section 2.3. Aliquots of spleen cells (10×10^6/ml) were incubated with anti-CD8α antibody for 5 min. on ice in the dark followed by incubation with $H\text{-}2K^bOva_{257-264}$ tetramers (Beckman Coulter, Fullerton, California) at room temperature for 30min. in the dark. After staining, cells were washed, permeabilized and incubated with DNAse for 30 min. at 37°C. Cells were stained with

Figure 2: The adoptive transfer model. OT-1 mice have been genetically engineered to have over 90% of the T cell receptors on their $CD8^+$ T cells specific for the $OVA_{257-265}$ (SIINFEKL) epitope. Splenocytes from these mice are adoptively transferred into naïve C57BL/6 recipients. Recipient mice are injected with LM-Ova or BCG-Ova as the experiment dictates.

Figure 2

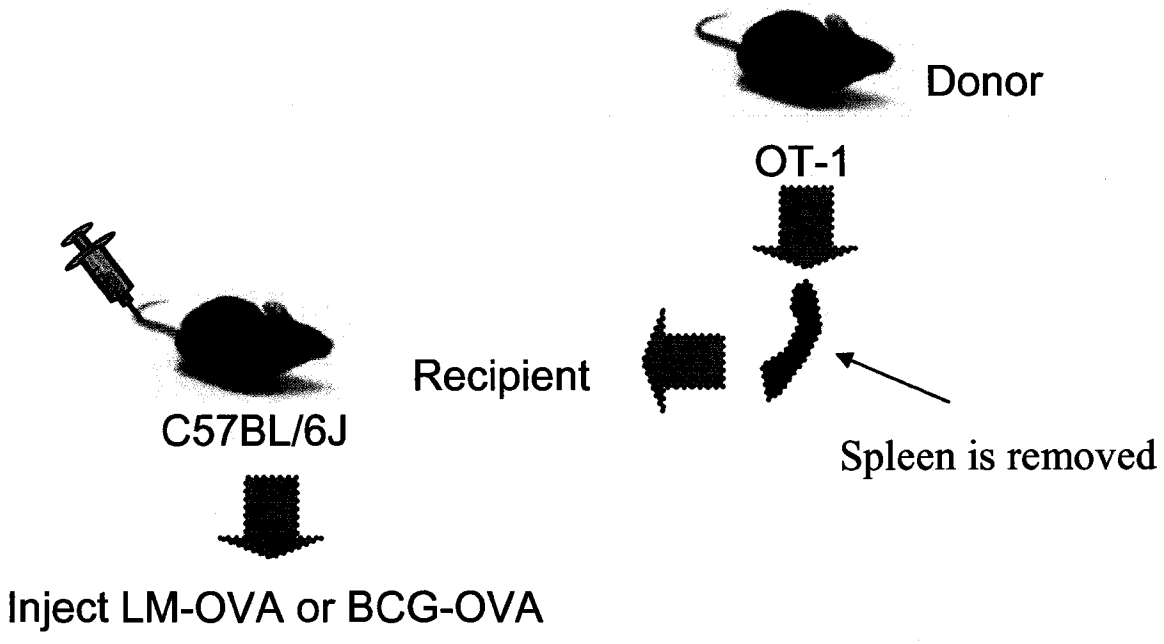
Donor
OT-1
Recipient
C57BL/6J
Spleen is removed
Inject LM-OVA or BCG-OVA

anti-BrdU antibody on ice for 30 min., washed, fixed in 0.5% Formaldehyde and acquired on EPICS XL Flow cytometer. BrdU is a base analog of thymidine, with the thymine replaced with bromouracil. It is used to detect proliferating cells within the tissue. During DNA replicating BrdU replaces thymidine thus incorporating itself into newly synthesized DNA. Antibodies specific for BrdU are then used to detect the thymidine analog and these antibodies can be detected using flow cytometry.

2.8 – Assessment of phenotype of antigen specific $CD8^+$ T cells

To assess the phenotype of the antigen specific $CD8^+$ T cells in the spleen $5x10^6$ spleen cells were incubated in 80 ul PBS-1%BSA with anti-CD16/32 at 4°C for 10 min. Cells were incubated with various antibodies to markers of interest (anti-CD8α, anti-CD62L, anti-CD44, anti CD25, anti-CD127, anti-CD69 or Rat IgG 2a) for 5 min. on ice in the dark. The lymphocytes were incubated with H-$2K^bOva_{257-264}$ tetramers (Beckman Coulter, Fullerton, California) at room temperature for 30min. in the dark. The lymphocytes were washed with PBS at room temperature and fixed with 0.5% formaldehyde and acquired on EPICS XL Flow Cytometer.

To assess the phenotype of the antigen specific $CD8^+$ T cells in the blood 100 ul of blood was collected in heparin coated tubes. The blood was incubated with various antibodies to markers of interest (anti-CD8α, anti-CD62L, anti-CD127 (IL-7Rα), or Rat IgG 2a) for 5 min. at room temperature in the dark. The lymphocytes were incubated with H-$2K^bOva_{257-264}$ tetramers (Beckman Coulter, Fullerton, California) at room temperature for 30min. in the dark. The lymphocytes were lysed with 1ml red blood cell lysis buffer in the dark for 8-10 min. After lysis the cells were washed with PBS at room temperature and fixed with 0.5% formaldehyde and acquired on EPICS XL Flow Cytometer.

2.9 – Assessment of Intracellular IFN-γ Production

Aliquots of spleen cells (10 x 10^6/ml) were incubated with anti-CD8α antibody for 5 min. on ice in the dark followed by incubation with H-2$K^b$$Ova_{257-264}$ tetramers (Beckman Coulter, Fullerton, California) at room temperature for 30 min. in the dark. The lymphocytes were washed with PBS and reconstituted in R8-A medium, and stimulated with $Ova_{257-264}$ peptide (1 μg/ml) in the presence of Golgi-stop (BD Biosciences) and plated into 96-well plates ($2x10^6$/well). After 1 h at 37°C, cells were harvested, washed, permeabilized and stained for intracellular IFN-γ using the IFN-γ staining kit (obtained from BD Biosciences). Cells were acquired on EPICS XL Flow cytometer and analyzed using the EXPO software.

2.10 – In vivo CTL

In vivo cytolytic activity of antigen-specific $CD8^+$ T cells was measured according to the protocol of Barber et al. [102]. Donor spleen cells were obtained from naïve C57BL/6J mice and prepared as stated above. The cell suspension was centrifuged and the red blood cells were lysed using a red blood cell lysing buffer (Sigma, Oakville, Ontario, Canada). 5 ml RBC lysing buffer was used per spleen, cells were mixed 5 times and cold PBS was added to stop the lysis. The spleen cells were pulsed at $1x10^7$cells/ml with 10 μM OVA peptide (SIINFEKL $OVA_{257-264}$) or without peptide in R8-A for 30 min. at 37°C. Each spleen cell population was stained at $2x10^7$ cells/ml in Diluent C (Sigma-Aldrich, St. Louis, MO, USA) with an equal volume of 4μM PKH26 membrane labeling dye diluted in Diluent C (Sigma-Aldrich, St. Louis, MO, USA) at room temperature for 3 min. PKH26 labeling was stopped by adding an equal volume of FBS for 3 min. Each cell population was labeled with a different concentration of carboxyfluorescein succinimidyl ester (CFSE). The cell suspensions were both stained in PBS at a concentration of $2x10^7$cells/ml. The peptide-pulsed population was stained with 5 μM CFSE (diluted in PBS) and the unpulsed

population was stained with 0.5 μM CFSE (diluted in PBS). CFSE labeling was stopped by adding an equal volume of FBS for 3 minutes. Cells were centrifuged and reconstituted in HBSS and $1x10^7$cells of each population was mixed together, and $2x10^7$cells of the mixture were injected i.v. into mice that were previously infected with either LM-Ova or BCG-Ova or uninfected. 24 hours after transfer, the infected mice were sacrificed, and their spleens were harvested. Spleens were prepared as in section 2.3 and $1x10^7$cells were washed with 3ml PBS/1%BSA and reconstituted in 1 ml of 0.5% fixative and analyzed by flow cytometry. Percent specific lysis of fluorescent donor spleen cells in each mouse was calculated as follows:

$$100\text{-}\ [\frac{\%pulsed\ \text{inf}\ ected\ /\ \%unpulsed\ \text{inf}\ ected}{\%pulsedun\ \text{inf}\ ected\ /\ \%unpulsedun\ \text{inf}\ ected} x100]$$

2.11 – T cell purifications

$CD8^+$ T cells were purified by positive selection using the Dynal CELLection Biotin Binder Bead Kit. CELLection Biotin Binder Dynabeads were pre-coated as per manufacture's instructions (Dynal Biotech, Great Neck, NY, USA), with biotin-conjugated rat anti-mouse CD8β.2 monoclonal antibody (BDbioscience, Franklin Lakes, NJ, USA, Catalogue# 553039). Briefly, beads were washed with PBS-tween 80 (0.05%). Beads were incubated with the CD8β antibody (10 ug/$1x10^8$ beads) for 1 hour at room temperature. After incubation with the antibody the beads were washed with PBS-tween 80 (0.05%) followed by washing with R8-A. Beads were stored in R8-A until needed (for a maximum of 7 days).

To purify the $CD8^+$ cells from spleens the spleen cells were processed as above and reconstituted to a concentration of $20x10^6$cell/ml. The pre-coated Dynabeads were added to the reconstituted cells at a ratio of five beads per cell, and incubated for 15-20 min. at 4°C in a rotating platform. $CD8\beta^+$ T cells were separated by magnetic isolation. $CD8\beta^+$ T cell-

Dynabead detachment was done using the CELLection Biotin Binder Kit Releasing Buffer (DNase; 188U/10^8 Dynabeads) and incubating at 37°C rotating for 15 min. This was followed by two to three rounds of washing and magnetic separation with R8-A.

2.12 – In vivo antigen presentation

Spleen cells were obtained from donor OT-1 or OT-1R mice, and stained with CFSE (Sigma, Oakville, Ontario, Canada) [103]. Spleen cell suspensions were prepared as mentioned above and cell numbers were assessed. Spleen cells were centrifuged and reconstituted in PBS at a concentration of $20x10^6$cells/ml. An equal volume of 5 μM CFSE in PBS was added to the cells and incubated with gentle shaking in the dark for 8 min. at room temperature. The reaction was quenched with an equal volume of cold FBS and the cells were put on ice for 3-5 min. The spleen cells were centrifuged and reconstituted in HBSS 25-30 million CFSE labeled OT-1 cells or 8 million CFSE labeled OT-1R cells were injected into recipient mice which had been pre-injected with LM-Ova or BCG-Ova. At different time intervals, recipient mice received the CFSE labeled OT-1 or OT-1R cells and four days or seven days post adoptive transfer, spleens, lungs, or livers were removed from the recipient mice and processed as above in section 2.3 and lymphocytes were evaluated for $OVA_{257-264}$-specific $CD8^+$ T cells and their reduction in CFSE intensity. The cells were incubated with anti-CD8α antibody for 5 min. on ice in the dark followed by incubation with H-$2K^bOva_{257-264}$ tetramers (Beckman Coulter, Fullerton, California, USA) at room temperature for 30 min. in the dark. The lymphocytes were washed with PBS at room temperature and fixed with 0.5% formaldehyde and acquired on EPICS XL Flow Cytometer.

2.13 – Quantification of Bacterial Gene Expression in infected spleens

Spleens were harvested from mice and snap frozen in a dry-ice/100 % ethanol bath and stored at -70°C. Total RNA was extracted from spleens using the Qiagen RNeasy mini

Kit (Qiagen, Mississauga, On, Canada) according to the manufactures instructions along with rapid mechanical lysis. The whole spleen was cut into 4 pieces and each piece was lysed in 1ml lysis buffer in a mini-Beadbeater 3110BX (BioSpec Products Inc. Bartlesville, OK, USA) with glass beads (Φ = 0.5mm and Φ = 0.1mm) (BioSpec Products, Bartlesville, OK, USA). Homogenates were extracted using the Qiagen RNeasy mini kit (Qiagen, Mississauga, On, Canada) according to the manufactures instructions and RNA was reconstituted in DEPC RNase free water 50 ul and stored at -70°C. Total RNA was quantified using a Nanodrop ND-1000 (Nanodrop Technologies, Wilmington, DE) and the pieces from one spleen were pooled so that all the RNA from one spleen was in one tube. The total RNA was treated with RNase free DNase I (Roche Applied Science, Penzberg Germany) for 30 min. at 37°C. The DNase was removed using the Qiagen RNeasy mini kit (Qiagen, Mississauga, On, Canada) according to the manufactures instructions. 15 ug of total RNA was taken for cDNA synthesis. cDNA was synthesized using N8 random primers purchased from Sigma. Reverse transcription was performed using the random primers (15 ug) and Superscript II (Invitrogen). RNA was made linear at 65°C for 5 minutes and cDNA was synthesized in a 40 ul reaction volume containing, 3 ul N8 Random Primers (5 ug/ul), 8 ul 5x 1st Strand Buffer, 4 ul DTT (100mM), 5 ul dNTP's (10mM), 1 ul RNase OUT (40 units/ul), 2 ul Superscript II (200 units/ul) and 15 ul of RNA template. Reverse transcription was performed in a Thermo Cycler 9700 (Applied Biosystems, Foster City, CA, USA) at 42°C for 15 min. and 45°C for 2 hours. Identical samples not treated with Thermo Script transcriptase were also prepared as controls to measure DNA carryover. After reverse transcription the RNA template was digested by hydrolysis with NaOH 1M at 65°C for 5 min. followed by neutralization with HCl 1M. cDNA was purified using Microcon YM-30 centrifugal filter unit (Millipore, Cambridge, On, Canada). The number of amplicons was measured by real-time PCR using

gene-specific primers and qPCR SYBR green supermix (ABgene, Surrey, UK). The primers used for the 16S rRNA cDNA were 5`-CTGGGAAACTGGGTCGTAATAC-3` and 5`-CCGTCGTCGCCTTGGTAG-3` and for the Ovalbumin cDNA 5'-CAACCTCACATCTGTCTTAATGG-3` and 5`-GCCTCTGCTGACCCTACC-3`. Primers were designed by inputting the gene sequence into the Beacon Designer 4.0 software and all default conditions were used except the fragment length was changed to 75-150bp which is the optimal size of primer length for the SYBR green method of quantification. To obtain a standard curve for each primer-template set, five different PCRs were performed in parallel by using as template 10-fold dilutions of known amounts of M. *Bovis* Pasteur chromosomal DNA (0.01 attomoles, 0.1 attomoles, 1 attomoles, 10 attomoles, and 100 attomoles), together with triplicate reactions of the uncharacterized samples. PCR conditions were optimized based on the melting curve of each primer and its target. PCR was performed in sealed tubes in a 96-well microtiter plate in an iCycler iQ Thermocycler (Bio-Rad Laboratories Inc., Hercules, CA, USA). The 26 ul reaction consisted of 12.5 ul qPCR SYBR green supermix (ABgene Surrey, UK), 1.2 ul of each primer, 9.1 ul DNase/RNase free doubly distilled H_2O and 1 ul of template. Thermal conditions were as follows: activation at 95°C for 15 min., followed by 40 cycles of denaturation at 95°C for 30 sec., annealing at 60°C for 30 sec., and extension at 72°C for 1min. Fluorescence was measured during the annealing step and plotted against the amplification cycle. Absolute quantitative analysis of the data was extrapolated from the standard curve. Primer efficiencies were between 100 % and 98 %.

3.0 - Results

3.1.0 – Bacterial burden in the spleens of mice infected with LM-Ova and BCG-Ova

The bacterial burden in the spleens of mice infected with LM-Ova or BCG-Ova was assessed by injecting $1x10^4$ LM-Ova or BCG-Ova i.v. via the lateral tail vein. At various time points throughout the course of infection the spleen was harvested and bacterial burden was evaluated by plating serial dilutions of the spleens. Figure 3 shows the bacterial burden in the spleen during LM-Ova and BCG-Ova infections. Two mice per time point were evaluated and the experiment was performed 4 times. So the graphs show the evaluation of 8 mice at each time point per group. During LM-Ova infection, bacterial burden is highest in the spleen around 3 days of infection and by 7 days of infection the burden is cleared. During BCG-Ova infection, bacterial burden rises slowly and peaks in the region of 15-28 days of infection. This is followed by a slight decline in burden but even at 60 days of infection the burden is still in the range of $1\text{-}2x10^3$ CFU. Since the gene for Ova contained in BCG-Ova is located on a plasmid which confers kanamycin resistance the bacterial burden in the spleen was also simultaneously assessed on 7H10 plates containing kanamycin. This was done in order to asses whether the pathogen was disposing of the plasmid bearing the antigen once it was in the mouse and the antibiotic selective pressure was therefore absent. Most of the time points evaluated did not seem to show much inconsistency between CFU on the antibiotic plates and the CFU without antibiotics. Since $CD8^+$ T cells are one of the members of the adaptive immune system responsible for directly destroying infected cells it was decided to evaluate the $CD8^+$ T cell response against BCG-Ova.

Figure 3: Bacterial burden in the spleens of mice infected with LM-Ova and BCG-Ova. C57BL/6J mice were infected with LM-Ova or BCG-Ova $1x10^4$ (i.v.). At various time intervals, spleens were harvested and the number of viable colonies was determined. Brain Heart Infusion plates were used for LM-Ova CFU growth and 7H10 agar plates containing OADC enrichment with and without kanamycin were used for BCG-Ova CFU growth. Each time point involved the evaluation of 2 mice per group and the experiment was performed 4 times.

Figure 3

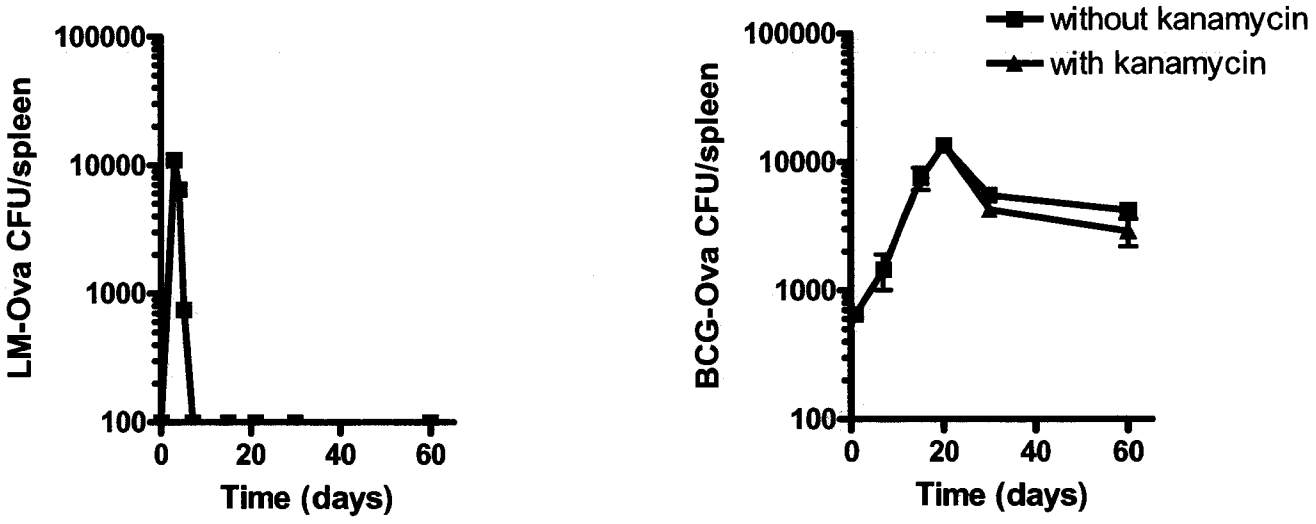
LM-Ova CFU/spleen
100000
10000
1000
100
0
20
40
60
Time (days)
BCG-Ova CFU/spleen
without kanamycin
with kanamycin
100000
10000
1000
100
0
20
40
60
Time (days)

3.2.0 – Characterization of the $CD8^+$ T cell response to LM-Ova and BCG-Ova

The frequency of IFN-γ producing $CD8^+$ T cells and subsequently the percentage of antigen specific $CD8^+$ T cells generated during the infection were evaluated along with the cycling and activation status of these cells.

3.2.1 – Evaluating the frequency of $CD8^+$ T cells against $Ova_{257-264}$ by ELISPOT assay

The frequency of IFN-γ producing $CD8^+$ T cells responding to LM-Ova and BCG-Ova were evaluated by ELISPOT assay as stated in section 2.5. The frequency of IFN-γ producing $CD8^+$ T cells responding to LM-Ova and BCG-Ova is shown in Figure 4 with the number of spots per $100x10^6$ spleen cells shown. Two mice per time point were evaluated. During the LM-Ova infection, the $CD8^+$ T cell frequency peaked around 7 days into the infection and then dropped considerably. However, during the BCG-Ova infection the $CD8^+$ T cell frequency was delayed and peaked around 15-30 days into the infection. Following this peak the frequency declined slowly as the response progressed. Overall, two major differences were noted in the $CD8^+$ T cell response to LM-Ova and BCG-Ova. The first being that there was a massive delay in the expansion of the $CD8^+$ T cells responding to BCG-Ova. The second major difference was that after the peak response during the BCG-Ova infection, the responding $CD8^+$ T cells showed little evidence of contraction. If the $CD8^+$ T cells are present, albeit in low frequencies, then why are they unable to control and eliminate the pathogen. To address this issue we decided to evaluate the phenotype of these $CD8^+$ T cells.

3.2.2 – Tracking Antigen Specific $CD8^+$ T cell response during LM-Ova and BCG-Ova infections.

We next wanted to track the antigen specific $CD8^+$ T cells using flow cytometry so their phenotype could be evaluated. To this end C57BL/6 mice were infected with LM-Ova

Figure 4: Frequency of endogenous Ova-specific $CD8^+$ T cells during LM-Ova and BCG-Ova infection. C57BL/6J mice were infected with LM-Ova or BCG-Ova $1x10^4$ (i.v.). At various time intervals, spleens were harvested and the frequency of IFN-γ-secreting $Ova_{257-264}$-specific $CD8^+$ T cells was enumerated using ELISPOT assay. Number of spots per $100x10^6$spleen cells is shown. Each time point involved the evaluation of 4 mice per group.

Figure 4

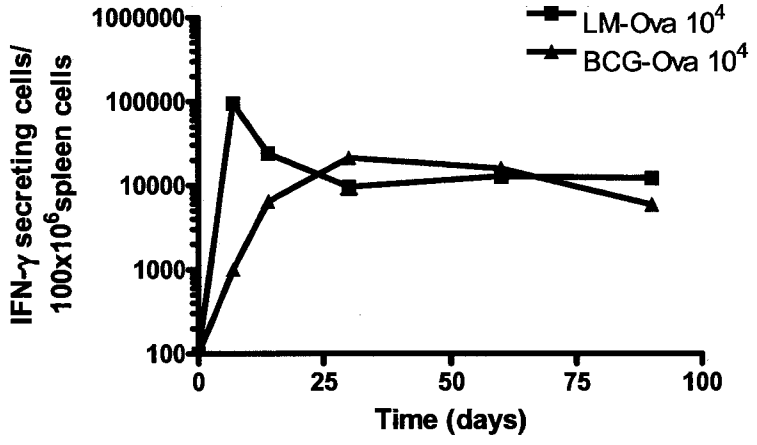
LM-Ova 10^4
BCG-Ova 10^4
IFN-γ secreting cells/ 100x10^6spleen cells
1000000
100000
10000
1000
100
0
25
50
75
100
Time (days)

or BCG-Ova $1x10^4$ i.v. At various time points the spleens from these mice were harvested and processed as in section 2.3. $1x10^7$ cells were obtained and stained with anti-CD8α antibody and H-$2K^b$$Ova_{257-264}$ tetramers as in section 2.8. The antigen specific $CD8^+$ T cell response is shown in Figure 5 and the percentages of $Ova_{257-264}$-specific $CD8^+$ T cells are shown in the graph. Three mice per time point were evaluated. The percentage of $Ova_{257-264}$-specific $CD8^+$ T cells was determined by gating on the lymphocytes in the forward scatter side scatter profile followed by gating on the $CD8^+$ population and further gating on the $Tetramer^+$ population. It was found that during LM-Ova infection the antigen specific $CD8^+$ T cells were detectable only during the peak phase (~day 7 of infection). In the case of BCG-Ova infection the population was undetectable at all the time points examined. Despite the acquisition of 200 000 $CD8^+$ events the frequency was not higher than the uninfected mice.

Thus, an adoptive transfer model was employed which used C57BL/6-Tg (TcraTcrb)1100Mjb mice commonly referred to as OT-1 mice. These mice are genetically modified to have > 90% of the T cell receptors on the $CD8^+$ T cell population specific for the $OVA_{257-264}$ (SIINFEKL) epitope. These cells were adoptively transferred into naïve C57BL/6 mice and those mice were infected with either LM-Ova or BCG-Ova as the experiment dictated Figure 2. This methodology resulted in the ability to detect the responding $CD8^+$ T cells which can be tracked for prolonged periods.

The antigen specific $CD8^+$ T cell response to LM-Ova and BCG-Ova was evaluated by injecting $1x10^6$ OT-1 splenocytes i.v. into naïve C57BL/6 mice and infecting them with either LM-Ova or BCG-Ova $1x10^4$ i.v. At various time points the spleens from these mice were harvested and processed as in section 2.3. The antigen specific $CD8^+$ T cell response is shown in Figure 6 and the percentages of $Ova_{257-264}$-specific $CD8^+$ T cells are shown in the

Figure 5: Using H2K^{b}Ova$_{257-264}$ tetramers to track endogenous Ova-specific CD8$^+$ T cells during LM-Ova and BCG-Ova infection. C57BL/6J mice were infected with LM-Ova or BCG-Ova 1x10^4 (i.v.). At various time intervals, spleens were harvested from the recipient mice and the number of OVA$_{257-264}$-specific CD8$^+$ T cells was evaluated after staining with H-2K^{b}OVA$_{257-264}$ tetramers and anti-CD8α antibody. Each time point involved the evaluation of 3 mice per group per time point. The graph shows the percentages of OVA $_{257-264}$-specific CD8$^+$ T cells at the given time points.

Figure 5

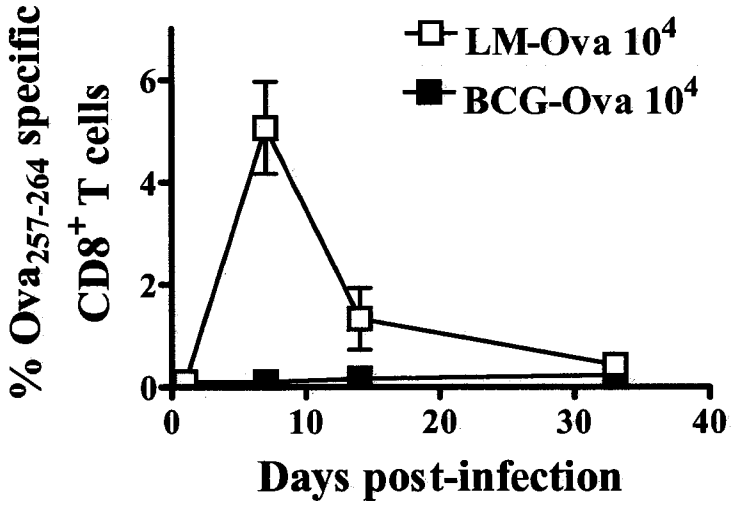
% Ova257-264 specific CD8+ T cells
LM-Ova 10^4
BCG-Ova 10^4
0
2
4
6
0
10
20
30
40
Days post-infection

Figure 6: Antigen-specific $CD8^+$ T cell response during LM-Ova and BCG-Ova infections. C57BL/6J recipient mice were injected with $1x10^6$ OT-1 donor cells and subsequently infected with LM-Ova or BCG-Ova $1x10^4$ (i.v.). At various time intervals, spleens were harvested from the recipient mice and the number of OVA $_{257-264}$-specific $CD8^+$ T cells were evaluated after staining with H-$2K^b$$OVA_{257-264}$ tetramers and anti-CD8α antibody. Each time point involved the evaluation of 2 mice per group. Numbers in the panel indicate the percentage of OVA-specific $CD8^+$ T cells at day 7 and day 21 (A). The change in the relative percentages of Ova-specific $CD8^+$ T cells was evaluated kinetically (B).

Figure 6

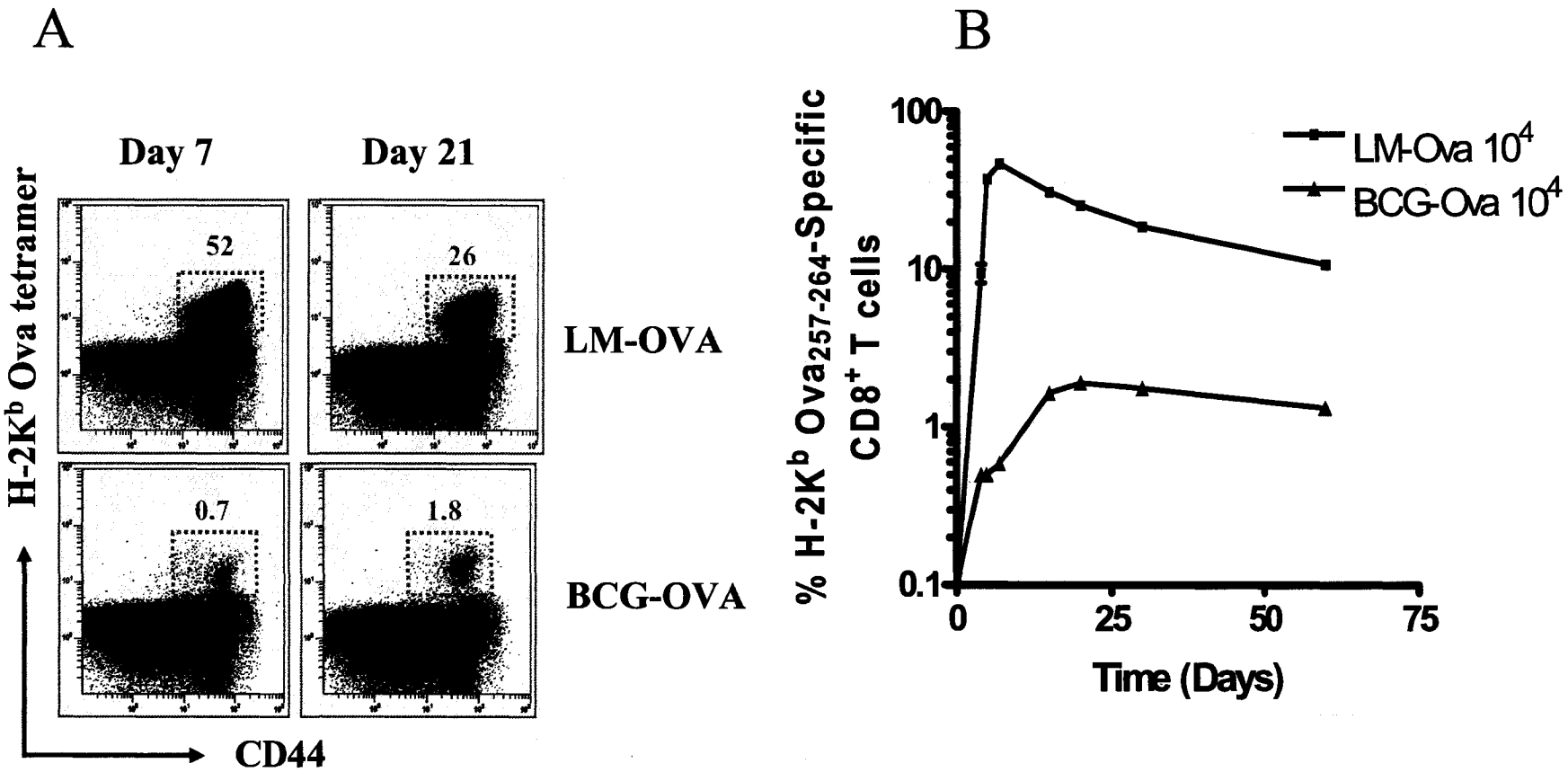
A
Day 7
Day 21
H-2K^b Ova tetramer
52
26
0.7
1.8
LM-OVA
BCG-OVA
CD44
B
% H-2K^b Ova$_{257-264}$-Specific CD8$^+$ T cells
100
10
1
0.1
0
25
50
75
Time (Days)
LM-Ova 10^4
BCG-Ova 10^4

graph. Two mice per time point were evaluated and the experiment was performed 4 times. The graph shows the evaluation of 8 mice at each time point. The percentages of $Ova_{257-264}$-specific $CD8^+$ T cells was determined by gating on the lymphocytes in the forward scatter side scatter profile followed by gating on the $CD8^+$ population and further gating on the $Tetramer^+$ population. In the case of LM-Ova infection the antigen specific $CD8^+$ T cell response peaks around 7 days of infection and is followed by rapid attrition of these $CD8^+$ T cells to about 10%. In the case of BCG-Ova infection the antigen specific $CD8^+$ T cell response is delayed and peaks between days 14-21 and this is followed by little attrition of these $CD8^+$ T cells.

3.2.2.1 – Has the $CD8^+$ T cell population responding to BCG-Ova arisen as a result of clonal burst or a gradual accumulation of cells over time?

The question as to whether the peak response in BCG-Ova infection is due to a gradual accumulation of cells over time, or to a rapid proliferation at a given time during the infection was sought. Naïve C57BL/6 mice were injected with BCG-Ova $1x10^4$ i.v. and at various time points throughout the infection $1x10^6$ OT-1 cells were injected i.v. and the spleen was harvested at a given time point post adoptive transfer as dictated by the time interval evaluated. The spleens were processed as in section 2.3. The graph of the results are shown in Figure 7 and the time intervals shown in Figure 7 are the time intervals during the infection in which the OT-1 cells were introduced into the system and the spleen was harvested. Three mice per time interval were evaluated. The percentage of Ova-specific $CD8^+$ T cells was determined by gating on the lymphocytes in the forward scatter side scatter profile followed by gating on the $CD8^+$ population and further gating on the $Tetramer^+$ population. It was observed that there was not much proliferation occurring in the first 7 days of infection. The majority of expansion of Ova-specific $CD8^+$ T cells appeared to have

Figure 7: Relative expansion of Ova-specific $CD8^+$ T cells during the different phases of BCG-Ova infection. Naïve C57BL/6 mice were injected with BCG-Ova $1x10^4$ i.v. at various time points. $1x10^6$ OT-1 cells were injected i.v. at various time points during the BCG-Ova infection and the spleens harvested a certain number of days later. So the time intervals shown in the graph are the time interval during the infection in which the OT-1 cells were introduced into the system and the spleen was harvested. Each time interval involved 3 mice per group. The graph shows the net percent of $Ova_{257-264}$-specific $CD8^+$ T cells that were generated during the given time interval.

Figure 7

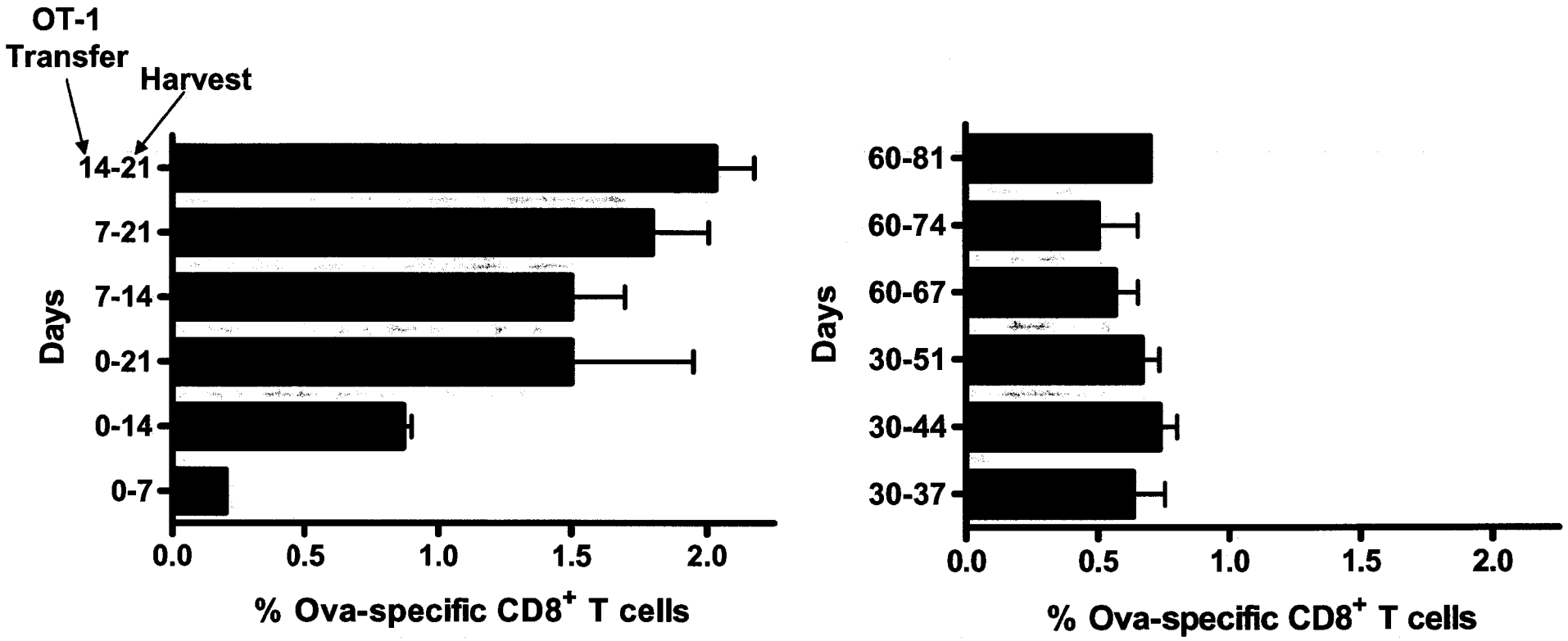
OT-1
Transfer
Harvest
14-21
7-21
7-14
0-21
0-14
0-7
Days
0.0
0.5
1.0
1.5
2.0
% Ova-specific CD8+ T cells
60-81
60-74
60-67
30-51
30-44
30-37
Days
0.0
0.5
1.0
1.5
2.0
% Ova-specific CD8+ T cells

occurred between 7-14 days of infection but continues into the range of 14-21 days of infection. When later time points were examined in the infection there was a low level of expansion indicating that antigen presentation is occurring at this time. Based on these findings the question arose as to the cell cycling status of the antigen specific $CD8^+$ T cells during BCG-Ova infection.

3.2.3 – Cycling status of antigen specific $CD8^+$ T cells during LM-Ova and BCG-Ova infections.

To assess the cycling status of antigen specific $CD8^+$ T cells during LM-Ova and BCG-Ova infections, $1x10^6$ OT-1 splenocytes were injected i.v. into naïve C57BL/6 mice and these mice were infected with either LM-Ova or BCG-Ova i.v. At various time points the spleens from these mice were harvested but prior to harvesting, the mice were given BrdU in their drinking water as in section 2.7. The spleens were processed as in section 2.3 and $1x10^7$ cells were obtained and stained with anti-CD8 antibody and H-$2K^b Ova_{257-264}$ tetramers followed by permeabilization and staining with anti-BrdU as in section 2.7. The cells were fixed and acquired on an EPICS XL Flow cytometer and data was analyzed using the EXPO software. Figure 8 shows the cycling status of antigen specific $CD8^+$ T cells during LM-Ova and BCG-Ova infections. Two mice per time point were evaluated. The percentage of Ova-specific $CD8^+$ T cells was determined by gating on the lymphocytes in the forward scatter side scatter profile followed by gating on the $CD8^+$ population and further gating on the $Tetramer^+$ population. Of these Ova-specific $CD8^+$ T cells, the percentage of those cells that were $BrdU^{hi}$ as based on the $Tetramer^-$ population of $CD8^+$ T cells are shown in the graph in Figure 8. It was observed that in the case of LM-Ova infections the majority of the Ova-specific $CD8^+$ T cells (approximately 90%) was cycling on day 7 of infection and

Figure 8: Cycling of antigen specific $CD8^+$ T cells during LM-Ova and BCG-Ova infections. C57BL/6J recipient mice were injected with $1x10^6$ OT-1 donor cells and subsequently infected with LM-Ova or BCG-Ova $1x10^4$ (i.v.). 3 days prior to harvest the mice were given BrdU in their drinking water (0.8mg/ml). At various time intervals, spleens were harvested from the recipient mice and the number of OVA $_{257-264}$-specific $CD8^+$ T cells were evaluated after staining with H-$2K^b$$OVA_{257-264}$ tetramers and anti-CD8α antibody. The cells were permeabilized and stained with anti-BrdU. Each time point involved the evaluation of 2 mice per group. Numbers in the panel indicate the percentage of $BrdU^+$ cells among the OVA-specific $CD8^+$ T cells at day 7 and day 21 (A). The change in the relative percentages of $BrdU^+$ Ova-specific $CD8^+$ T cells was evaluated kinetically (B).

Figure 8

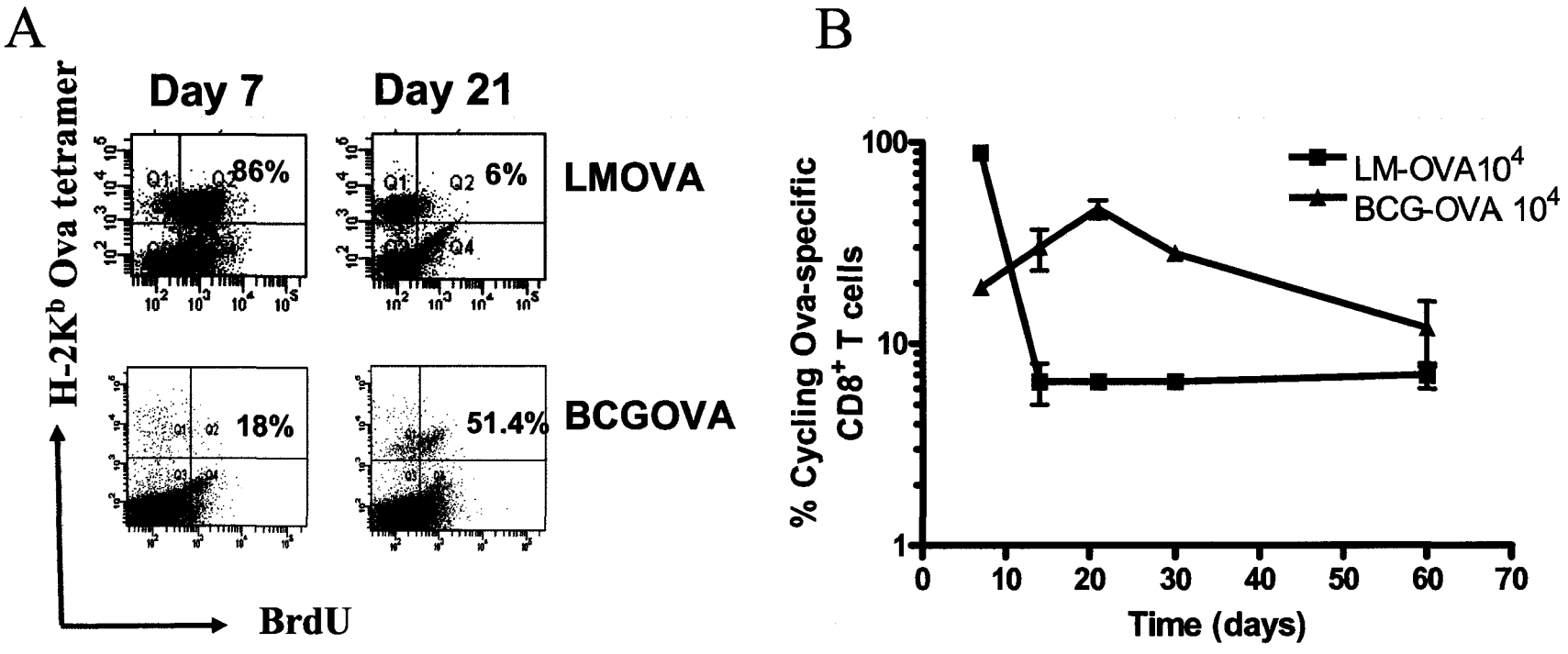
A
Day 7
Day 21
LMOVA
BCGOVA
86%
6%
18%
51.4%
Q1
Q2
Q3
Q4
H-2K^b Ova tetramer
BrdU
B
% Cycling Ova-specific CD8$^+$ T cells
Time (days)
LM-OVA10^4
BCG-OVA 10^4
100
10
1
0
10
20
30
40
50
60
70

by day 14 cycling had returned to homeostatic levels. In the case of BCG-Ova infection the cycling of Ova-specific $CD8^+$ T cells were highest around day 15 of infection and cycling of these cells declined to near homeostatic levels. Since there seemed to be a delay in the cycling status of the antigen specific $CD8^+$ T cells generated against BCG-Ova it was decided that certain key cell surface activation markers should be examined. The $CD8^+$ T cells may be faulty with respect to the up-regulation or down-regulation of key activation markers which would have implications on their phenotypic response.

In summary, BCG-Ova induced a delayed and muted $CD8^+$ T cell response with delayed cycling. As the $CD8^+$ T cell response to BCG-Ova progresses the population does not increase despite the pathogen burden present, instead it plateaus, and cycling of these $CD8^+$ T cells became curtailed. However, naïve OT-1 cells did respond by proliferating when introduced into mice at later stages of the BCG-Ova infection. This indicated that there may still be antigen presentation occurring at this time but for some reason it was occurring at lower levels. To this end the differentiation and activation status of these $CD8^+$ T cells was evaluated in order to evaluate the phenotype of the $CD8^+$ T cells responding to BCG-Ova.

3.3.0 – Evaluating the activation and differentiation status of the $CD8^+$ T cells generated during BCG-Ova infection

There was a delay in the $CD8^+$ T cell response to BCG-Ova and the overall percentage of Ova-specific $CD8^+$ T cells generated was quite low as compared to that generated during LM-Ova infections. It was thought that this delay may be due to reduced stimulation that may be occurring in this infection model. To this end some key activation markers along with the differentiation profile of the antigen specific $CD8^+$ T cells generated against BCG-Ova were examined in order to assess the activation status of the $CD8^+$ T cells generated during BCG-Ova infection.

3.3.1 – Evaluation of activation markers on antigen specific $CD8^+$ T cells during LM-Ova and BCG-Ova infections

C57BL/6 mice were injected with $1x10^6$ OT-1 splenocytes i.v. and infected with either $1x10^4$ LM-Ova or BCG-Ova i.v. At various time points the spleens from these mice were harvested and processed as in section 2.3. $1x10^7$ cells were obtained and stained with anti-CD8, anti-CD127, anti-CD25, and anti-CD69 antibodies, followed by staining with H-$2K^bOva_{257-264}$ tetramers as in section 2.8. The activation markers on antigen specific $CD8^+$ T cells responding to LM-Ova and BCG-Ova are shown in Figure 9. In the case of each marker, two mice per group per time point were evaluated and the experiment was performed twice. So the graphs show the evaluation of 4 mice per group at each time point. The percentages of $Ova_{257-264}$-specific $CD8^+$ T cells that are high for the given cell surface marker are shown in the graph. This was determined by gating on the lymphocytes in the forward scatter/side scatter profile followed by gating on the $CD8^+$ population and further gating on the $Tetramer^+$ population. Figure 9 shows the percentage Ova-specific $CD8^+$ T cells that were $CD69^{hi}$ (Figure9a), $CD25^{hi}$ (Figure9b), or $CD127^{hi}$ (Figure9c) as based on the Tetramer-positive population of $CD8^+$ T cells. During the LM-Ova infection, cell surface expression of CD69 and CD25 are high early in infection and after 7 days of infection they are both undetectable on the cell surface of the antigen specific $CD8^+$ T cells. During BCG-Ova infection the cell surface expression of both CD69 and CD25 were undetectable on the cell surface throughout the infection indicating weaker stimulation. The cell surface expression of CD127 was down-regulated early in LM-Ova infection, and as the pathogen was cleared and the $CD8^+$ T cell response was allowed to progress, the numbers of CD127-expressing cells increased. In the case of BCG-Ova infection however, the cell surface expression of CD127 was delayed in it's down-regulation from the cell surface of antigen

Figure 9: CD69, CD25, and CD127 cell surface expression on antigen specific $CD8^+$ T cells during LM-Ova and BCG-Ova infections. C57BL/6J recipient mice were injected with $1x10^6$ OT-1 donor cells and subsequently infected with LM-Ova or BCG-Ova $1x10^4$ (i.v.). At various time intervals, spleens were harvested from the recipient mice and the number of $OVA_{257-264}$-specific $CD8^+$ T cells were evaluated after staining with anti-CD8α antibody and H-$2K^bOVA_{257-264}$ tetramers, and anti-CD69 (A) anti-CD25 (B) and anti-CD127 (C) antibodies. Each time point involved the evaluation of 4 mice per group. The graphs show the average percentage of the cell surface expression of the given marker on the $OVA_{257-264}$-specific $CD8^+$ T cells of the 4 mice at each given time point.

Figure 9

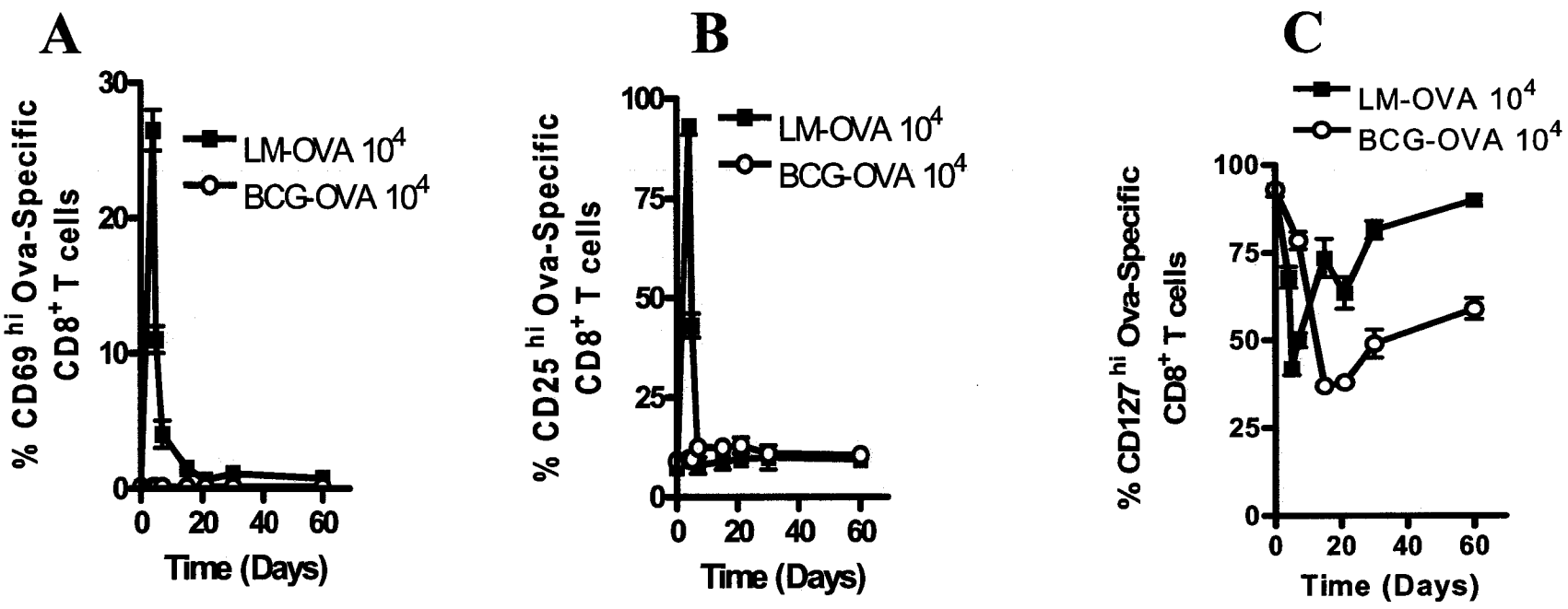
A
% CD69 hi Ova-Specific CD8+ T cells
LM-OVA 10^4
BCG-OVA 10^4
Time (Days)
B
% CD25 hi Ova-Specific CD8+ T cells
LM-OVA 10^4
BCG-OVA 10^4
Time (Days)
C
% CD127 hi Ova-Specific CD8+ T cells
LM-OVA 10^4
BCG-OVA 10^4
Time (Days)

specific $CD8^+$ T cells. Also, throughout the BCG-Ova infection, the numbers of CD127-expressing cells did not increase to levels seen with LM-Ova.

3.3.2 – Evaluation of the differentiation profile of $CD8^+$ T cells during LM-Ova and BCG-Ova infections

$CD8^+$ T cells have been shown to differentiate into three distinct phenotypes: Effector cells ($CD62L^{low}CD44^{hi}CD127^{low}$), effector memory cells ($CD62L^{low}CD44^{hi}CD127^{hi}$) and central memory cells ($CD62L^{hi}CD44^{hi}CD127^{hi}$) [59]. Using these markers the differentiation profile of Ova-specific $CD8^+$ T cells induced during LM-Ova and BCG-Ova infections was discerned kinetically. Two mice per group per time point were evaluated and the experiment was performed twice. The graphs show the evaluation of 4 mice per group at each time point. The percentages of $Ova_{257-264}$-specific $CD8^+$ T cells that are $CD44^{hi}CD62L^{hi}$, or $CD44^{hi}CD62L^{low}$ for the given cell surface marker are shown in the graph in Figure 10. This was determined by gating on the lymphocytes in the forward scatter side scatter profile followed by gating on the $CD8^+$ population and further gating on the $Tetramer^+$ population. In the case of LM-Ova infection the majority of the primed $CD8^+$ T cells display an effector ($CD44^{hi}CD62L^{low}$) phenotype. As the pathogen is cleared from the system and the $CD8^+$ T cells differentiation progresses, the dominant phenotype of the antigen specific $CD8^+$ T cells is that of a central ($CD44^{hi}CD62L^{hi}$) phenotype. From Figure 9 it is already clear that majority of the Ova-specific $CD8^+$ T cells induced against LM-Ova express high levels of CD127 at these late time points. On the other hand, $CD8^+$ T cells responding to BCG-Ova infection differentiated early on into a central phenotype ($CD44^{hi}CD62L^{hi}$) and the majority of the cells did not differentiate into either effector or effector memory state (Figure 10).

In summary during BCG-Ova infection, both CD69 and CD25 were not up-regulated on the responding $CD8^+$ T cells. As well, there was a delay in the down-regulation of

Figure 10: Contrasting differentiation of antigen specific $CD8^+$ T cells during LM-Ova and BCG-Ova infections. C57BL/6J recipient mice were injected with $1x10^6$ OT-1 donor cells and subsequently infected with LM-Ova or BCG-Ova $1x10^4$ (i.v.). At various time intervals, spleens were harvested from the recipient mice and the number of OVA $_{257-264}$-specific $CD8^+$ T cells were evaluated after staining with H-$2K^b$$OVA_{257-264}$ tetramers and anti-CD8α, anti-CD44, and anti-CD62L antibodies. Each time point involved the evaluation of 4 mice per group per time point. FACS data from a representative mouse at the day 7 time point is shown and the line graphs show the average percentages of central and effector phenotype $OVA_{257-264}$-specific $CD8^+$ T cells.

Figure 10

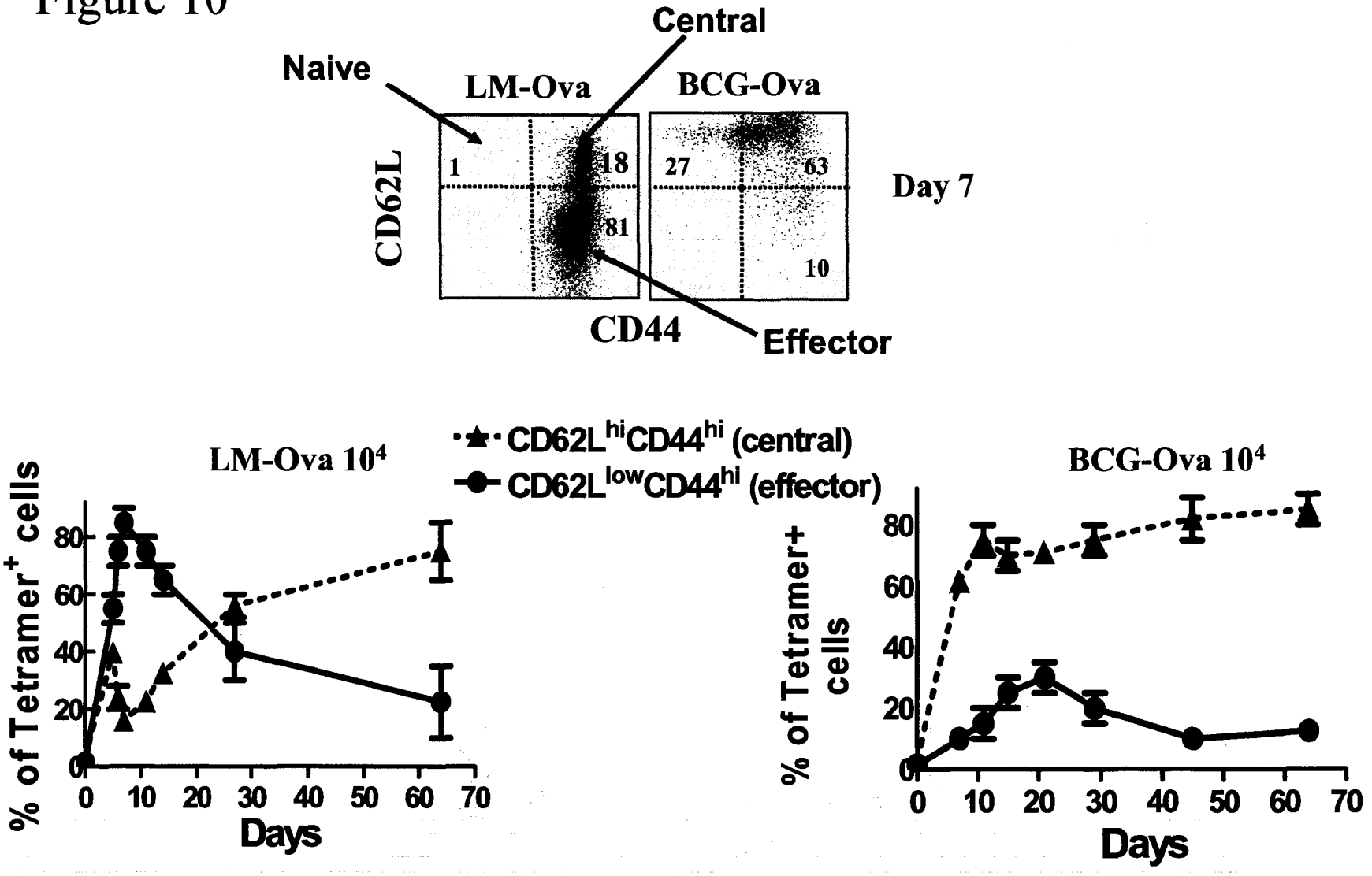
Naive
Central
LM-Ova
BCG-Ova
CD62L
CD44
1
18
81
27
63
10
Day 7
Effector
CD62L^hiCD44^hi (central)
CD62L^lowCD44^hi (effector)
LM-Ova 10^4
BCG-Ova 10^4
% of Tetramer+ cells
Days
0
10
20
30
40
50
60
70
80

CD127. The $CD8^+$ T cells responding to BCG-Ova also differentiated into a predominantly central phenotype. This indicated that the stimulation conditions are quite weak in the BCG model. The CD127 cell surface expression doesn't return to naïve levels like what is seen in an LM-Ova infection. This may be due to the presence of peptide or increased inflammation that may be persisting during the chronic BCG infection.

3.4.0 – Maintenance of antigen specific $CD8^+$ T cells during BCG-Ova infection

The numbers of CD127-expressing $CD8^+$ T cells do not increase during the later stages of BCG-Ova infection. It is possible that this could be due to the persistent inflammation induced by the chronic infection, or due to the chronic presence of low-levels of Ova. Based on these findings the maintenance of the $CD8^+$ T cells responding to BCG-Ova was evaluated. Specifically examined was whether inflammation or antigen was dictating the lack of up-regulation of CD127 at later time periods.

3.4.1 – Evaluation of the effects of inflammation on CD127 expression in $CD8^+$ T cells

To evaluate the effects of inflammation on the cell surface expression of CD127 on antigen specific $CD8^+$ T cells responding to BCG-Ova, an Ova specific memory $CD8^+$ T cell population was generated that was $CD127^{hi}$ and inflammation was induced in order to observe any down-regulation of CD127. Since one may argue that BCG may not induce enough inflammation, virulent *Salmonella typhimurium* (ST) was also used to address this question since it seems to induce more inflammation than BCG [10]. To do this, naïve B6.129F1 mice were injected with $1x10^6$ OT-1 splenocytes i.v Figure11. B6.129F1 mice are generated via mating a 129XsvJ female with a C57BL/6 male. The C57BL/6 strain of mice is highly susceptible to infection with ST and dies within 5-8 days of infection but does not

Figure 11: Experimental layout to assess the effects of inflammation on CD127 cell surface expression on $CD8^+$ T cells responding to BCG-Ova. $1x10^6$ OT-1 splenocytes were injected into naïve B6.129F1 mice. On day 1 and day 21 archeosomes containing entrapped $Ova_{257-264}$ peptide were injected s.c. 30days later on day 51 these mice were challenged with ST $1x10^3$ or BCG $1x10^4$ (i.v.) to induce inflammation. 30 days later on day 81 the spleens from these mice were harvested and stained with anti-mouse CD8α antibody, anti-CD127 antibody and H-$2K^b$ $Ova_{257-264}$ tetramers and analyzed by flow cytometry.

Figure 11

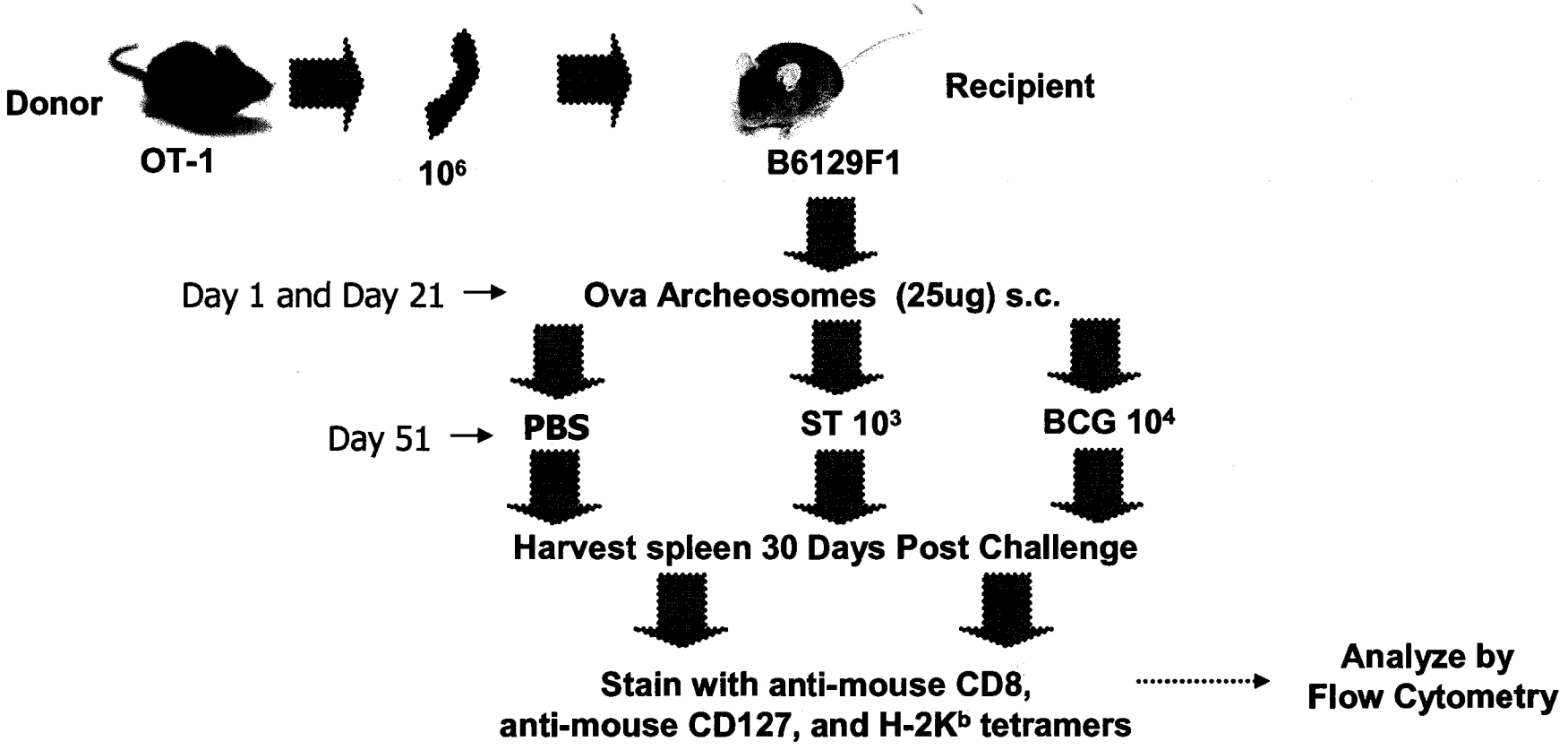
Donor
OT-1
10⁶
Recipient
B6129F1
Day 1 and Day 21
Ova Archeosomes (25ug) s.c.
Day 51
PBS
ST 10³
BCG 10⁴
Harvest spleen 30 Days Post Challenge
Stain with anti-mouse CD8,
anti-mouse CD127, and H-2Kᵇ tetramers
Analyze by
Flow Cytometry

reject the OT-1 cells. The 129XsvJ mice are resistant to ST but reject the OT-1 cells due to MHC incompatibility. So the F1 hybrid of these mice, B6.129F1, were used because they maintain the adoptively transferred OT-1 cells and are still resistant to infection with ST [10]. These B6.129F1 mice were injected on day 1 and boosted on day 21 with 25ug *M. Smithii*-Ova-archeosomes s.c. [97-100] to generate an antigen specific population of memory $CD8^+$ T cells that are $CD127^{hi}$. These mice were infected 30 days later on day 51 with $1x10^3$ ST or $1x10^4$ BCG i.v. to induce inflammation. Spleens were harvested 30 days post infection on day 81 and processed as in section 2.3. The percentages of $Ova_{257-264}$-specific $CD8^+$ T cells that are $CD127^{low}$ are shown in the graph (Figure 12 A). This was determined by gating on the lymphocytes in the forward scatter side scatter profile followed by gating on the $CD8^+$ population and further gating on the $Tetramer^+$ population. Despite the inflammation induced by ST or BCG as seen in Figure 12 B, no differences were observed in the cell surface expression of CD127 on antigen specific $CD8^+$ T cells between the control group and the groups in which inflammation was induced by BCG or ST. The mean fluorescence intensity remained similar in all the three groups of mice (data not shown).

3.4.2 – Evaluation of the effects of the presence of antigen on the cell surface expression of CD127 on antigen specific $CD8^+$ T cells responding to BCG-Ova

To evaluate the effects of the presence of antigen on the cell surface expression of CD127 on antigen specific $CD8^+$ T cells responding to BCG-Ova $1x10^6$, OT-1 splenocytes were injected i.v. into naïve C57BL/6 mice and these mice were infected with $1x10^4$ BCG-Ova i.v Figure 13. After 90 days of infection half these mice were treated with an antibiotic cocktail of 0.1mg/mL isoniazid and 0.15mg/mL rifampicin in their drinking water to eliminate the pathogen. Mice were kept continuously on antibiotics. On day 90 the bacterial

Figure 12: The effects of inflammation on CD127 cell surface expression. $1x10^6$ OT-1 splenocytes were injected into naïve B6.129F1 mice. On day 1 and day 21 archeosomes containing entraped $Ova_{257-264}$ peptide were injected s.c. 30 days later on day 51 these mice were challenged with ST $1x10^3$ or BCG $1x10^4$ (i.v.) to induce inflammation. 30 days later on day 81 the spleens from these mice were harvested and stained with anti-mouse CD8α and anti-mouse CD127 antibodies and H-$2K^b Ova_{257-264}$ tetramers and analyzed by flow cytometry. Two mice per group were evaluated and the bar graph shows the percentage of $Ova_{257-264}$-specific $CD8^+$ T cells that were $CD127^{low}$ (A). The presence of massive splenomegaly indicating inflammation is shown in the bar graph of the average spleen cell numbers of the 2 mice in each group (B).

Figure 12

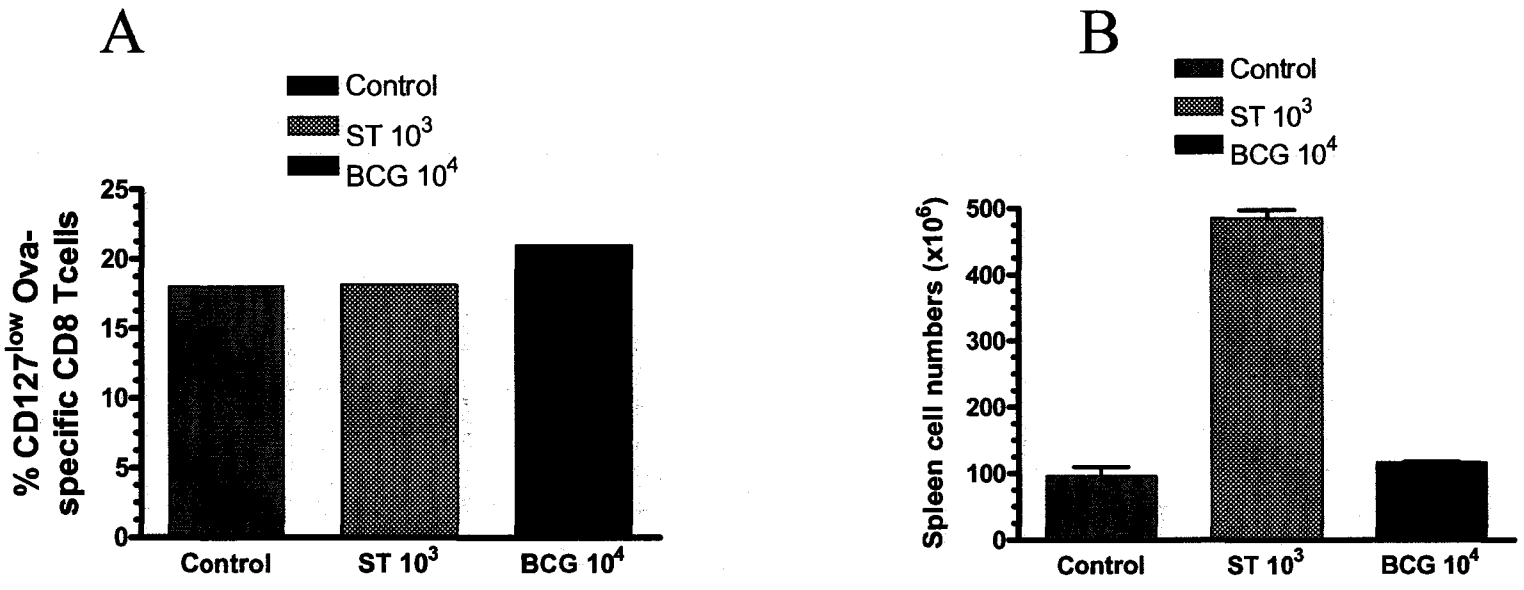
A
Control
ST 10^3
BCG 10^4
% CD127^low Ova-specific CD8 Tcells
25
20
15
10
5
0
Control
ST 10^3
BCG 10^4
B
Control
ST 10^3
BCG 10^4
Spleen cell numbers (x10^6)
500
400
300
200
100
0
Control
ST 10^3
BCG 10^4

Figure 13: Experimental layout to assess the effects of antigen persistence on CD127 cell surface expression on $CD8^+$ T cells responding to BCG-Ova. $1x10^6$ OT-1 splenocytes were injected into naïve C57BL/6 mice. These mice were injected with BCG-Ova 10^4 (i.v.). After 90 days of infection half the mice were given an isoniazid/rifampicin antibiotic cocktail containing 0.1mg/ml isoniazid and 0.15mg/ml rifampicin in their drinking water to eliminate the pathogen. The blood from these mice was harvested at a variety of time points and stained with anti-mouse CD8α, anti-mouse CD62L, and anti-mouse CD127 antibodies and H-$2K^b$$Ova_{257-264}$ tetramers and analyzed by flow cytometry. On day 157 the bacterial burden in the spleen was assessed by performing serial dilutions and plating on 7H10+OADC agar plates.

Figure 13

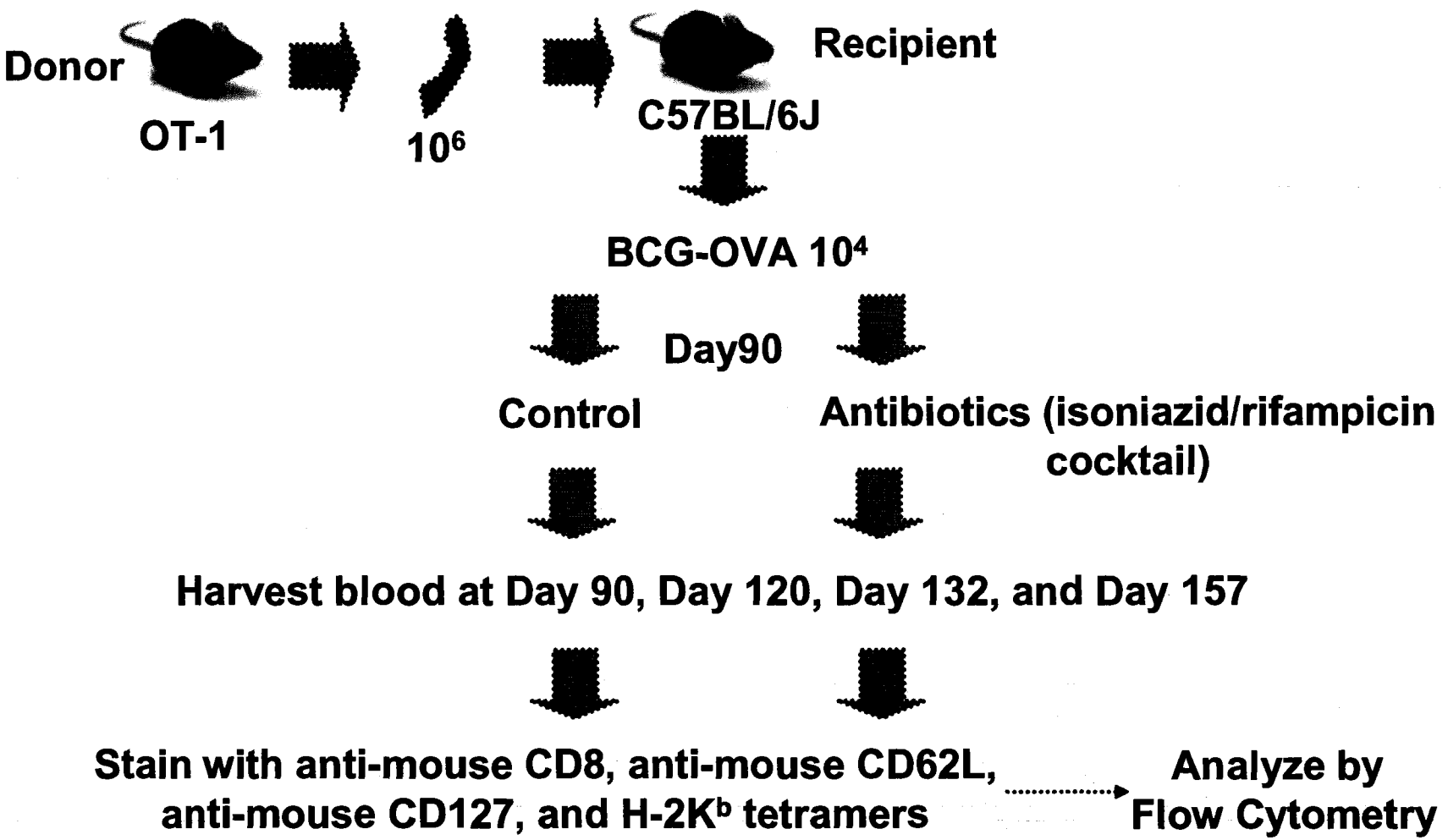
Donor
OT-1
10^6
Recipient
C57BL/6J
BCG-OVA 10^4
Day90
Control
Antibiotics (isoniazid/rifampicin cocktail)
Harvest blood at Day 90, Day 120, Day 132, and Day 157
Stain with anti-mouse CD8, anti-mouse CD62L, anti-mouse CD127, and H-2K^b tetramers
Analyze by Flow Cytometry

burden was assessed in the spleen prior to antibiotic treatment by performing serial dilutions in PBS-T80 and plating on 7H10+OADC agar plates as in section 2.4. This was done in order to confirm the burden was similar among the mice prior to antibiotic treatment. The bacterial burden in the spleens of the mice after the antibiotic treatment on day 157 (60 days of continuous antibiotic therapy) was also assessed to confirm the pathogen had been eliminated from the spleen. Data in Figure 14 A confirms that the pathogen was eliminated from the spleen of the antibiotic treated mice. The blood from these mice was harvested at various time points and processed as in section 2.8. 100 ul of peripheral blood was obtained and stained with anti-CD8 and anti-CD127 antibodies, followed by staining with H-$2K^bOva_{257-264}$ tetramers as in section 2.8. Firstly, for the first thirty days of antibiotic therapy, no change was noted in the relative percentage of Ova-specific $CD8^+$ T cells in the control versus antibiotic treated mice (Figure 14 B). However, continued antibiotic therapy resulted in a reduction in Ova-specific $CD8^+$ T cells indicating that antigenic persistence seems to be necessary for maintenance of Ova-specific $CD8^+$ T cells during the chronic BCG-Ova infection. Removal of BCG-Ova with antibiotics also resulted in an increase in the numbers of cells expressing CD127 (Figure 14C) indicating that antigenic persistence restricts the development of antigen-specific $CD8^+$ T cells that are $CD127^{hi}$.

In summary, CD127 expression seems to be influenced by the direct presence of peptide rather than the presence of inflammation. Thus, the lack of CD127 up-regulation is likely due to the presence of antigen still in the system during BCG-Ova infections. Evidence to support this is also seen when naïve OT-1 cells responded by proliferating when introduced into mice at later stages of the BCG-Ova infection (Figure 7) indicating that any antigen presentation that may be occurring is also preventing the up-regulation of CD127.

Figure 14: The effects of antigen persistence on CD127 cell surface expression. $1x10^6$ OT-1 splenocytes were injected into naïve C57BL/6 mice. These mice were injected with BCG-Ova 10^4 (i.v.). After 90 days of infection half the mice were given an isoniazid/rifampicin antibiotic cocktail containing 0.1mg/ml isoniazid and 0.15mg/ml rifampicin in their drinking water to eliminate the pathogen. The blood from these mice was harvested at a variety of time points and stained with anti-mouse CD8α and anti-mouse CD127 antibodies and H-$2K^bOva_{257-264}$ tetramers and analyzed by flow cytometry. On day 90 and day 157 the bacterial burden in the spleen was assessed by performing serial dilutions and plating on 7H10+OADC agar plates (A). Dotted line indicates the threshold of detection. When the antigen (pathogen) is removed from the system by antibiotic treatment (A), the overall percentage of antigen specific $CD8^+$ T cells declines gradually (B), and the CD127 expression on the cell surface of the antigen specific $CD8^+$ T cells increases compared to that of the control group (C).

Figure 14

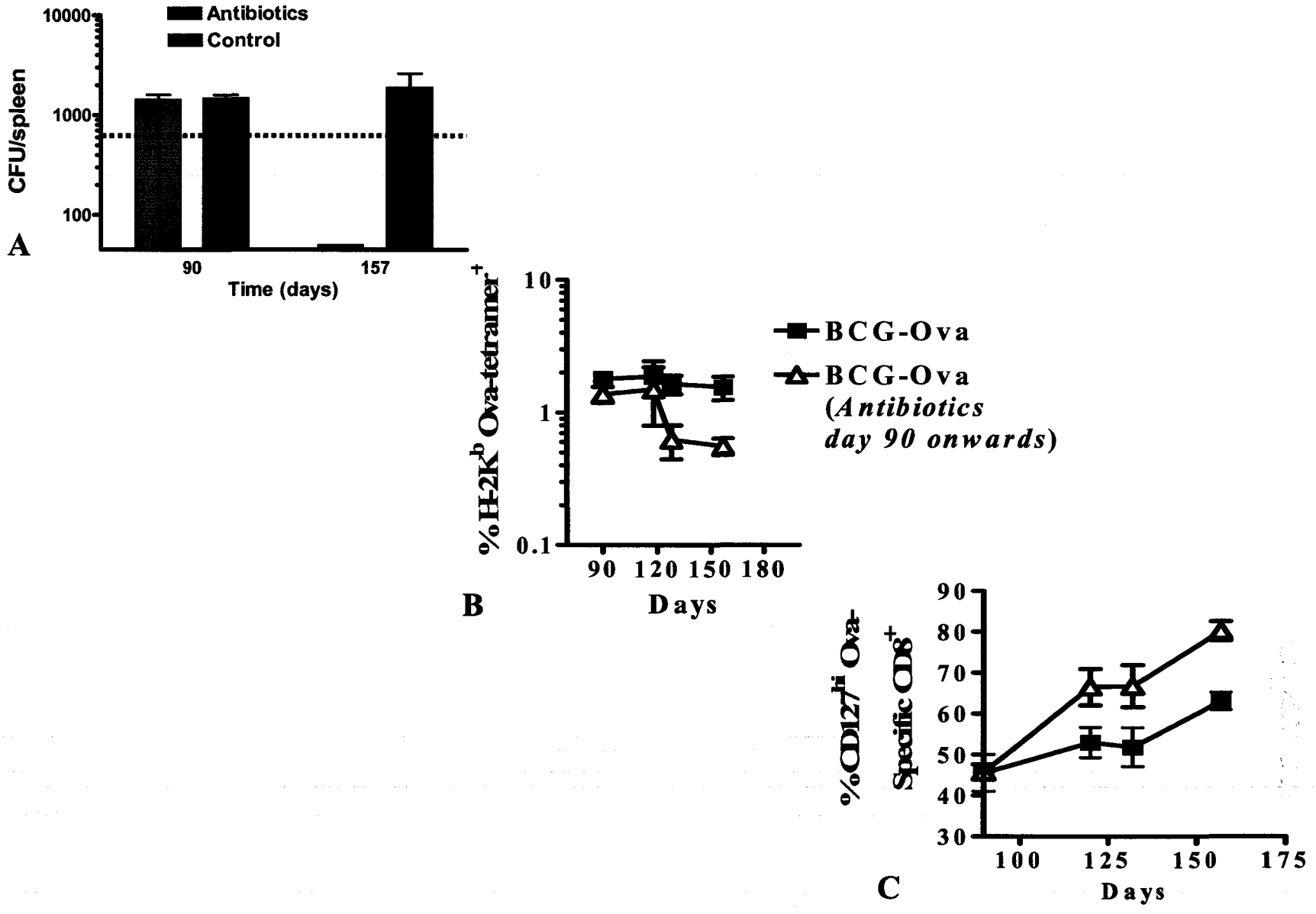
Antibiotics
Control
10000
1000
100
CFU/spleen
90
157
Time (days)
A
10
1
0.1
%H-2K^b Ova-tetramer+
90 120 150 180
Days
B
BCG-Ova
BCG-Ova
(Antibiotics
day 90 onwards)
90
80
70
60
50
40
30
%CD127^hi Ova-Specific CD8+
100 125 150 175
Days
C

3.5.0 – Evaluation of the functionality of the $CD8^+$ T cells responding to a BCG-Ova infection

Considering that reduced stimulation of $CD8^+$ T cells was observed (reduced CD69, CD25 up-regulation and decreased down-regulation of CD62L) in BCG-Ova infected mice, it was hypothesized that $CD8^+$ T cells generated against BCG may be functionally incompetent. This is because in some chronic viral infections the $CD8^+$ T cells have been shown to become exhausted or lose some of their effector functions [104;105]. To this end the functionality of the $CD8^+$ T cells responding to BCG-Ova was evaluated with respect to their ability to produce IFN-γ, exhibit lytic activity, and to respond rapidly in response to antigenic stimulation in vivo.

3.5.1 – Evaluation of IFN-γ production by $CD8^+$ T cells responding to LM-Ova or BCG-Ova infections

To assess the IFN-γ production by antigen specific $CD8^+$ T cells during LM-Ova and BCG-Ova infection, $1x10^6$ OT-1 splenocytes were injected i.v. into naïve C57BL/6 mice and these mice were infected with either LM-Ova or BCG-Ova $1x10^4$ i.v (Figure 15). At various time points the spleens from these mice were harvested. The spleens were processed as in section 2.3 and $1x10^7$ cells were obtained and stained with anti-CD8 antibody and H-$2K^bOva_{257-264}$ tetramers followed by permeabilization and staining with anti-IFN-γ as in section 2.9. Figure 16 shows the percentage of IFN-γ producing antigen specific $CD8^+$ T cells responding to LM-Ova and BCG-Ova infections. The percentage of Ova-specific $CD8^+$ T cells was determined by gating on the lymphocytes in the forward scatter/side scatter profile followed by gating on the $CD8^+$ population and further gating on the $Tetramer^+$ population. Of these Ova-specific $CD8^+$ T cells, the percentage of those cells that were IFN-γ^+ as based on the $Tetramer^+$ population of $CD8^+$ T cells are shown in the graph in Figure 16.

Figure 15: Experimental layout to evaluate the ability of $CD8^+$ T cells responding to BCG-Ova to produce IFN-γ. $1x10^6$ OT-1 splenocytes were injected into naïve C57BL/6 mice. These mice were injected with LM-Ova 10^4 or BCG-Ova 10^4 (i.v.). The spleens from these mice were harvested at a variety of time points and stained with anti-mouse CD8α antibody and H-$2K^b$$Ova_{257-264}$ tetramers and then stimulated with the Ova peptide for 1 hour. The cells were then permeabilized and stained intracellularly with anti-mouse IFN-γ antibody. The cells were fixed and analyzed by flow cytometry.

Figure 15

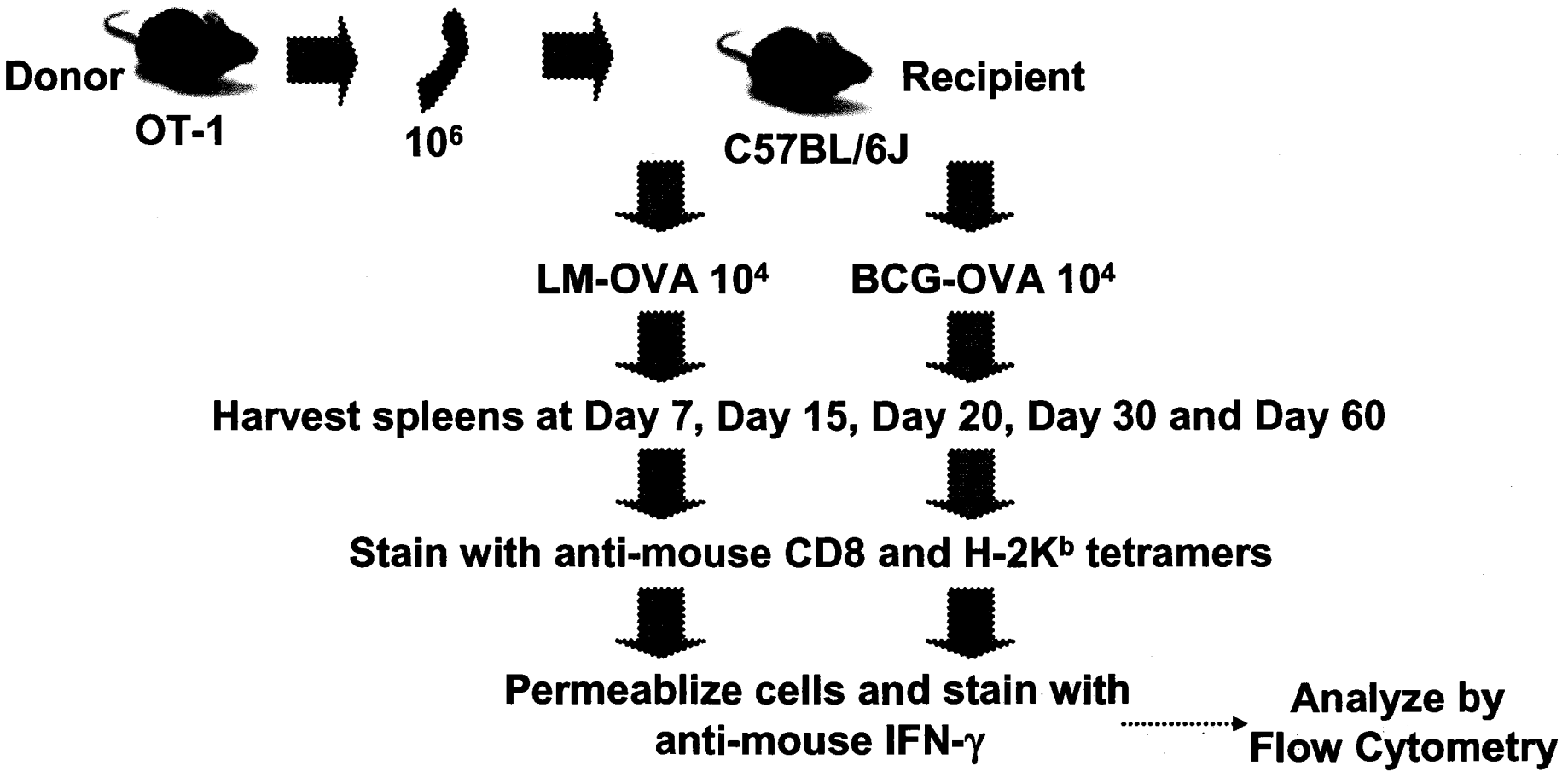
Donor
OT-1
10^6
Recipient
C57BL/6J
LM-OVA 10^4
BCG-OVA 10^4
Harvest spleens at Day 7, Day 15, Day 20, Day 30 and Day 60
Stain with anti-mouse CD8 and H-2K^b tetramers
Permeablize cells and stain with anti-mouse IFN-γ
Analyze by Flow Cytometry

Figure 16: Intracellular IFN-γ expression of antigen specific $CD8^+$ T cells during LM-Ova and BCG-Ova infections. C57BL/6J recipient mice were injected with $1x10^6$ OT-1 donor cells and subsequently infected with LM-Ova or BCG-Ova $1x10^4$ (i.v.). At various time intervals, spleens were harvested from the recipient mice and the number of $OVA_{257-264}$-specific $CD8^+$ T cells were evaluated after staining with H-$2K^bOVA_{257-264}$ tetramers and anti-CD8α antibody and then stimulated with the Ova peptide for 1 hour. The cells were then permeabilized and stained with anti-IFN-γ antibody. Each group involved the evaluation of 4 mice per time point. A representative FACS data is shown for the day 7, day 14 and day 28 time point. Numbers in the panels indicate the numbers of IFN-γ-secreting cells among $tetramer^+$ cells (A). The graph (B) shows the average percentage of IFN-γ –secreting $OVA_{257-264}$-specific $CD8^+$ T cells kinetically.

Figure 16

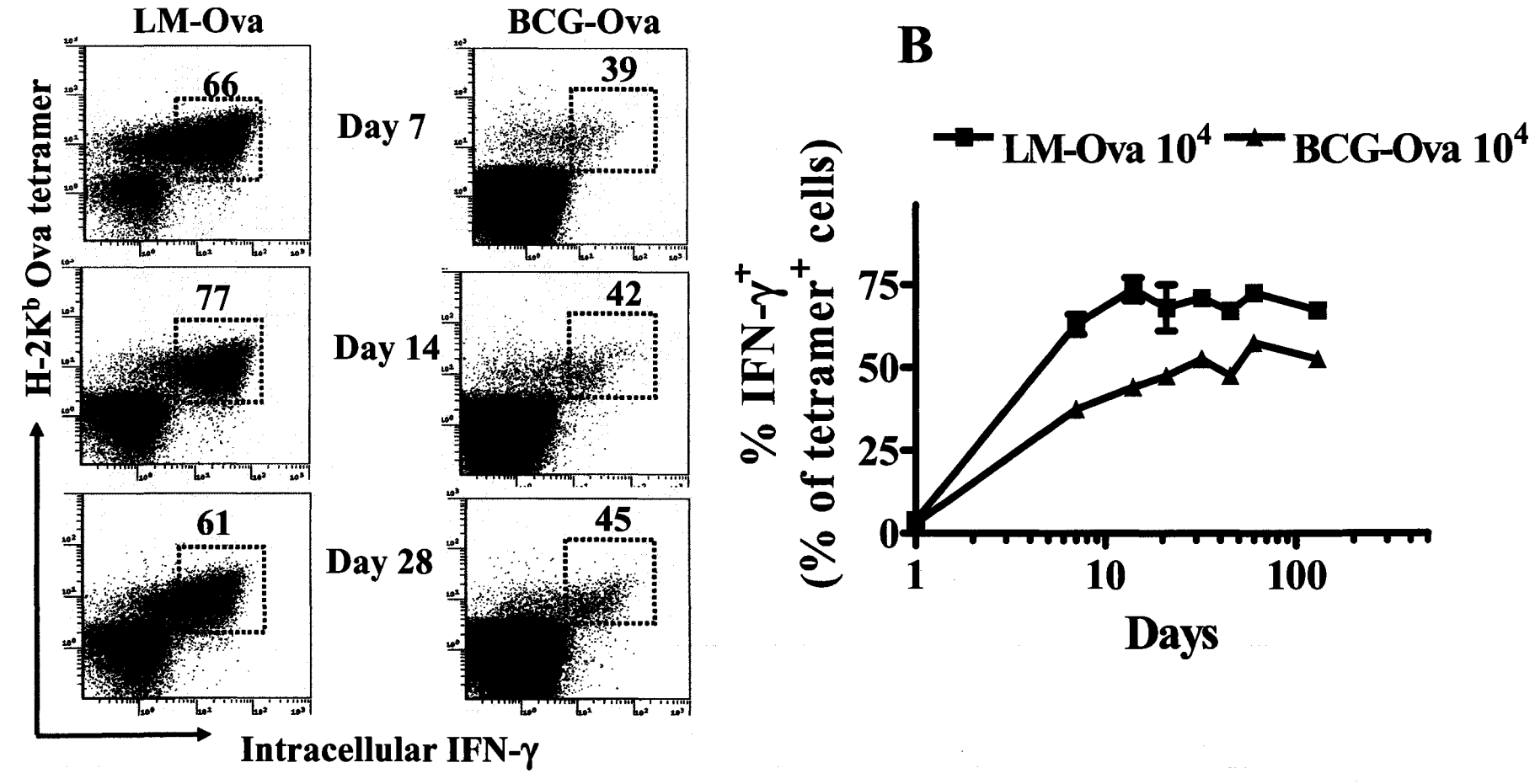
A
LM-Ova
BCG-Ova
66
39
77
42
61
45
Day 7
Day 14
Day 28
H-2K^b Ova tetramer
Intracellular IFN-γ
B
LM-Ova 10^4
BCG-Ova 10^4
% IFN-γ$^+$ (% of tetramer$^+$ cells)
75
50
25
0
1
10
100
Days

Two mice per time point were evaluated and the experiment was performed twice. The graph shows the evaluation of 4 mice at each time point. It was observed that during LM-Ova infection the percentage of IFN-γ expressing Ova-specific $CD8^+$ T cells was high throughout the infection. In the case of BCG-Ova infection the percentage of IFN-γ expressing Ova-specific $CD8^+$ T cells was also high throughout the infection but at levels slightly lower than those responding to LM-Ova. Thus, considering that BCG may induce a weak stimulation and chronic infection, $CD8^+$ T cells that are induced do not appear to be functionally incompetent in terms of their ability to produce IFN-γ.

3.5.2 – Evaluation of in vivo lytic activity of antigen specific $CD8^+$ T cells responding to LM-Ova or BCG-Ova

To asses the in vivo lytic activity of antigen specific $CD8^+$ T cells responding to LM-Ova or BCG-Ova, naïve C57BL/6 mice were injected with either LM-Ova or BCG-Ova $1x10^4$ i.v (Figure17). Splenocytes from a naïve C57BL/6 donor mouse were obtained and half the population was pulsed with 10 μM Ova peptide and the other half with no peptide. The cells were stained with PKH26 and the pulsed population was stained with 5 μM CFSE and the un-pulsed population was stained with 0.5 μM CFSE as in section 2.10. Both populations were mixed in a 1:1 ratio and injected into the infected recipient mice along with uninfected recipient mice at various time points. 24 hours later the spleens were harvested from the recipient mice and processed as in section 2.3. The specific lytic activity of antigen specific $CD8^+$ T cells responding to LM-Ova and BCG-Ova infections is shown in Figure 18. Two mice per time point were evaluated and the experiment was performed twice. The graph shows the evaluation of 4 mice at each time point. The lytic activity was determined by first gating on the $PKH26^+$ donor cells followed by gating on the $CFSE^{hi}$ and $CFSE^{lo}$

Figure 17: Experimental layout to evaluate the ability of $CD8^+$ T cells responding to BCG-Ova to exhibit lytic activity. C57BL/6J recipient mice were injected with LM-Ova or BCG-Ova $1x10^4$ (i.v.). At various time intervals, splenocytes from a naïve donor C57BL/6J mouse were obtained. Half were pulsed with 10μM Ova peptide and the other half with no peptide. Both populations were stained with PKH26 and the peptide pulsed population was stained with 5μM CFSE and the un-pulsed with 0.5μM CFSE. These populations were mixed in a 1:1 ratio and injected into the infected mice. The spleen was harvested 24hours later and analyzed by flow cytometry for specific lysis. The formula shown was used to calculate the specific lytic activity.

Figure 17

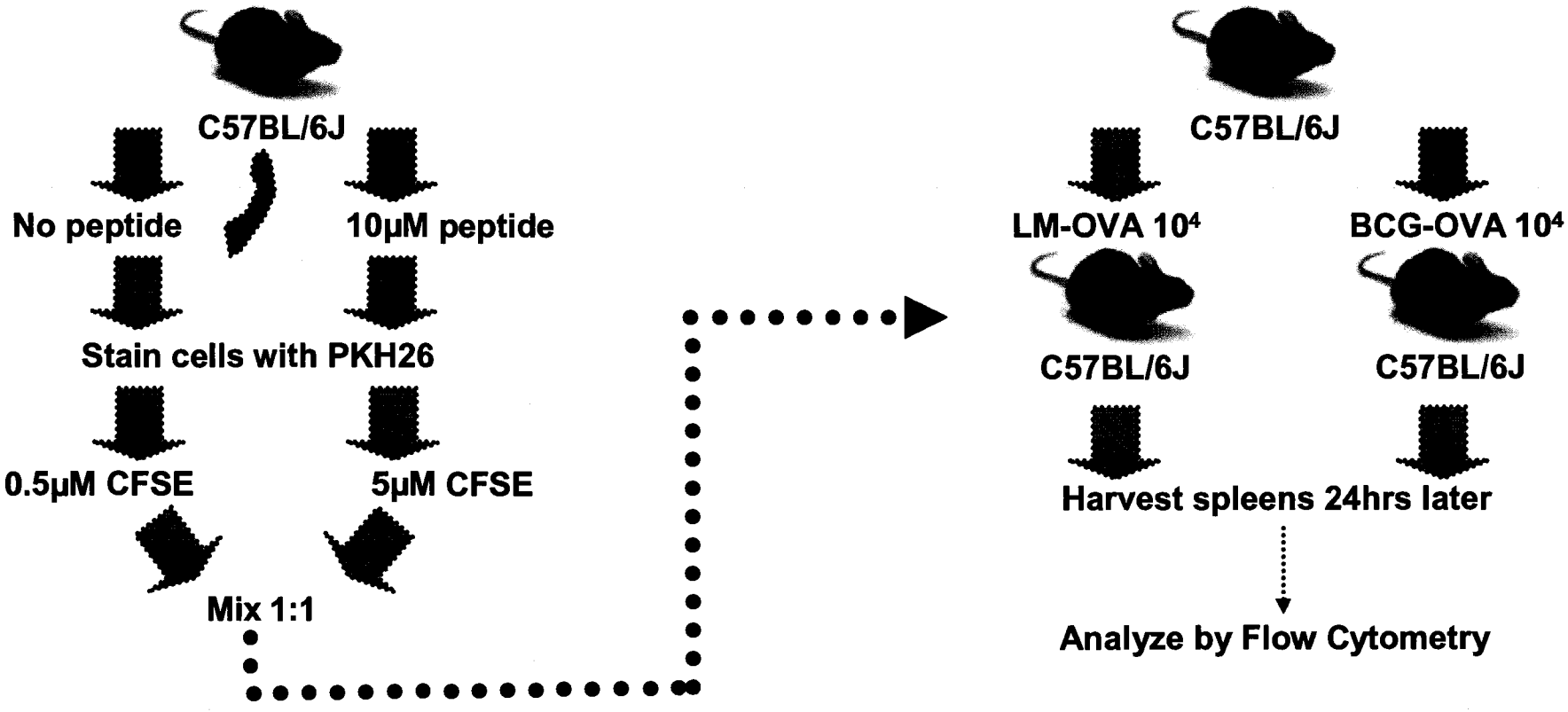

The percent specific lysis of donor spleen cells in each mouse was be calculated as follows:

$$100 - \left[\frac{\text{number of peptide-pulsed targets in infected /number of unpulsed targets in infected}}{\text{number of peptide-pulsed targets in naive/number of unpulsed targets in naive}} \times 100 \right]$$

Figure 18: In vivo lytic activity of antigen specific $CD8^+$ T cells during LM-Ova and BCG-Ova infections. C57BL/6J recipient mice were injected with LM-Ova or BCG-Ova $1x10^4$ (i.v.). At various time intervals, splenocytes from a naïve donor C57BL/6J mouse were obtained. Half were pulsed with 10μM Ova peptide and the other half with no peptide. Both populations were stained with PKH26 and the peptide pulsed population was stained with 5μM CFSE and the un-pulsed with 0.5μM CFSE. These populations were mixed in a 1:1 ratio and injected into the infected mice. The spleen was harvested 24hours later and analyzed by flow cytometry for specific lysis. Each time point involved the evaluation of 2 mice per group. Numbers in the panel show the relative proportions of non-pulsed versus Ova-pulsed populations (A). The graph (B) shows the average percentage of antigen specific lysis occurring for the 2 mice per group at each of the given time points. The graph (C) shows the overall numbers of $Ova_{257-264}$-specific $CD8^+$ T cells in the spleens of mice at various time points as determined by ELISPOT assay.

Figure 18

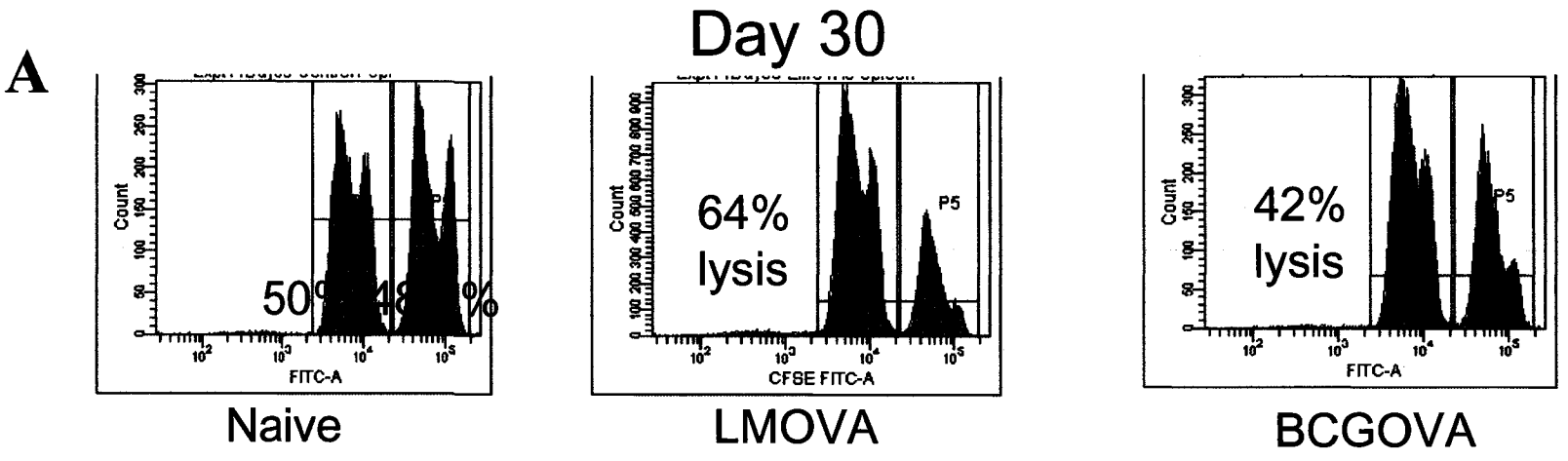
A
Day 30
Count
FITC-A
Naive
64%
lysis
P5
CFSE FITC-A
LMOVA
42%
lysis
P5
FITC-A
BCGOVA

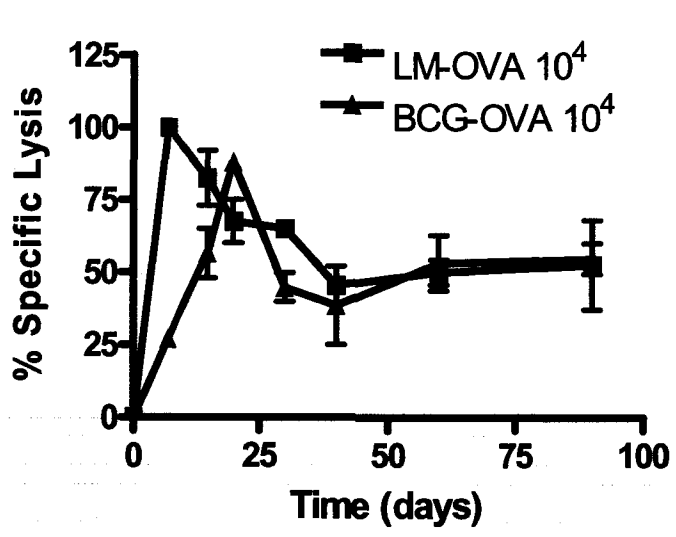
B
% Specific Lysis
LM-OVA 10^4
BCG-OVA 10^4
Time (days)

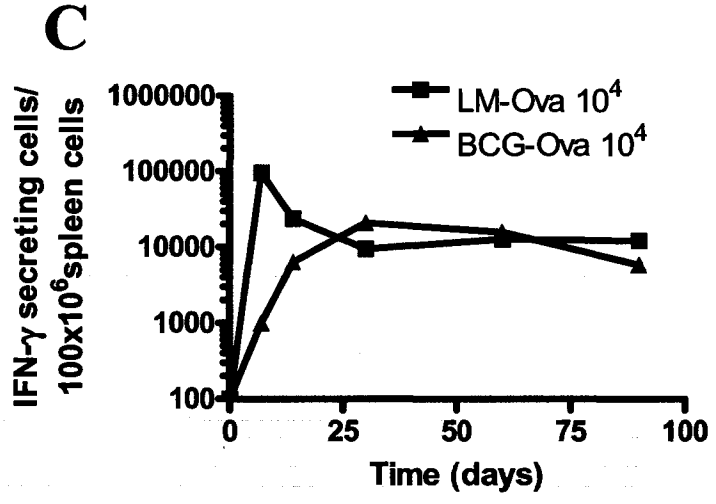
C
IFN-γ secreting cells/ 100x10^6spleen cells
LM-Ova 10^4
BCG-Ova 10^4
Time (days)

populations. The percentages obtained by each of these two populations was entered into a formula shown in section 2.10 to obtain the specific lytic activity of the antigen specific $CD8^+$ T cells within 24 hours at that time in the infection. In the case of LM-Ova infection it was observed that the lytic activity of the antigen specific $CD8^+$ T cells is highest around day 7 of infection and as the bacterial burden is eliminated and the response is allowed to progress, their lytic activity declines to about 50 %. In the case of BCG-Ova infection there was little lytic activity on day 7 of infection but lytic activity peaked around the third week of infection and declined to approximately 50 % subsequently. The lytic activity graph (Figure 18 B) correlated with the frequency of Ova-specific $CD8^+$ T cells (Figure 18 C). Thus, the lytic function of $CD8^+$ T cells was not compromised during the chronic stage of the BCG infection.

3.5.3 – Memory recall ability of antigen specific memory $CD8^+$ T cells generated during LM-Ova and BCG-Ova infections

The memory recall ability of memory $CD8^+$ T cells generated by LM-Ova and BCG-Ova infections was evaluated by injecting $1x10^6$ OT-1 splenocytes i.v. into naïve C57BL/6 mice and infecting them with either $1x10^4$ LM-Ova or BCG-Ova i.v (Figure 19). Thirty days post infection, the spleens were harvested from these mice and $CD8^+$ T cells were purified as in section 2.11. Approximately 10 % of the $CD8^+$ T cells from LM-Ova injected mice were $Ova_{257-264}$-specific whereas only 1 % of $CD8^+$ T cells from BCG-Ova infected mice were $Ova_{257-264}$-specific. Purified $CD8^+$ T cells were injected i.v. ($4x10^6$/mouse) into groups of naïve C57BL/6 mice. Both groups of mice, those containing memory $CD8^+$ T cells generated by LM-Ova infection and those containing memory $CD8^+$ T cells generated by BCG-Ova infection were challenged with LM-Ova or BCG-Ova $1x10^4$ i.v. At various time points after

Figure 19: Experimental layout to evaluate the response of memory $CD8^+$ T cells to re-challenge. C57BL/6J donor mice were injected with $1x10^6$ OT-1 donor cells and subsequently infected with LM-Ova or BCG-Ova $1x10^4$ (i.v.). After 30 days, spleens from these mice were harvested and the $CD8^+$ cells were purified and injected $4x10^6$ (i.v.) into naïve C57BL/6J recipient mice. The recipient mice were infected with LM-Ova or BCG-Ova $1x10^4$ (i.v.). At various time intervals, spleens were harvested from the recipient mice and the number of $OVA_{257-264}$-specific $CD8^+$ T cells was evaluated after staining with H-$2K^bOVA_{257-264}$ tetramers and anti-mouse CD8α antibody.

Figure 19

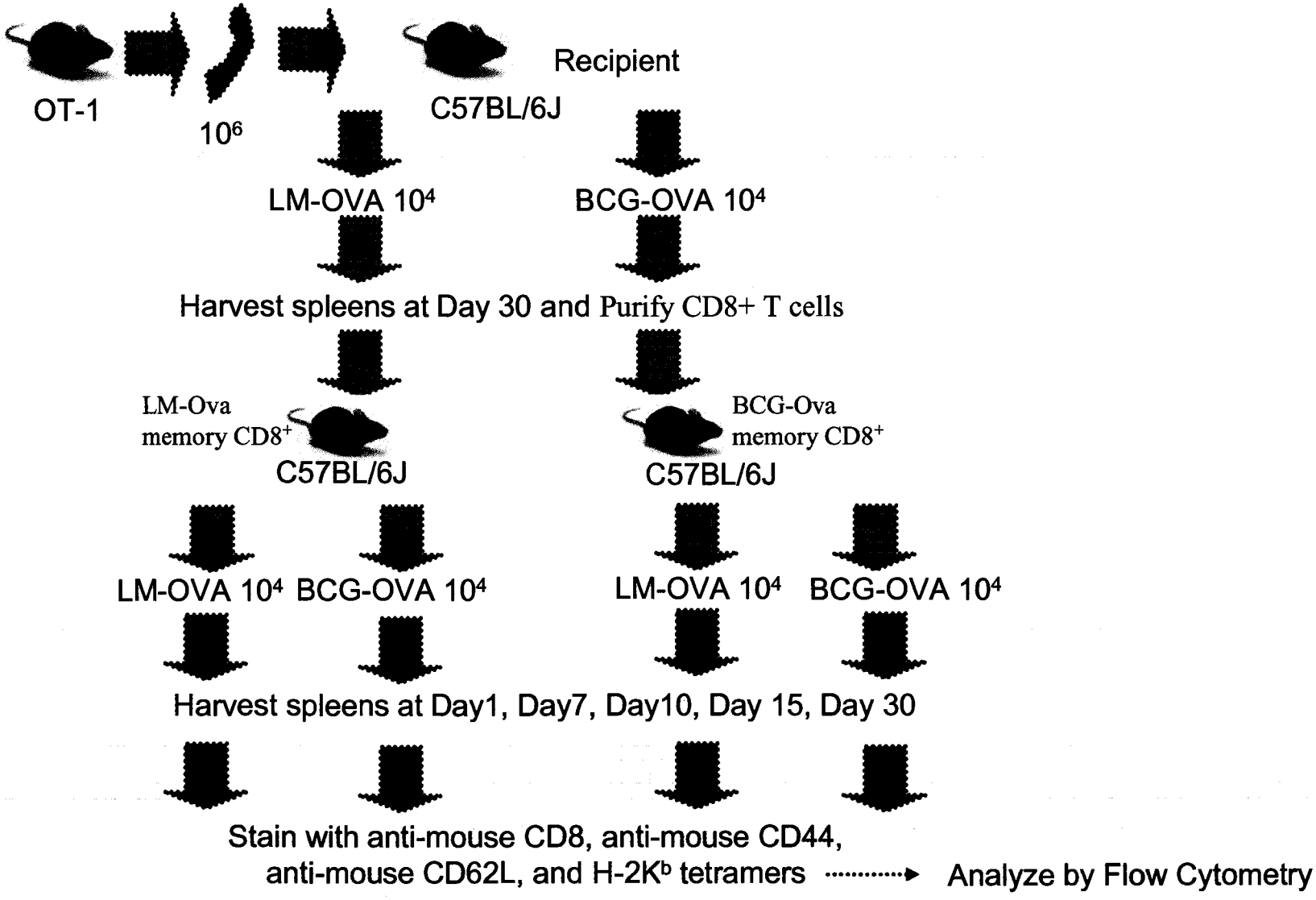
OT-1
10^6
Recipient
C57BL/6J
LM-OVA 10^4
BCG-OVA 10^4
Harvest spleens at Day 30 and Purify CD8+ T cells
LM-Ova memory $CD8^+$
C57BL/6J
BCG-Ova memory $CD8^+$
C57BL/6J
LM-OVA 10^4
BCG-OVA 10^4
LM-OVA 10^4
BCG-OVA 10^4
Harvest spleens at Day1, Day7, Day10, Day 15, Day 30
Stain with anti-mouse CD8, anti-mouse CD44,
anti-mouse CD62L, and H-2K^b tetramers
Analyze by Flow Cytometry

challenge, spleens were harvested and processed as in section 2.3. Figure 20 shows the antigen specific recall response of Ova-specific memory $CD8^+$ T cells that were derived from LM-Ova or BCG-Ova infected mice. Two mice per time point were evaluated and the experiment was performed twice. The graph shows the evaluation of 4 mice at each time point. The percentage of Ova-specific $CD8^+$ T cells was determined by gating on the lymphocytes in the forward scatter/side scatter profile followed by gating on the $CD8^+$ population and further gating on the $Tetramer^+$ population. Not surprisingly, Ova-specific memory $CD8^+$ T cells derived from LM-Ova infected mice proliferated rapidly in response to LM-Ova infection in naïve mice (Figure 20 A). However, the same memory $CD8^+$ T cells displayed a very delayed and muted response in response to BCG-Ova infection, indicating that even conventional memory $CD8^+$ T cells respond to BCG-Ova infection with protracted kinetics (Figure 20 B). The memory $CD8^+$ T cells generated in BCG-Ova infected mice proliferated efficiently in response to LM-Ova infection in naïve mice (Figure 20 C), indicating that the memory recall ability of BCG-Ova induced memory cells is not compromised. As with LM-Ova induced memory cells, BCG-Ova induced memory $CD8^+$ T cells also responded to BCG-Ova infection in naïve mice with delayed and protracted kinetics (Figure 20 D).

In the previous experiment recipient mice were challenged with LM-Ova and BCG-Ova immediately after adoptively transferring memory $CD8^+$ T cells. It was therefore speculated that a defect might become noticeable if sufficient time was given for memory $CD8^+$ T cells to undergo homeostatic proliferation after adoptive transfer into recipient mice before they were challenged with LM-Ova and BCG-Ova. In fact is has been shown that $CD8^+$ T cells induced during chronic viral infections undergo poor homeostatic proliferation

Figure 20: Response of memory $CD8^+$ T cells to re-challenge. C57BL/6J donor mice were injected with $1x10^6$ OT-1 donor cells and subsequently infected with LM-Ova or BCG-Ova $1x10^4$ (i.v.). After 30 days, cells from these mice were harvested and the $CD8^+$ cells were purified and injected $4x10^6$ (i.v.) into naïve C57BL/6J recipient mice. The recipient mice were infected with LM-Ova or BCG-Ova $1x10^4$ (i.v.). At various time intervals, spleens were harvested from the recipient mice and the number of $OVA_{257-264}$-specific $CD8^+$ T cells were evaluated after staining with H-$2K^bOVA_{257-264}$ tetramers and anti-mouse CD8α antibody. Each group involved the evaluation of 4 mice per time point. Each graph shows the average percentage of $OVA_{257-264}$-specific $CD8^+$ T cells at the given time points. LM-Ova memory $CD8^+$ T cells challenged with LM-Ova (A), LM-Ova memory $CD8^+$ T cells challenged with BCG-Ova (B), BCG-Ova memory $CD8^+$ T cells challenged with LM-Ova (C), BCG-Ova memory $CD8^+$ T cells challenged with BCG-Ova (D).

Figure 20

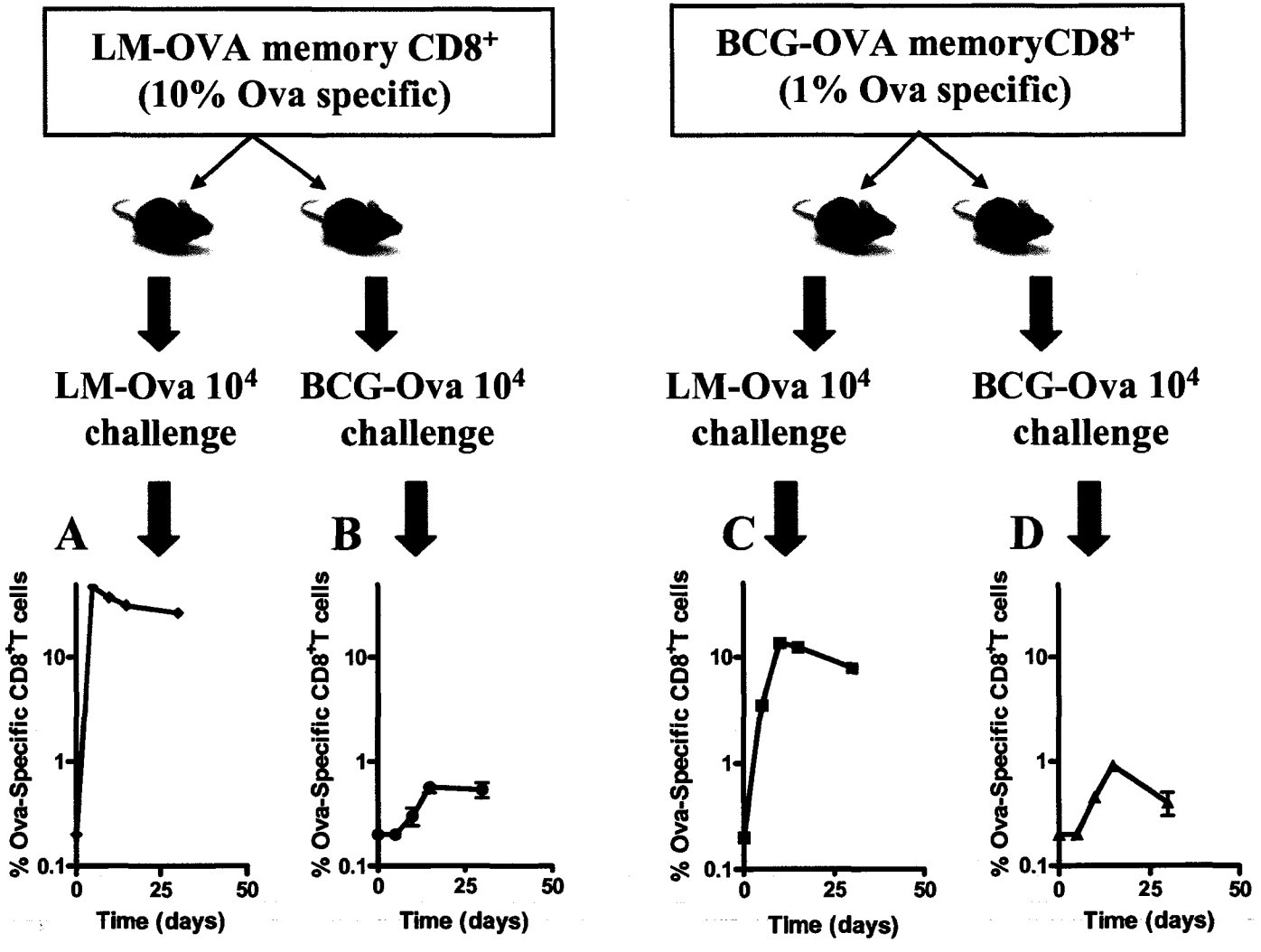
LM-OVA memory CD8+
(10% Ova specific)
BCG-OVA memoryCD8+
(1% Ova specific)
LM-Ova 10^4
challenge
BCG-Ova 10^4
challenge
LM-Ova 10^4
challenge
BCG-Ova 10^4
challenge
A
B
C
D
% Ova-Specific CD8+T cells
10
1
0.1
0
25
50
Time (days)

and thus are not maintained efficiently in naïve mice [106]. Thus, in a separate set of experiments, memory $CD8^+$ T cells from LM-Ova or BCG-Ova infected mice were adoptively transferred into naïve recipient C57BL/6 mice. Memory $CD8^+$ T cells were allowed to undergo homeostatic proliferation for a short time (5 days) or a long time (30 days) before their ability to mount a recall response to antigenic stimulation (LM-Ova challenge) was tested. The spleens were harvested at various time points after LM-Ova challenge and processed as in section 2.3 and $1x10^7$ cells were obtained and stained with anti-CD8α antibody and H-$2K^b$$Ova_{257-264}$ tetramers. The cells were fixed and acquired on EPICS XL Flow cytometer and analyzed using the EXPO software. As is evident in Figure 21 Ova-specific memory $CD8^+$ T cells generated from LM-Ova as well as BCG-Ova infected mice proliferated efficiently in response to LM-Ova re-challenge. Furthermore, there was no significant difference in the response if memory $CD8^+$ T cells were allowed to undergo homeostatic proliferation for a short or long duration.

In summary since BCG-Ova induced a chronic infection the functional phenotype of the responding $CD8^+$ T cells was called into question. However the data showed that the $CD8^+$ T cells are fully functional in that they are capable of producing IFN-γ, they exhibit in vivo lytic activity and they are capable of proliferating in response to a previously experienced peptide. Thus, the $CD8^+$ T cells responding to BCG-Ova don't seem to be functionally affected by the reduced stimulation or the chronic nature of the infection. Since the $CD8^+$ T cells responding to BCG-Ova are fully functional this does not seem to be the reason behind the decline in cycling at later stages of infection. Since antigen presentation directly contributes to the cycling of $CD8^+$ T cells it was decided that the response to in vivo antigen presentation should be evaluated in this infection model.

Figure 21: Response of memory $CD8^+$ T cells to re-challenge after homeostatic equilibration. C57BL/6J donor mice were injected with $1x10^6$ OT-1 donor cells and subsequently infected with LM-Ova or BCG-Ova $1x10^4$ (i.v.). After 30 days, cells from these mice were harvested and the $CD8^+$ cells were purified and injected $4x10^6$ (i.v.) into naïve C57BL/6J recipient mice. The recipient mice were infected with LM-Ova or BCG-Ova $1x10^4$ (i.v.) either 5 days post adoptive transfer or 30 days post adoptive transfer. Spleens were harvested from the recipient mice at various time intervals after LM-Ova re-challenge and the number of $OVA_{257-264}$-specific $CD8^+$ T cells evaluated after staining with H-$2K^bOVA_{257-264}$ tetramers and anti-mouse CD8α antibody. Each group involved the evaluation of 4 mice per time point. Each graph shows the average percentage of $OVA_{257-264}$-specific $CD8^+$ T cells at the given time points.

Figure 21

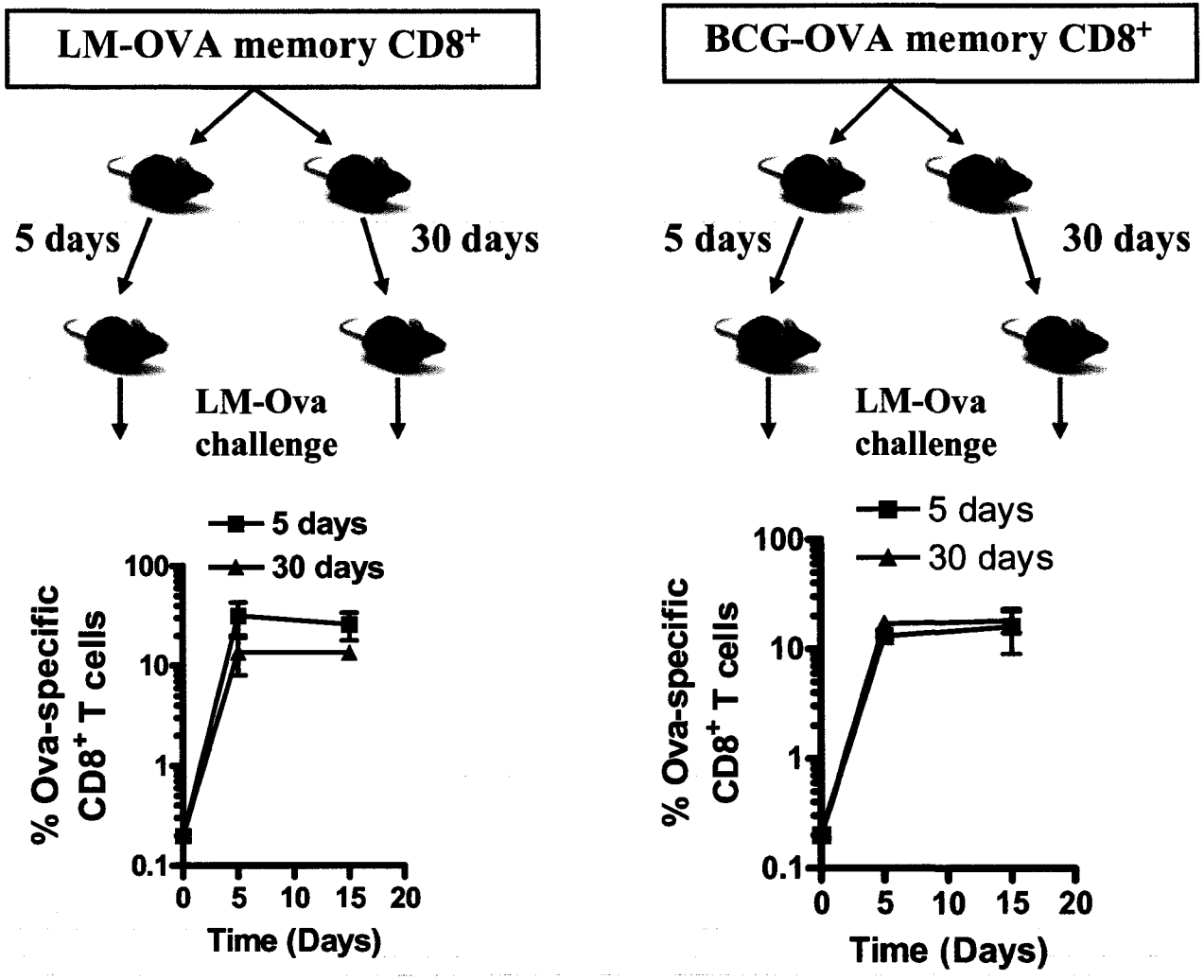
LM-OVA memory CD8+
5 days
30 days
LM-Ova challenge
5 days
30 days
% Ova-specific CD8+ T cells
100
10
1
0.1
0
5
10
15
20
Time (Days)
BCG-OVA memory CD8+
5 days
30 days
LM-Ova challenge
5 days
30 days
% Ova-specific CD8+ T cells
100
10
1
0.1
0
5
10
15
20
Time (Days)

3.6.0 – Evaluation of in vivo antigen presentation

Since the $CD8^+$ T cells generated during BCG-Ova infection are functionally competent at later time points and reduced stimulation is observed initially in this infection model the question arose as to what is causing the delay in the $CD8^+$ T cell response and why there is a decline in cycling despite pathogen persistence. Thus, it was decided that in vivo antigen presentation should be evaluated in this model and the contribution of cytokines and lymphocytes to this process should also be examined. The stability of the antigen mRNA was also addressed as a possible contributing factor to the decline in cycling despite pathogen persistence.

3.6.1 – Evaluation of in vivo antigen presentation during LM-Ova and BCG-Ova infections

The model for testing in vivo antigen-presentation is described in detail in section 2.12 and Figure 22. The model rests on the premise that if Ova-peptide/MHC complexes are displayed on APCs in vivo this should lead to proliferation of adoptively transferred naive Ova-specific OT-1 transgenic $CD8^+$ T cells. Thus, the read-out of in vivo antigen-presentation is the proliferation of responding T cells which is detected by measuring the down-regulation of CFSE staining which gets halved with each cell division.

At day -1, day -7, day-14, day -30 and day -60, LM-Ova 10^4 or BCG-Ova 10^4 was injected into naïve C57BL/6 mice. On day 0, ~$25x10^6$ CFSE labeled splenocytes from OT-1 mice were injected into these mice. The spleens were removed 4 days post adoptive transfer and processed as in section 2.3. Spleen cells were stained with anti-CD8α antibody and $Ova_{257-264}$-tetramers, and the proliferation of donor OT-1 cells was measured by determining the reduction in the intensity of CFSE, which gets halved with each cell division. Figure 23 shows the response to in vivo antigen presentation of the naïve OT-1 $CD8^+$ T cells

Figure 22: Experimental layout to evaluate the kinetics of antigen presentation to $CD8^+$ T cells infections. C57BL/6J mice were injected with LM-Ova or BCG-Ova (10^4 i.v.). At various time points post infection CFSE-labelled cells from an OT-1 transgenic donor mouse were injected into the recipient mice i.v. ($25\text{-}30x10^6$). After 4 days of parking, the spleens from the recipient mice were harvested and stained with H-$2K^bOVA_{257\text{-}264}$ tetramer and anti-mouse CD8α antibody and analyzed by flow cytometry. The expression of CFSE was assessed based on $Tetramer^+$ donor $CD8^+$ T cells. Each time point involved the evaluation of 4 mice per group.

Figure 22

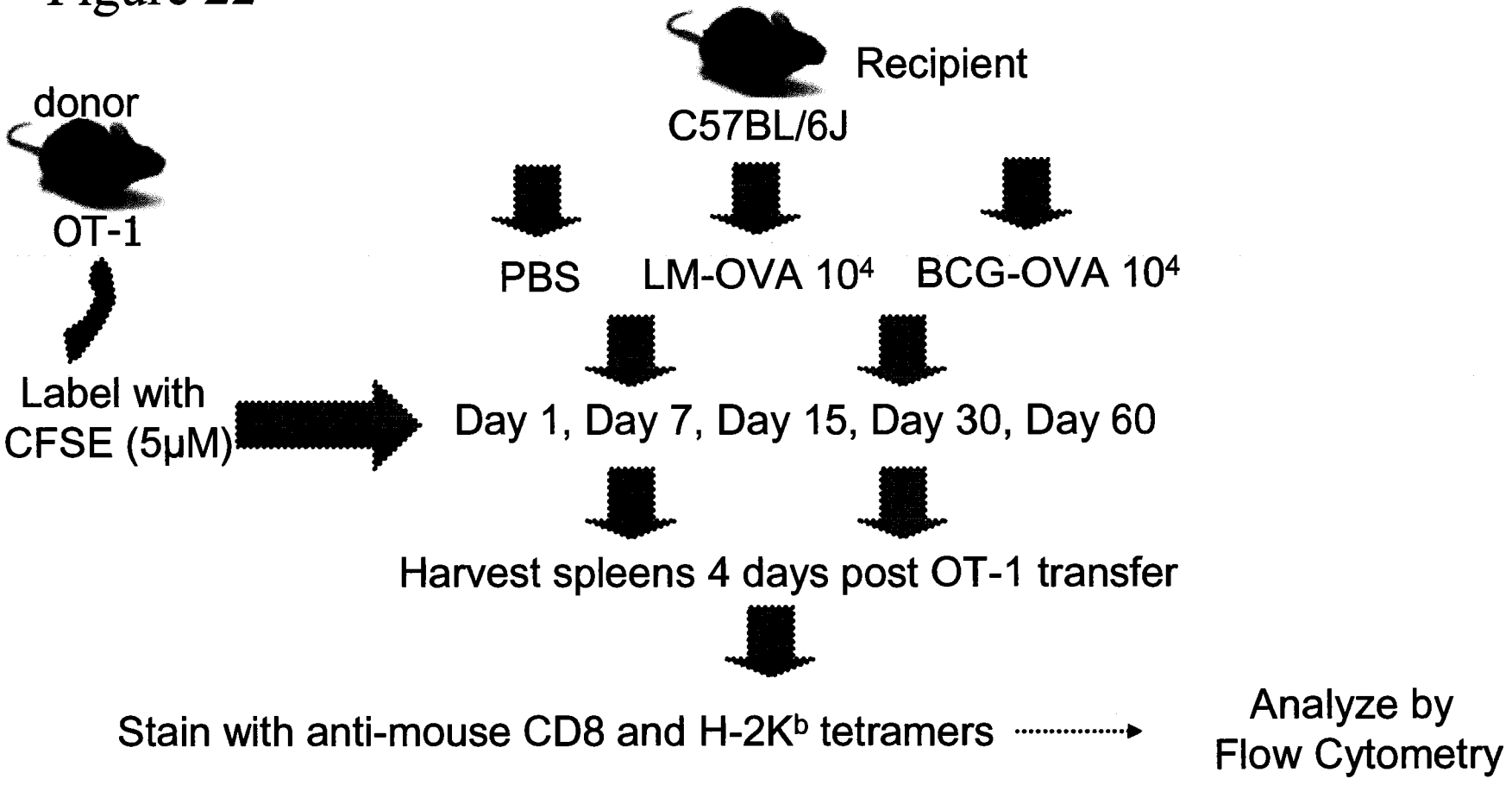
donor
OT-1
Label with
CFSE (5μM)
Recipient
C57BL/6J
PBS
LM-OVA 10⁴
BCG-OVA 10⁴
Day 1, Day 7, Day 15, Day 30, Day 60
Harvest spleens 4 days post OT-1 transfer
Stain with anti-mouse CD8 and H-2K^b tetramers
Analyze by
Flow Cytometry

Figure 23: Kinetics of antigen presentation during LM-Ova and BCG-Ova infections. C57BL/6J mice were injected with LM-Ova or BCG-Ova (10^4 i.v.). At various time points post infection CFSE-labelled cells from an OT-1 transgenic donor mouse were injected into the recipient mice i.v. ($25\text{-}30x10^6$). After allowing 4 days for the cells to respond, the spleens from the recipient mice were harvested and stained with H-2K^{b}OVA$_{257\text{-}264}$ tetramers and anti-mouse CD8α antibody. The expression of CFSE was assessed based on Tetramer$^+$ donor CD8$^+$ T cells. Each time point involved the evaluation of 4 mice per group per time point. A representative FACS data for the Day 0-4 time point and the Day 6-10 time point are shown for both groups (A). The graph (B) shows the average percentages of CFSE^{lo} OVA$_{257\text{-}264}$-specific CD8$^+$ T cells for the 4 mice at each given time point based on a PBS control group.

Figure 23

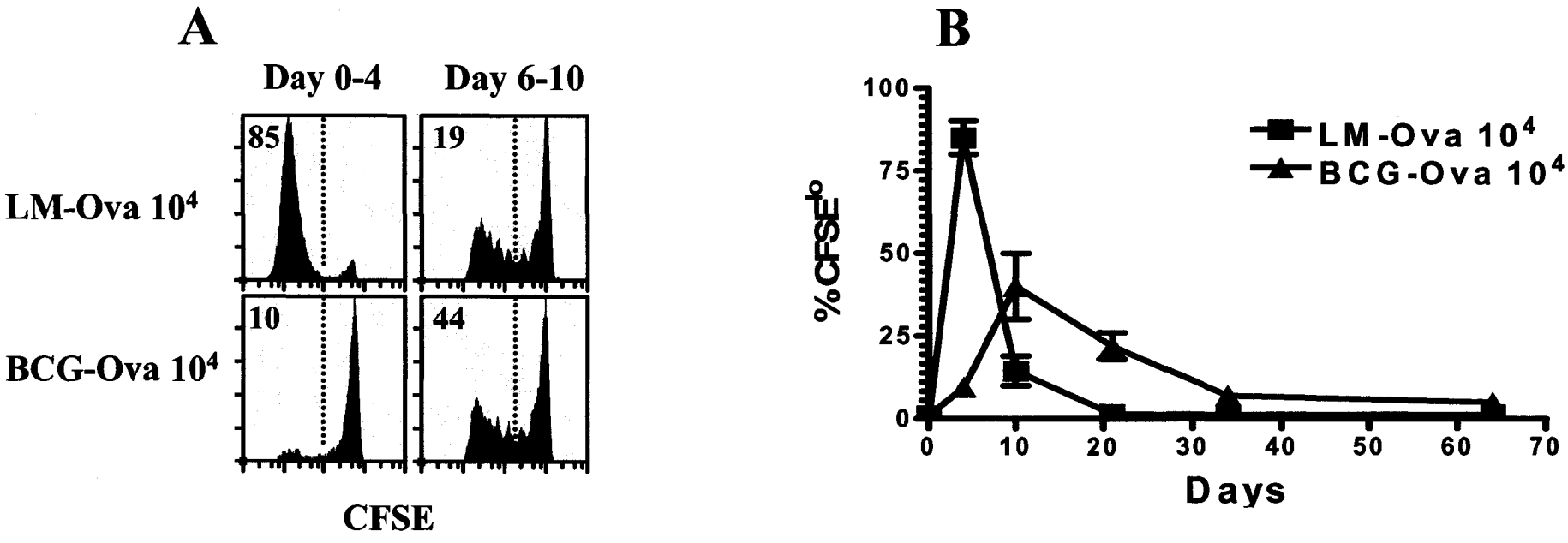
A
Day 0-4
Day 6-10
LM-Ova 10^4
BCG-Ova 10^4
85
19
10
44
CFSE
B
100
75
50
25
0
%CFSE^lo
0
10
20
30
40
50
60
70
Days
LM-Ova 10^4
BCG-Ova 10^4

responding to LM-Ova or BCG-Ova. Two mice per time point were evaluated and the experiment was performed twice. The graph shows the evaluation of 4 mice at each time point. It was observed that during LM-Ova infection massive antigen presentation occurs early in infection. Antigen presentation peaks within the first few days of infection and declines enormously thereafter when the pathogen is eliminated. In contrast, in BCG-Ova infection, antigen-presentation was almost undetectable during the first week of infection, peaking around the second week of infection and getting curtailed to low levels despite the persistence of BCG-Ova.

3.6.2 – Evaluation of in vivo antigen presentation during BCG-Ova infection when increased response time for donor OT-1 cells is provided

Since there was a curtailment in antigen presentation (Figure 23) and cycling (Figure 8) during BCG-Ova infection despite pathogen persistence (Figure 2), it was speculated that the curtailment in antigen-presentation during the later time intervals might not be as pronounced if OT-1 cells were allowed to respond for 7 days as opposed to 4 days. At day -1, day -7, day-14, day -30 and day -60, BCG-Ova 10^4 was injected into naïve C57BL/6 mice. On day 0, ~$25x10^6$ splenocytes from OT-1 mice were labeled with 5 μM CFSE and injected into these mice as in section 2.12. The spleens from these mice were harvested 4 or 7 days post adoptive transfer. The spleens were processed as in section 2.3 and $1x10^7$ cells were obtained and stained with anti-CD8α antibody and H-$2K^bOva_{257-264}$ tetramers. Figure 24 shows that the increased time in parking did not seem to rescue the curtailment in antigen presentation seen in this BCG-Ova infection model. There was still a delay in antigen presentation early on, and the peak of antigen presentation was still approximately 7-11 days of infection and antigen presentation still became curtailed on day 30 despite pathogen presence in the spleen.

Figure 24: Kinetics of antigen presentation during BCG-Ova infection with longer parking interval of donor OT-1 cells. C57BL/6J mice were injected with BCG-Ova (10^4 i.v.). At various time points post infection CFSE-labelled cells from an OT-1 transgenic donor mouse were injected into the recipient mice i.v. ($25\text{-}30\text{x}10^6$). The CFSE labelled donor cells were allowed to respond for 4 days or 7 days in the recipient mice. The spleens from the recipient mice were harvested and stained with H-2K^{b}OVA$_{257\text{-}264}$ tetramers and anti-mouse CD8α antibody. The expression of CFSE was assessed based on Tetramer$^+$ donor CD8$^+$ T cells. Each time point involved the evaluation of 2 mice per group per time point. The graph shows the average percentages of CFSE^{lo} OVA$_{257\text{-}264}$-specific CD8$^+$ T cells for the 2 mice at each given time point based on a PBS control group.

Figure 24

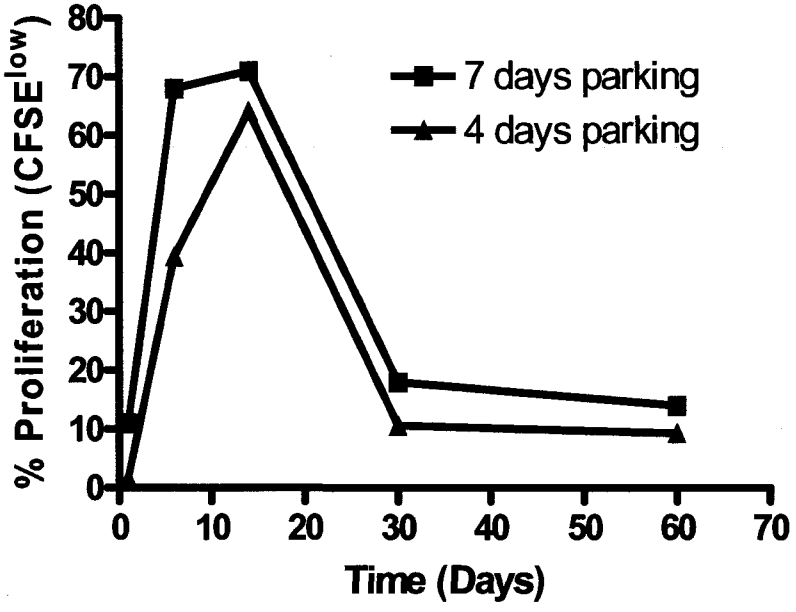
% Proliferation (CFSE^{low})
80
70
60
50
40
30
20
10
0
0
10
20
30
40
50
60
70
Time (Days)
7 days parking
4 days parking

3.6.3 – Evaluation of the mechanisms that contribute to the curtailment in antigen-presentation during the later time intervals of BCG-Ova infection.

A curtailment in antigen presentation (Figure 23) and cycling (Figure 8) was observed during BCG-Ova infections despite pathogen persistence, and this did not seem to be rescued by longer parking of the donor CFSE labeled OT-1 cells (Figure 24). Therefore, the contribution of T cells and inflammatory cytokines to this phenomenon. To this end antigen presentation was evaluated in mice that are deficient in T, B cells (Rag-$1^{-/-}$) and those that are lacking in key inflammatory molecules (TNF-Rαβ, IFN-γ and iNOS-2). Rag-1 knockouts lack the ability to generate lymphocytes so they were used to assess the contribution of lymphocytes to the delay and curtailment of antigen presentation during BCG-Ova infection. The TNF-Rαβ knockout mice are unable to respond to the TNF cytokine which is one of the key inflammatory cytokines produced by APCs, NK cells, and T cells. These mice were used to evaluate the contribution of the TNF cytokine to the delay and curtail of antigen presentation in BCG-Ova infections. iNOS-2 deficient mice are unable to produce the inducible nitrous oxide synthase and are thus unable to make nitrous oxide which is used by APCs to destroy bacteria in their phago-lysosomes. These mice were used to evaluate the contribution of nitrous oxide production to the delay and curtailment of antigen presentation in BCG-Ova infections. IFN-γ-deficient mice are unable to produce IFN-γ which is a signature inflammatory cytokine produced by T cells and NK cells and activates macrophages. These mice were used to evaluate the contribution of the IFN-γ cytokine to the delay and curtailment of antigen presentation in BCG-Ova infections. Antigen presentation was also evaluated in C57BL/6 mice as a control.

To assess in vivo response to antigen presentation, BCG-Ova 10^4 i.v. was injected at day -1, day -7, day-14, day -30 and day -60 into Rag-1 knockouts, TNF-Rαβ knockouts, iNOS-2 knockouts, IFN-γ knockouts, along with naïve C57BL/6 mice. On day 0, 5 μM CFSE labeled splenocytes (8 x10^6 cells, described in section 2.12) from OT-1R mice were injected into these mice. OT-1R mice were used because these mice lack endogenous non-transgenic lymphocytes which may lead to increased background in the various knockout mice. The spleens from the recipient mice were harvested 4 days post adoptive transfer and processed as in section 2.3. 1x10^7 cells were obtained and stained with anti-CD8α antibody and H-2K^{b}Ova$_{257-264}$ tetramers. The cells were fixed and acquired on EPICS XL Flow cytometer and analyzed using the EXPO software.

Figure 25 shows the response to in vivo antigen presentation of the naïve Ova-specific CD8$^+$ T cells during BCG-Ova infection in various mutant mice (Figure 25 A) along with the bacterial burden in those mice (Figure 25 B). Two mice per time point were evaluated and the experiment was performed twice. The graph shows the evaluation of 4 mice at each time point. In all the knock-out mice there was a delay in antigen-presentation indicating that the proposed cytokines do not contribute to the delay in antigen-presentation during BCG-Ova infection. In fact, the delay in antigen presentation was further exacerbated in the Rag-1 knockout mice in contrast to controls in that antigen presentation did not appear to begin till day 20 of infection. The degree of antigen-presentation was enhanced in the various knock-out mice. More importantly, the curtailment in antigen-presentation that was noted in control mice at later time intervals was reduced (IFN-$\gamma^{-/-}$, iNOS2$^{-/-}$, TNF-Rαβ$^{-/-}$) or even absent (Rag-1$^{-/-}$) in the various knock-out mice. Higher burden was noted in all the knock-out mice in comparison to the controls (Figure 25 B). Although the higher BCG-Ova burden could explain the reduced curtailment in antigen-presentation in the knock-out mice,

Figure 25: Kinetics of antigen presentation during BCG-Ova infections in knockout mice. Normal C57BL/6 (WT) and various knock-out mice on C57BL/6 background (Rag-$1^{-/-}$, TNFR-$\alpha\beta^{-/-}$, iNOS-$2^{-/-}$, and IFN-$\gamma^{-/-}$) were injected with BCG-Ova (10^4 i.v.). At various time points post infection CFSE-labelled cells from OT-1R transgenic donor mice were injected into the recipient mice i.v. ($8x10^6$). The CFSE labelled donor cells were allowed to respond for 4 days in the recipient mice. The spleens from the recipient mice were harvested and stained with H-$2K^bOVA_{257-264}$ tetramers and anti-mouse CD8α antibody. The expression of CFSE was assessed based on $Tetramer^+$ donor $CD8^+$ T cells. Each time point involved the evaluation of 4 mice per group per time point. The graphs show the average percentages of $CFSE^{lo}$ $OVA_{257-264}$-specific $CD8^+$ T cells for the 4 mice at each given time point based on a PBS control group (A). The bacterial burden in the spleens of the mice was assessed by performing serial dilutions of the homogenized spleen in PBS-T80 and plating on 7H10+OADC agar plates (B).

Figure 25

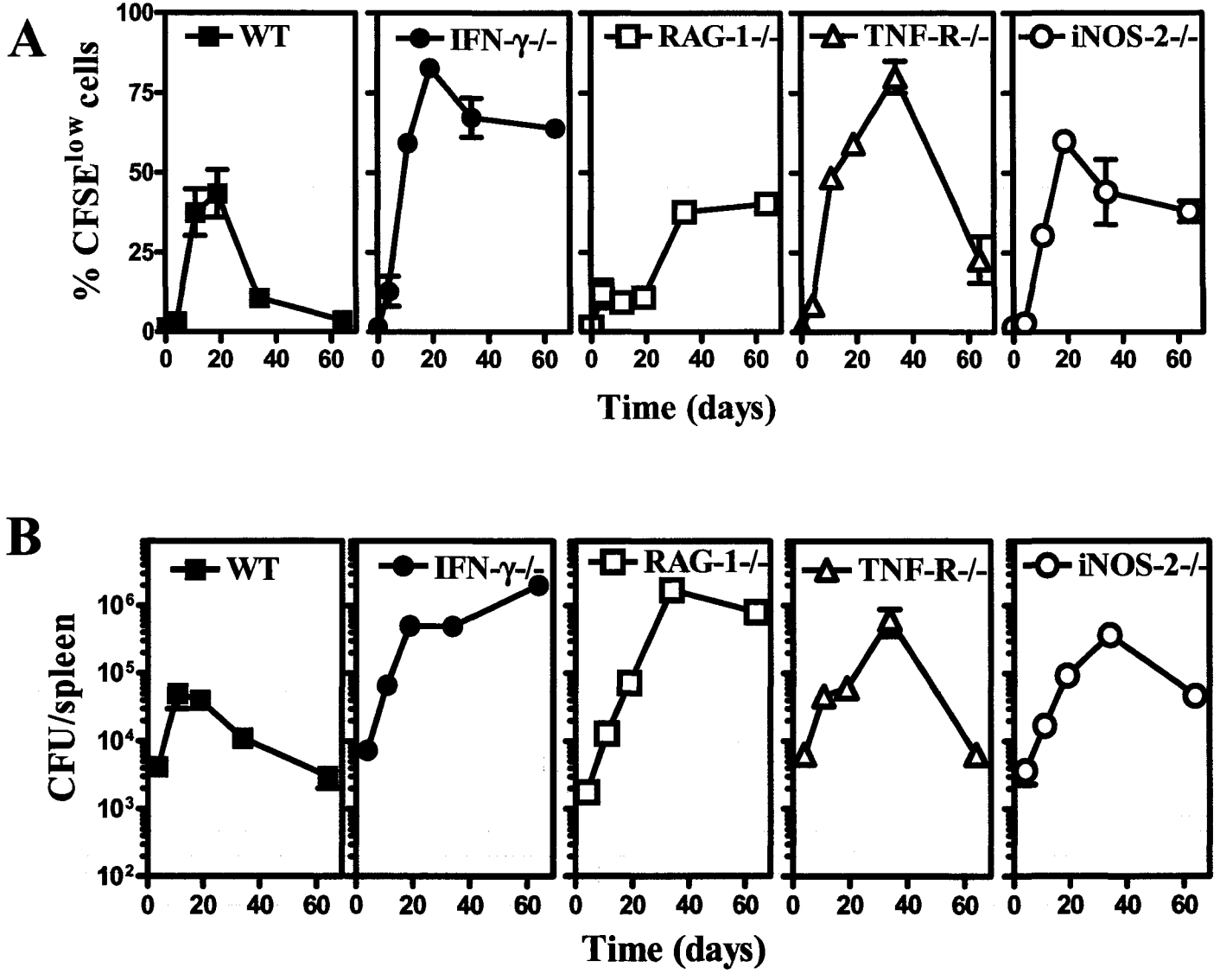
A
% CFSE^low cells
100
75
50
25
0
WT
IFN-γ-/-
RAG-1-/-
TNF-R-/-
iNOS-2-/-
0 20 40 60
Time (days)
B
CFU/spleen
10^6
10^5
10^4
10^3
10^2
WT
IFN-γ-/-
RAG-1-/-
TNF-R-/-
iNOS-2-/-
0 20 40 60
Time (days)

on close examination this may not be the case. For example, at day 30 of infection, bacterial burden is similar in the various knockout mice and yet antigen presentation at this time is quite varied between the various knock out mice.

Antigen presentation was also evaluated in the non-lymphoid organs. The lungs were evaluated for antigen presentation in the Rag-1 knockouts, TNF-Rαβ knockouts, iNos-2 knockouts, IFN-γ knockouts and the C57BL/6 control mice. The liver was also evaluated for antigen presentation in the control mice. Both lungs and livers were harvested 4 days post adoptive transfer of the CFSE labeled OT-1R donor cells. Both the lungs and livers were processed as in section 2.3. The lungs and livers were pooled for two mice at each time point throughout the BCG-Ova infection and the experiment was performed twice. The graphs show the evaluation of 4 mice at each time point. The lymphocytes were stained with anti-CD8α antibody and H-2K^{b}Ova$_{257-264}$ tetramers. In the non-lymphoid organs the overall trend seemed to be the same as what was observed in the spleen (Figure 26) in that there was a delay in antigen-presentation earlier which was followed by a massive curtailment of antigen-presentation in controls but not in the various knock-out mice.

3.6.4 – Contribution of CD4$^+$ and CD8$^+$ T cells to the delay and curtailment of antigen-presentation during BCG-Ova infection.

Having noted in the previous figure that antigen-presentation is enormously delayed in Rag-1 knockout mice and does not get curtailed at all even at day 60 of infection, the next step was to determine whether the endogenous CD4$^+$ and CD8$^+$ T cells are responsible for these effects. To assess in vivo response to antigen presentation, BCG-Ova 10^4 i.v. was injected at day -1, day -7, day-14, day -30 and day -60 into CD4-knockout and CD8-knockout mice, along with normal C57BL/6 mice as controls. On day 0, 8 x10^6 CFSE labeled splenocytes from OT-1R mice were injected into these mice. The spleens from the

Figure 26: Kinetics of antigen presentation during BCG-Ova infections in non-lymphoid organs in knockout mice. Normal C57BL/6 (WT) and various knock-out mice on C57BL/6 background ($Rag1^{-/-}$, $TNFR\alpha\beta^{-/-}$, $iNOS\text{-}2^{-/-}$ and $IFN\text{-}g^{-/-}$) were injected with BCG-Ova (10^4, iv). At various time points post infection CFSE-labelled cells from an OT-1R transgenic donor mouse were injected into the recipient mice i.v. ($8x10^6$). The CFSE labelled donor cells were parked for 4 days in the recipient mice. The lungs or livers from the recipient mice were harvested and stained with $H\text{-}2K^bOVA_{257\text{-}264}$ tetramers and anti-mouse CD8α antibody. The expression of CFSE was assessed based on $Tetramer^+$ donor $CD8^+$ T cells. Each time point involved the evaluation of 2 mice per group per time point. The lungs were pooled for each time point. The graphs show the percentages of $CFSE^{lo}$ $OVA_{257\text{-}264}$-specific $CD8^+$ T cells for the 2 pooled mice at each given time point based on a PBS control group.

Figure 26

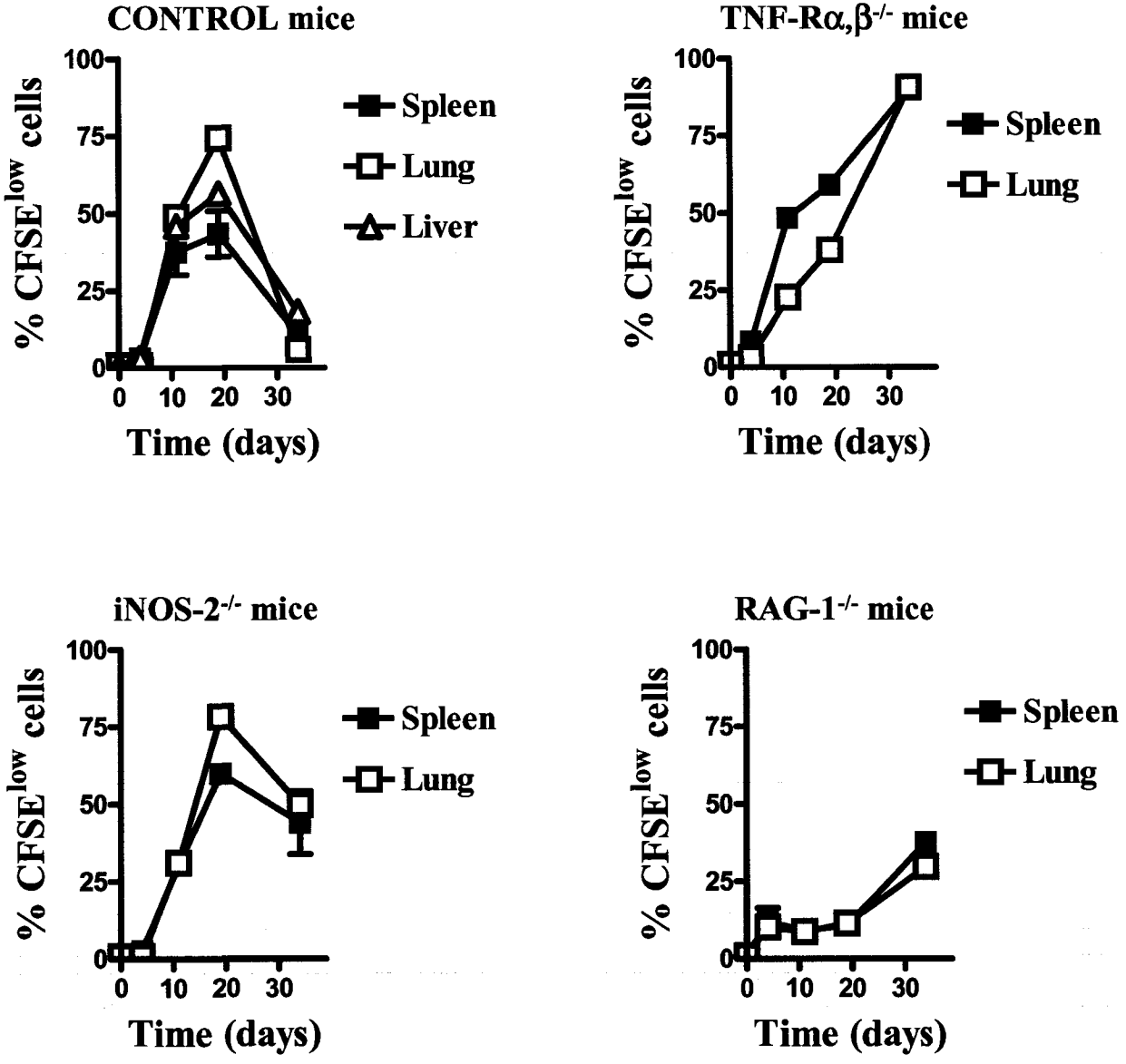
CONTROL mice
% CFSE low cells
100
75
50
25
0
0 10 20 30
Time (days)
Spleen
Lung
Liver
TNF-Rα,β-/- mice
% CFSE low cells
100
75
50
25
0
0 10 20 30
Time (days)
Spleen
Lung
iNOS-2-/- mice
% CFSE low cells
100
75
50
25
0
0 10 20 30
Time (days)
Spleen
Lung
RAG-1-/- mice
% CFSE low cells
100
75
50
25
0
0 10 20 30
Time (days)
Spleen
Lung

recipient mice were harvested 4 days post adoptive transfer and processed as in section 2.3. $1x10^7$ cells were obtained and stained with anti-CD8α antibody and H-2K^{b}Ova$_{257-264}$ tetramers. Two mice per time point were evaluated and the experiment was performed twice. The graph shows the evaluation of 4 mice at each time point. As is clear from Figure 27 A the delay in antigen-presentation was comparable in the controls and the CD4 and CD8-knockout mice. However, at later time periods the curtailment in antigen-presentation was considerably reduced in CD8- but not in CD4 deficient mice, indicating that endogenous $CD8^+$ T cells are partly responsible for

regulating the persistence of antigen-presentation. Higher burden at later time points was also noted in the CD4-knockout mice more so than the CD8-knockout mice in comparison to the controls (Figure 27 B). At day 30 of infection, CD4-knockout mice harbor a 10-fold increased bacterial burden relative to controls, yet the antigen presentation is curtailed similar to the controls. On the other hand, CD8-knockout mice having a BCG-Ova burden similar to the controls at this time point, yet antigen-presentation was not curtailed in these mice as strongly as controls. This lends validity to the idea that the higher BCG-Ova burdens seen in the various knock-out mice (in Figure 25) do not seem to be contributing to the rescue of curtailment in antigen-presentation.

3.6.5 – Effects of early inflammation on the delayed $CD8^+$ T cell response to BCG-Ova.

The delayed $CD8^+$ T cell response in BCG-Ova infected mice (Figures 3-7) correlates very well with the delayed antigen-presentation that was noted in control as well as the various knock-out mice (Figures 25-27). Since BCG is a highly attenuated pathogen that doubles very slowly, it was speculated that BCG might induce reduced inflammatory signals initially in comparison to other potent pathogens such as LM. To this end, the development

Figure 27: Kinetics of antigen presentation during BCG-Ova infection in CD4 and CD8 knockout mice. C57BL/6 mice (WT) and CD4 and CD8 knock-out mice on C57BL/6 background were injected with BCG-Ova (10^4 i.v.). At various time points post infection CFSE-labelled cells from OT-1R transgenic donor mice were injected into the recipient mice i.v. ($8x10^6$). The CFSE labelled donor cells were parked for 4 days in the recipient mice. The spleens from the recipient mice were harvested and stained with H-2K^{b}OVA$_{257-264}$ tetramers and anti-mouse CD8α antibody. The expression of CFSE was assessed based on Tetramer$^+$ donor CD8$^+$ T cells. Each time point involved the evaluation of 4 mice per group per time point. The graph shows the average percentages of CFSE^{lo} OVA$_{257-264}$-specific CD8$^+$ T cells for the 2 mice at each given time point based on a PBS control group (A). The bacterial burden in the spleens of the mice was assessed by performing serial dilutions of the homogenized spleen in PBS-T80 and plating on 7H10+OADC agar plates (B).

Figure 27

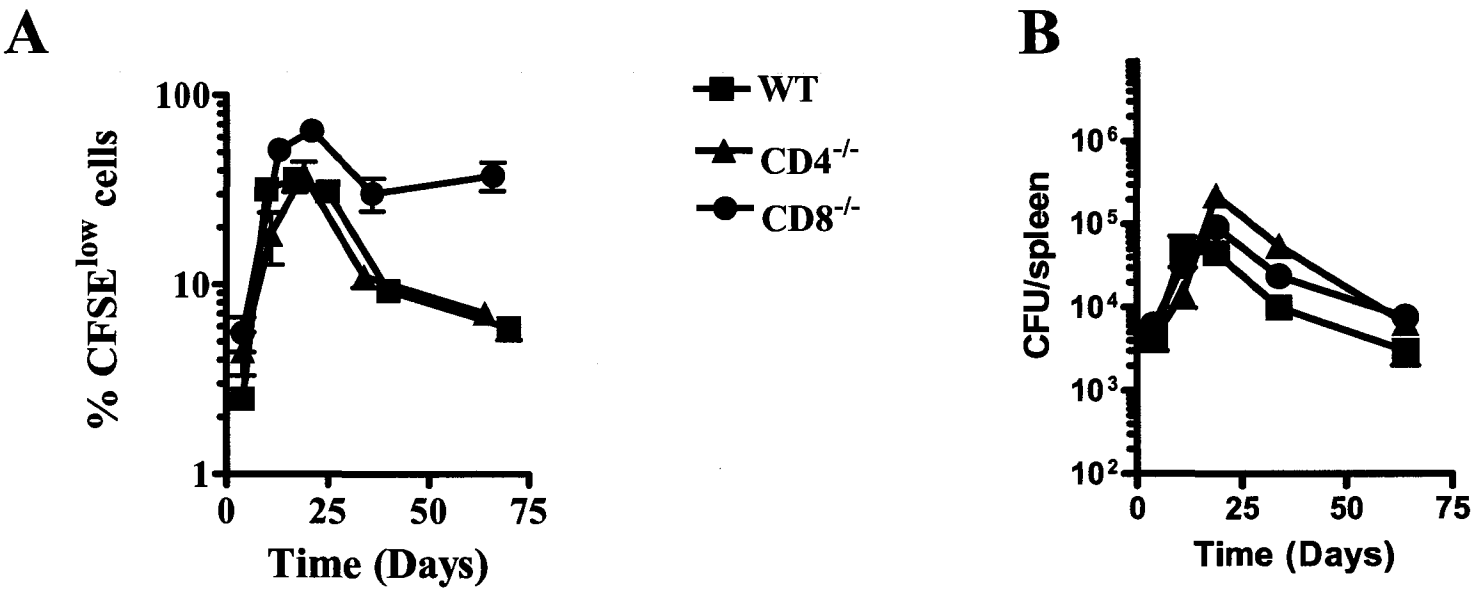
A
100
10
1
% CFSE^low cells
0
25
50
75
Time (Days)
WT
CD4-/-
CD8-/-
B
10^6
10^5
10^4
10^3
10^2
CFU/spleen
0
25
50
75
Time (Days)

of $CD8^+$ T cell response was evaluated by co-injecting mice with additional factors that induce potent inflammation (such as CpG, polyI-C and even LM).

To see if the delay in the antigen specific $CD8^+$ T cell response during BCG-Ova infections could be rescued, $1x10^6$ OT-1 splenocytes were injected i.v. into naïve C57BL/6 mice. These mice were injected with BCG-Ova 10^4 i.v. On day 0, day3, and day 5 one group of mice received CpG i.p., and on the same days a control group of mice received PBS i.p. as a control. CpG was given to induce inflammation early in a BCG-Ova infection to see if the delayed $CD8^+$ T cell response could be rescued. The blood from these mice were harvested on days 7, 14 and 21 post infection and processed as in section 2.8. 100ul of blood was obtained and stained with anti-CD8α and H-$2K^b$$Ova_{257-264}$ tetramers as in section 2.8. Enhancement of early inflammation by CpG did not seem to rescue the delay in the antigen specific $CD8^+$ T cell response (Figure 28A). Rather an opposite effect was noted. Massive splenomegaly was noted in the CpG treated group (figure 28 B) commensurate with increased inflammation. Similarly, the $CD8^+$ T cell response was not enhanced when mice were injected with other stimulants such as poly I-C, or LM (data not shown). Thus, the delay in $CD8^+$ T cell priming during BCG-Ova infection does not seem to be due to a lack of appropriate inflammatory signals.

In summary the data indicates that antigen-presentation, $CD8^+$ T cell priming and expansion is delayed during BCG-Ova infection and that this delay cannot be rescued by enhancement of inflammatory signals early on, or removal of inflammatory signals, such as TNF, IFN-γ and iNOS-2. Further, despite persistence of the pathogen, antigen-presentation and $CD8^+$ T cell expansion are curtailed after the second week of infection and this curtailment of antigen-presentation seemed to be regulated by multiple mechanisms involving endogenous $CD8^+$ T cells and inflammatory cytokines such as IFN-γ.

Figure 28: Influence of enhancement of early inflammation on the $CD8^+$ T cell response to BCG-Ova. C57BL/6 mice were injected with OT-1 cells ($1x10^6$) followed by BCG-Ova (10^4 i.v.). On day 0, day3, and day 5 one group of mice received CpG i.p., and on the same days, a control group of mice received PBS i.p. as a control. Blood was harvested 7 days and 14 days post infection and stained with H-$2K^b$$OVA_{257-264}$ tetramers and anti-mouse CD8α antibody. The percentage of $Ova_{257-264}$-specific $CD8^+$ T cells was determined by gating on $CD8^+$ cells followed by further gating on $tetramer^+$ cells. Each time point involved the evaluation of 3 mice per group per time point. The graph shows the average percentages of $OVA_{257-264}$-specific $CD8^+$ T cells for the 3 mice at each given time point (A). CpG induced massive splenomegaly as a result of inflammation as indicated by the spleen cell numbers (B).

Figure 28

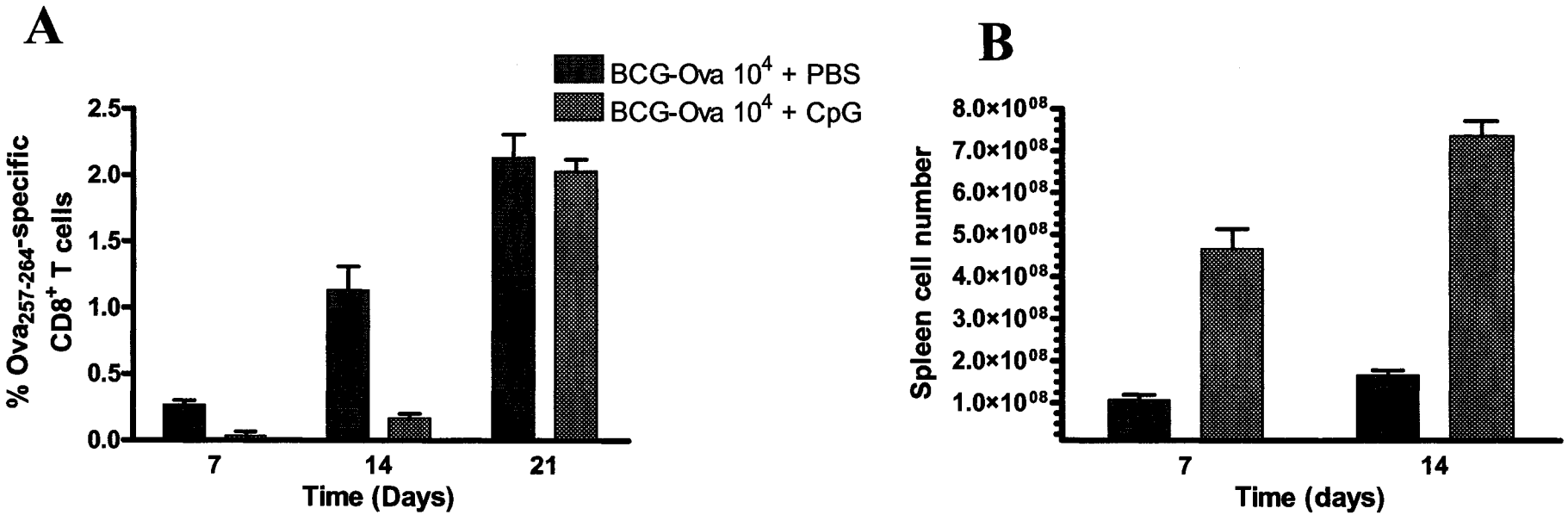
A
BCG-Ova 10^4 + PBS
BCG-Ova 10^4 + CpG
% Ova257-264-specific CD8+ T cells
2.5
2.0
1.5
1.0
0.5
0.0
7
14
21
Time (Days)
B
Spleen cell number
8.0×10^08
7.0×10^08
6.0×10^08
5.0×10^08
4.0×10^08
3.0×10^08
2.0×10^08
1.0×10^08
7
14
Time (days)

3.7.0 – Influence of antigenic dose on the delay in $CD8^+$ T cell priming during BCG-Ova infection

Although it is clear that higher antigenic doses induce stronger T cell responses, the kinetics of $CD8^+$ T cell expansion and contraction remain identical in the various viral infection models as well as against LM [55]. However, the aim of this study was to determine why the delay in $CD8^+$ T cell priming was occurring despite using a BCG-Ova dose as high as 10^4 iv. Since the enhancement of inflammation in the spleen did not seem to rescue the delay in the antigen specific $CD8^+$ T cell response it was thought that maybe increasing the amount of antigen initially would rescue the delay.

3.7.1 – The influence of initial amount of pathogen burden on $CD8^+$ T cell activation.

C57BL/6 mice were injected with $1x10^6$ OT-1 splenocytes i.v. and challenged with 10^4 or 10^6 dose of BCG-Ova or LM-Ova 10^4 i.v. At various time points the spleens from these mice were harvested and processed as in section 2.3. $1x10^7$ cells were obtained and stained with anti-CD8α, anti-CD127, anti-CD25, and anti-CD69 antibodies, followed by staining with H-$2K^bOva_{257-264}$ tetramers as in section 2.8. The cells were fixed and acquired on EPICS XL Flow cytometer and analyzed using the EXPO software. Surprisingly, infection with a 100-fold higher dose of BCG-Ova (10^6 iv) resulted in a rapid $CD8^+$ T cell response which peaked by day 7 of infection followed by contraction subsequently (Figure 29 A), a situation that seemed to be similar to LM-Ova. Thus, from this data it appeared that the initial amount of antigenic stimulation was the reason for the delay in $CD8^+$ T cell priming. Correlating with early activation of $CD8^+$ T cells, infection of mice with 10^6 BCG-Ova resulted in detectable increase in the expression of CD69 (Figure 29 B), an early T cell activation marker. Expression of this marker remained undetectable with the 10^4 dose of BCG-Ova. However, another early T cell activation marker, CD25, was not detected on the

Figure 29: Influence of BCG-Ova dose on CD69, CD25, and CD127 cell surface expression on antigen specific $CD8^+$ T cells. C57BL/6J recipient mice were injected with $1x10^6$ OT-1 donor cells and subsequently infected with LM-Ova or BCG-Ova $1x10^4$ (i.v.) or BCG-Ova $1x10^6$ (i.v.). At various time intervals, spleens were harvested from the recipient mice and the percentage of $OVA_{257-264}$-specific $CD8^+$ T cells were evaluated after staining with anti-CD8α and H-$2K^bOVA_{257-264}$ tetramers (a), and anti-CD69 (b), anti-CD25 (c), and anti-CD127 (d) antibodies. Each group involved the evaluation of 4 mice per time point. The graphs show the average percentage of the cell surface expression of the given marker on the $OVA_{257-264}$-specific $CD8^+$ T cells of the 4 mice at each given time point.

Figure 29

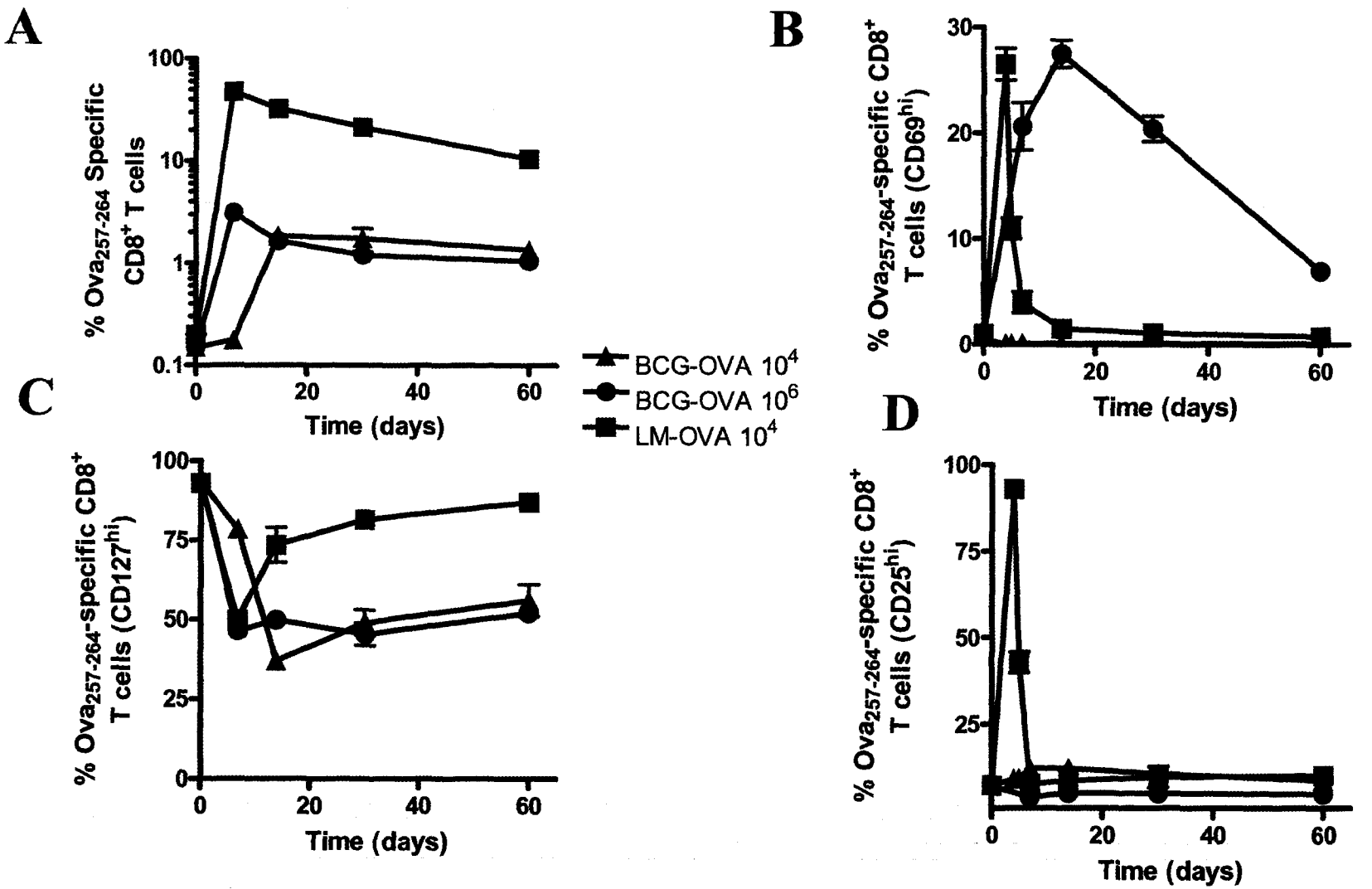
A
% Ova257-264 Specific CD8+ T cells
100
10
1
0.1
0
20
40
60
Time (days)
BCG-OVA 10^4
BCG-OVA 10^6
LM-OVA 10^4
B
% Ova257-264-specific CD8+ T cells (CD69hi)
30
20
10
0
0
20
40
60
Time (days)
C
% Ova257-264-specific CD8+ T cells (CD127hi)
100
75
50
25
0
0
20
40
60
Time (days)
D
% Ova257-264-specific CD8+ T cells (CD25hi)
100
75
50
25
0
20
40
60
Time (days)

cell surface with the 10^6 dose of BCG-Ova similar to that seen with the 10^4 dose. Throughout BCG-Ova infection with the 10^4 dose, the cell surface expression of CD127 was delayed in its down-regulation from the cell surface of antigen specific $CD8^+$ T cells. Also, CD127 cell surface expression never returned to levels seen on naïve $CD8^+$ T cells even after 30 days of infection as in section 3.3.1. Infection with the 10^6 dose of BCG-Ova resulted in a rapid down-regulation of the cell surface expression of CD127, similar to that in LM-Ova infected mice (Figure 29 C). Thus, these results clearly indicate that a higher dose of BCG-Ova induces stronger activation of $CD8^+$ T cells which results in rapid expansion of $CD8^+$ T cell response which is detectable at day 7.

3.7.2 – The influence of initial amount of pathogen burden on antigen-presentation during BCG-Ova infection.

Considering that a higher dose of BCG-Ova induced an early detectable population of Ova-specific $CD8^+$ T cells which underwent attrition subsequently, it was speculated that the onset of antigen-presentation during infection with the high dose of BCG-Ova might be earlier. To evaluate in vivo response to antigen presentation in a higher dose of BCG-Ova, BCG-Ova 10^4 or 10^6 i.v. was injected at day -1, day -7, day-14, day -30 and day -60 into naïve C57BL/6 mice. On day 0, $8x10^6$ CFSE labeled splenocytes from OT-1R mice were injected into these mice. The spleens from the recipient mice were harvested 4 days post adoptive transfer and processed as in section 2.3. $1x10^7$ cells were obtained and stained with anti-CD8α antibody and H-$2K^bOva_{257-264}$ tetramers. The cells were fixed and acquired on EPICS XL Flow cytometer and analyzed using the EXPO software. Figure 30 shows the response to in vivo antigen presentation of the OT-1 $CD8^+$ T cells responding to low or high dose of BCG-Ova (Figure 30 A), along with the bacterial burden in those mice (Figure 30 B). Two mice per time point were evaluated and the experiment was performed twice. Compared

Figure 30: Influence of BCG-Ova dose on the kinetics of antigen presentation. C57BL/6 mice were injected with BCG-Ova 10^4 i.v. or BCG-Ova $1x10^6$ i.v. At various time points post infection CFSE-labelled cells from an OT-1R transgenic donor mouse were injected into the recipient mice i.v. ($8x10^6$). The CFSE labelled donor cells were parked for 4 days in the recipient mice. The spleens from the recipient mice were harvested and stained with H-$2K^bOVA_{257-264}$ tetramers and anti-mouse CD8α antibody. The expression of CFSE was assessed based on $Tetramer^+$ donor $CD8^+$ T cells. Each time point involved the evaluation of 4 mice per group per time point. The graph shows the average percentages of $CFSE^{lo}$ $OVA_{257-264}$-specific $CD8^+$ T cells for the 4 mice at each given time point based on a PBS control group (A). The bacterial burden in the spleens of the mice was assessed by performing serial dilutions of the homogenized spleen in PBS-T80 and plating on 7H10+OADC agar plates (B).

Figure 30

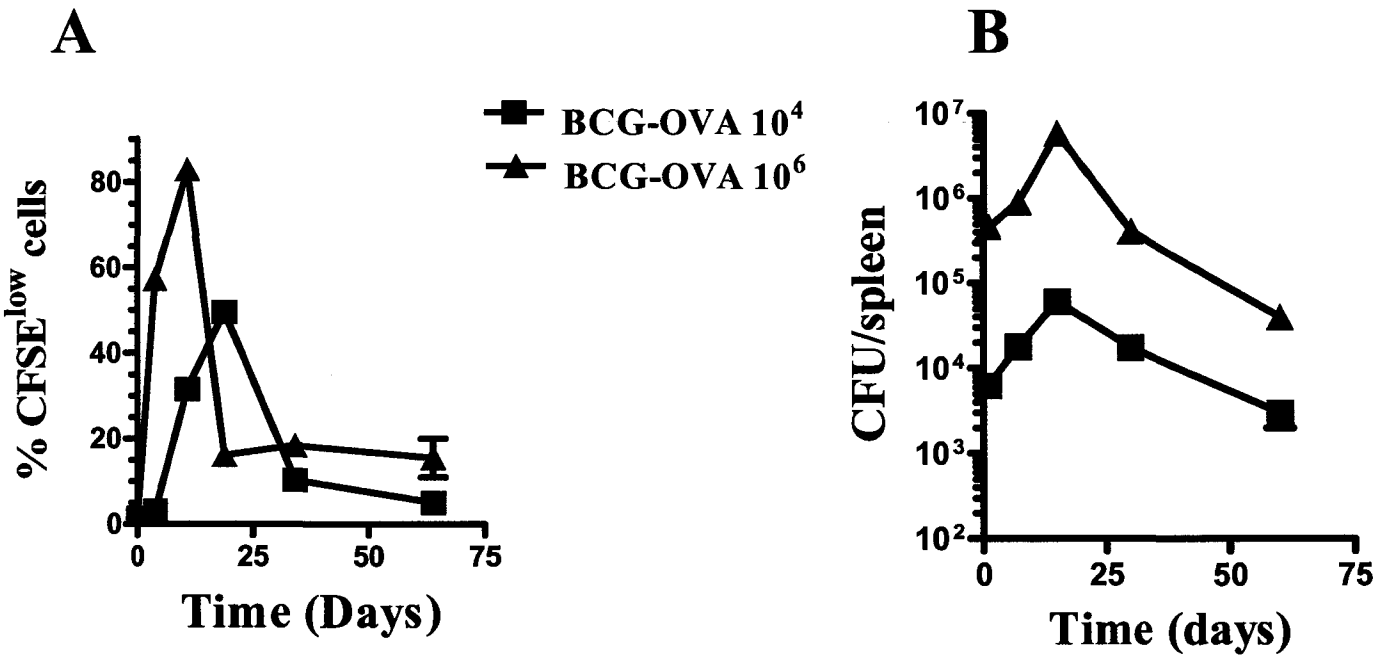
A
B
BCG-OVA 10^4
BCG-OVA 10^6
% CFSE^low cells
0
20
40
60
80
0
25
50
75
Time (Days)
CFU/spleen
10^2
10^3
10^4
10^5
10^6
10^7
0
25
50
75
Time (days)

to the 10^4 dose of BCG-Ova, infection with the 10^6 dose of BCG-Ova resulted in an early onset of antigen-presentation (Figure 30 A), which was followed by an earlier curtailment of antigen-presentation. As expected the higher dose of BCG-Ova resulted in higher bacterial burden (~100 fold) at all the time intervals (Figure 30 B), yet antigen-presentation was still curtailed at later time intervals, further indicating that the reduced curtailment in antigen-presentation that was seen with the various knock-out mice (Figure 25) was not mainly due to increased bacterial burden.

3.7.3 – Quantification of the mRNA expression of Ova in spleens of mice infected with BCG-Ova

mRNA expression of Ova in spleens of mice infected with BCG-Ova was quantified using quantitative real-time PCR. Naïve C57BL/6 mice were injected with BCG-Ova 10^6 i.v. and the spleens were harvested at various time points during the infection. Absolute quantification of the expression of Ova by BCG-Ova was carried out using the SYBR green method of quantification as in section 2.13. Primer efficiencies were between 100% and 98%. Figure 31 shows the quantification of mRNA of Ova and 16S rRNA in BCG-Ova infected spleens along with the corresponding CFU/spleen. Four mice per time point were evaluated. Four naïve C57BL/6 mice were processed along side and used as a control. Expression of 16S rRNA and Ova are highest on day 7 and decline thereafter. This seemed to correlate with the drop in the bacterial burden. When the ratio of Ova mRNA expression to 16S rRNA mRNA expression was measured there was no apparent change in the ratio of expression. This indicates that the stability of the Ova mRNA expression is similar to that of the 16S rRNA mRNA expression. Overall in quantitative terms, higher dose of BCG-Ova resulted in higher mRNA expression of Ova. Further, the expression of Ova was at its peak during the first few weeks of infection, which was followed by a gradual reduction in Ova-

Figure 31: Ova mRNA and 16S mRNA expression in BCG-Ova infected spleens. C57BL/6 mice were injected with BCG-Ova (10^4 i.v.) or with BCG-Ova (10^6 i.v.). At various time points post infection spleens from these mice were harvested and snap frozen in dry-ice ethanol bath. Total RNA was extracted and 15ug of RNA was taken to make cDNA. The cDNA was the quantified using gene-specific primers for Ova and 16S rRNA and the SYBR green method of quantification as outlined in the materials and methods (section 2.13) and in the results section. Each time point involved the evaluation of 4 mice per time point. The graphs show the average attomoles of mRNA for each gene and the corresponding CFU's within the spleen at that particular time point. The bacterial burden in the spleens of the mice was assessed by performing serial dilutions of the homogenized spleen in PBS-T80 and plating on 7H10+OADC agar plates.

Figure 31

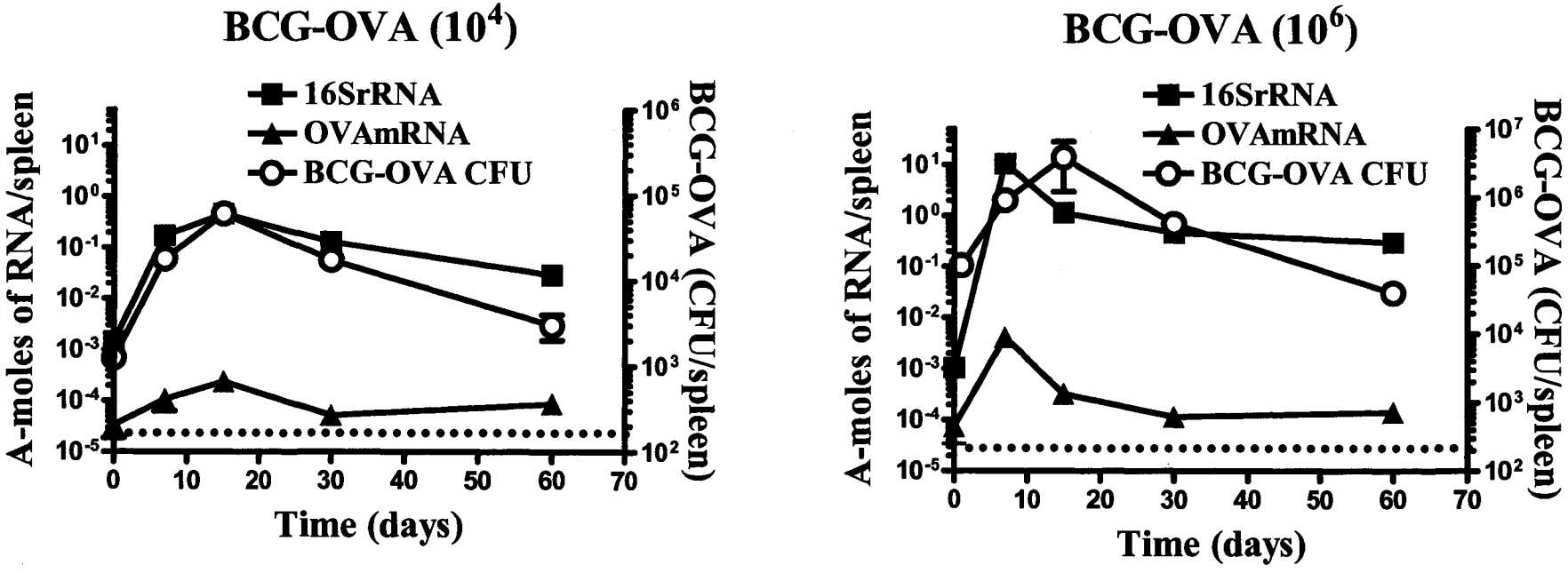
BCG-OVA (10^4)
16SrRNA
OVAmRNA
BCG-OVA CFU
A-moles of RNA/spleen
BCG-OVA (CFU/spleen)
Time (days)
BCG-OVA (10^6)
16SrRNA
OVAmRNA
BCG-OVA CFU
A-moles of RNA/spleen
BCG-OVA (CFU/spleen)
Time (days)

expression thereafter and maintenance of low-level expression subsequently.

In summary, in contrast to other infection models, where the relative timing of antigen presentation and the timing of expansion and contraction of T cell response are not governed by the antigenic dose [55], in the BCG-Ova infection model dose seems to be an important factor. Infection with the higher dose of BCG-Ova causes an earlier onset of antigen-presentation, followed by a rapid expansion of $CD8^+$ T cell response followed by a greater contraction subsequently. This correlated with the expression of Ova mRNA in the spleens and with the rapid and increased activation status on primed $CD8^+$ T cells.

4.0 - Discussion

The ability of memory $CD8^+$ T cells to exhibit cytolytic activity, produce inflammatory cytokines and most importantly to persist for long periods of time and respond rapidly upon secondary infection make them crucial for effective elimination of a given pathogen. Antigen presentation is a key initial event during an immune response that directly affects the differentiation and magnitude of the $CD8^+$ T cell response and consequently has profound implications for long term protection against pathogens [107-109]. However, the mechanisms that dictate the induction and maintenance [8;110;111] along with the differentiation [112-115] of $CD8^+$ T cells are still not fully clear. The general paradigm of T cell memory has been derived mainly from viral infection models which indicate that antigen-presentation occurs rapidly within the first few days of infection which results in massive clonal expansion of antigen-specific $CD8^+$ T cells which peak around day 7 of infection followed by an equally swift contraction phase [111;113]. Complicating matters however, is that this general paradigm of differentiation, expansion, and contraction of $CD8^+$ T cells [111;113] does not seem to apply in the case of pathogens that reside within the phagosomes [10;116;117]. Understanding the mechanisms that govern antigen presentation to $CD8^+$ T cells along with their induction, differentiation, and maintenance when combating a phagosome-residing pathogen are key to developing novel vaccine strategies to combat these types of pathogens.

Each pathogenic encounter with the host results in host-pathogen interactions that are unique to that particular pathogen and it can be misleading to generalize the paradigm when intracellular pathogens display enormous differences. For example, pathogens have differences in virulence, replication and intracellular niche. Pathogens vary in the nature of lipid content on their surface which influences the nature of inflammation that is induced.

Some or all of these factors can influence the relative host-pathogen interactions which could have an impact on T cell response and memory generation.

In order to track the $CD8^+$ T cells responding to LM-Ova and BCG-Ova an adoptive transfer model was employed using OT-1 mice. These cells were adoptively transferred into naïve C57BL/6 mice and those mice were infected with either LM-Ova or BCG-Ova as the experiment dictated. OVA was used as a model antigen because the CTL epitope, $OVA_{257-264}$, has been well characterized, $CD8^+$ T cells against $OVA_{257-264}$ have been shown to elicit protection in vivo against a challenge with OVA-expressing tumor cells [95]. Additionally, by using the adoptive transfer model with OT-1 transgenic mice the response of $CD8^+$ T cells to two different pathogens could be tracked directly by flow cytometry because the T cells are responding to the same antigen. This avoids the problem of $CD8^+$ T cells responding to different endogenous peptides that vary between the pathogens and that would have varying immunodominance. These models have been commonly used and the results have been shown to correlate very well to those obtained in the absence of transgenic cells [117]. Thus, the results obtained in this study can be extrapolated to physiological circumstances.

The $CD8^+$ T cell response to BCG-Ova is both delayed and quantitatively reduced in comparison to that induced against LM-Ova. This may be attributed to various factors such as differences in their doubling times (~ 46 min for LM versus ~ 30 hours for BCG), their different intracellular niches (cytosolic versus phagosomal), their virulence, and the type of infection they induce (chronic versus acute). While the slow replication of BCG implies that this may be one of the reasons for the delayed and muted $CD8^+$ T cell response, however, in a recent study the $CD8^+$ T cell response against the virulent *Salmonella typhimurium*, an intracellular bacterium that persists within phagosomes and replicates faster than LM, was reported to be delayed and muted in comparison to that induced against LM-Ova [10;116]. It

is most likely that the differing intracellular niches contribute to the differences in the kinetics and magnitude of the CD8+ T cell response. Since LM escapes from the phagosome and enters the cytosol, it is now exposed to the classical MHC class I pathway of antigen processing and presentation, where as phagosomal pathogens such as BCG remain in the confines of the phagosome, hidden from this pathway. Although both LM and BCG survive within APCs, they exhibit differences in their intracellular life-style. LM escapes from the phagosome and proliferates in the cytosol of infected cells. In contrast, BCG replicates inside the phagosome that poses a hostile and changing environment characterized by poor nutrient content, progressive decrease of the pH, and delivery of antibacterial peptides and lysosomal enzymes. Thus, Mycobacteria have evolved ways to survive this environment by inhibiting phagosome maturation [118;119], and interfering with nitrous oxide synthesis [120]. This, in combination with the rapid growth of LM, which would result in massive amounts of antigen being processed and presented, may explain why the response to BCG is muted as compared to LM.

Another important difference between LM and BCG lies in the relative virulence of the two pathogens. While a virulent strain of LM was used in this study, BCG is a highly attenuated pathogen and it is possible that virulence of the pathogen profoundly influences $CD8^+$ T cell priming. In that context, although the doubling time of LM and BCG was measured in vitro, it is still not clear what the doubling time of the two pathogens would be once inside the macrophage in vivo.

The muted $CD8^+$ T cell response observed in BCG-Ova infection is highlighted by the lack of CD69 and CD25 up-regulation. This indicates that $CD8^+$ T cells that are primed during BCG-Ova infection do not get stimulated profoundly. In fact it has been shown that the lack of STAT3 or STAT5a expression prevents the expression of CD25 in response to

signaling via either TCR or the IL-2 cytokine/receptor engagement, leading to a failure of IL-2-driven T cell proliferation [121;122]. It may be that the reduced stimulation via the TCR in the case of BCG infection does not activate the Jak3-STAT pathway even with the high dose. Since CD25 associates with CD122 and the common gamma chain to generate the high affinity receptor for IL-2, it may be possible that CD25 expression is needed more so in order to increase the magnitude of the response [123] rather than initially promoting the response [123;124]. This may be why in the high dose the priming of $CD8^+$ T cell response is not delayed, but the clonal expansion and the magnitude of the response was still low due to lack of CD25 expression. Another important indicator of the reduced stimulation experienced by $CD8^+$ T cells during BCG-Ova infection are the results of the CD62L cell surface expression. The vast majority of the Ova-specific $CD8^+$ T cells induced during BCG-Ova infection did not down-regulate CD62L expression. It was recently reported that reduced stimulation of naïve $CD8^+$ T cells results in their reduced down-regulation of CD62L expression [117]. Interestingly, it has been reported that during infection with the virulent phagosomal intracellular bacteria, ST, the majority of the primed $CD8^+$ T cells expressed low levels of CD62L and high levels of CD69 [10]. This suggests that pathogen virulence may influence the activation and phenotype of primed cells.

The pathway that $CD8^+$ T cells embark on to differentiate into memory cells is still not clear. Some suggest T cells become effectors immediately after priming and the surviving effectors gradually differentiate into the central phenotype memory cells [113]. Others contend that T cells differentiate into a central state first and the intensity of stimulation governs the extent to which the cells will differentiate into the effector phenotype [112;125] and some others argue that central and effector cells arise from separate lineages completely and do not differentiate into one-another [126;127]. The results presented in this

thesis indicate that the $CD8^+$ T cells induced during BCG-Ova infection display a central phenotype early on and do not appear to differentiate overwhelmingly into the effector phenotype. This tends to imply that the central and effector cells may perhaps represent separate lineages. However, the responses were evaluated only in the spleen and the interpretations may be misleading when responses are measured only in one organ. It is possible that the profile in the blood or other non-lymphoid organs is different. Overall, the $CD8^+$ T cell differentiation pathway may be sensitive to modulation by pathogens, and the specific interplay of host cells with varied pathogens may explain the occurrence of the different differentiation models.

The delay in the overall $CD8^+$ T cell response to BCG has also been observed in murine infection models with salmonella [10;116]. This delayed response is highlighted by the delayed down-regulation of CD127, and the delay in cycling, and antigen presentation. Surprisingly, this delay in antigen-presentation and T cell activation is observed even when conventional memory $CD8^+$ T cells respond to BCG-Ova. This was observed in the case of salmonella infection models as well [10]. In comparison to naïve $CD8^+$ T cells, conventional memory $CD8^+$ T cells are bestowed with increased ability and sensitivity to rapidly respond to antigenic encounter. These results further highlight that antigen-presentation is delayed during infection with phagosomal intracellular bacteria. This raises an important issue as to how effective vaccine-induced memory cells would be at clearing such phagosomal residing intracellular pathogens? As a result of these findings it would seem that new strategies would need to be developed in order to control and eliminate these pathogens.

Infection of mice with higher doses of LM or various viruses while increasing the magnitude of $CD8^+$ T cell response does not change the timing of expansion and contraction of the $CD8^+$ T cell response [55]. The extent of $CD8^+$ T cell contraction remains constant as

~90% of the primed $CD8^+$ T cells are eliminated by apoptosis irrespective of the pathogen dose used. In the majority of the experiments in this study a BCG-Ova dose of 10^4 was used. However, when a 100-fold higher dose of BCG-Ova (10^6) was used, rapid expansion of Ova-specific $CD8^+$ T cells was noted as the peak $CD8^+$ T cell response shifted from day 21 to day 7. Most likely the $CD8^+$ T cells experienced stronger stimulation with the higher dose of BCG-Ova since an increase in the expression of CD69 and a more rapid decrease in the expression of CD127 was detected on the cell surface of Ova-specific $CD8^+$ T cells. Furthermore, unlike the lower dose of BCG-Ova where little contraction of the response was noted, contraction of the $CD8^+$ T cell response was greater with the higher dose of BCG-Ova. It should also be noted that the overall response was still muted despite the expression of CD69 and this could be because the antigenic levels would still be lesser than those generated during LM-Ova infection. Increased activation of $CD8^+$ T cells during infection with the higher dose of BCG-Ova could be due to excess levels of antigen or due to excess inflammation induced by the glycol-lipids present on the bacterial surface. However, several other immune stimulants were injected into mice that received the reduced dose of BCG-Ova and there was no enhancement in the $CD8^+$ T cell priming, thereby indicating that increased stimulation of $CD8^+$ T cells that occurs with the higher dose of BCG-Ova is due to the presence of higher antigenic levels. In fact repeated administration of mice with CpG while increasing inflammation resulted in a decreased number of Ova-specific $CD8^+$ T cells implying that too much inflammation may be deleterious to $CD8^+$ T cell priming. In fact it has been shown that reduced antigen-MHC complexes lead to the delayed activation of TCRVβ-bearing T cells [128] and this would have implications for the overall effector function and quality of the response [129]. It is thought that due to BCG's unique phagosomal intracellular location in combination with it's slow growth, that the amount of antigen

generated would be quite low and thus there would be few Ova-MHC complexes causing the delayed response.

The delayed antigen presentation was found to be exacerbated in Rag-1 knockouts suggesting that the lymphocytes that are lacking in these mice are necessary to promote antigen presentation early in infection. However, when antigen presentation was evaluated in $CD4^+$ and $CD8^+$ deficient mice the delay was similar to that of the control mice. It should be noted that the APCs in the Rag-1 knockout mice are functional in terms of maturation and ability to induce $CD8^+$ T cells [130]. It is possible that the exacerbated delay in antigen-presentation in Rag1-knockout mice may be due to a lack of inflammatory cytokines present early in infection being produced by members of the innate immune system such as gamma-delta T cells which are also absent in the Rag-1 knockouts. In fact gamma-delta T cells have been shown to present mycobaterial antigens via an MHC-independent pathway and provide key cytokines initially to drive the adaptive response [131-133] and these T cells would not be present in the Rag-1 knockout mice [134]. This may be especially important in the case of BCG because the antigens mainly presented by the MHC-independent pathway to gamma-delta T cells are lipid and glycolipid antigens in the hydrophobic cavity of the CD1 molecule and Mycobacteria have a very lipid rich cell wall. In fact it has been shown that in Mycobacterial infections, the peak of gamma-delta T cell expansion occurs at 7 days postinfection preceding the 2-3 week peak of the alpha-beta T cell expansion and peak bacterial burden [131]. These gamma-delta T cells in the lungs of BCG-infected mice secreted IFN-gamma and were cytotoxic against BCG-infected peritoneal macrophages [131].

A surprising observation during the $CD8^+$ T cell response is that antigen-presentation seems to be drastically curtailed after the third week of BCG-Ova infection despite the continued persistence of the bacterium. One would think that since the pathogen is present,

antigen would continue to be presented to the $CD8^+$ T cells and they would continue to differentiate/divide. The various mechanisms that can potentially contribute to this decline in antigen-presentation are listed below:

The first comes from studies on antigen-presentation during LM infection model. In typical acute infections such as LM antigen presentation peaks very early in infection in the first few days (0-4 days) and becomes curtailed as T cell responses develop around 6-10 days of infection to counteract the proliferating pathogen. After 10 days, once the pathogen has been eliminated from the system, antigen presentation ceases. Proliferating LM-specific T cells would rapidly kill antigen-bearing APCs and hence prevent their ability to present antigen. This mechanism would limit continued activation of $CD8^+$ T cells even during an acute infection and hence help in preserving the fate and function of the primed $CD8^+$ T cells. As with LM [135], the development of host T cell responses may also restrict antigen-presentation during BCG-Ova infection. It should be noted as well that the decline in antigen presentation coincides with the peak of the $CD8^+$ T cell response and thus the cytolytic $CD8^+$ T cells may be destroying the APCs. Furthermore, the curtailment in antigen-presentation was reduced in Rag1- and CD8-knockout mice. The length of time needed for the dying APCs to be replenished by new ones is not known.

The second possibility is that the inflammatory mediators produced by members of the innate and acquired immune system, such as IFN-γ, TNF and nitrite ions might also cause rapid demise of antigen-bearing target cells during BCG-Ova infection, thus preventing their ability to present antigens continually. Considering that BCG induces a chronic infection and possesses a cell wall that is loaded with highly stimulatory lipid structures [97] it is quite likely that inflammatory mediators are produced chronically during BCG infection. Indeed, antigen-presentation was not strongly curtailed after the third week of BCG-Ova infection in

mice that are deficient in IFN-γ, iNOS2 and TNF-Rαβ. In such knock-out mice the bacterial burden was higher than the control mice and it appears that this may be the reason that antigen-presentation does not get curtailed strongly after the first few weeks of infection. However, when one looks closely at the bacterial burden at day 30 for example, the bacterial burden is similar in the various knock-out strains of mice yet antigen presentation is so varied.

The third possibility is that the curtailment in antigen presentation may be occurring due to BCG-Ova disposing of the plasmid containing the gene for Ova. The gene for Ova in BCG-Ova is contained on a plasmid which confers resistance to the antibiotic kanamycin. In the mouse there is no selective pressure forcing the bacteria to maintain the plasmid. Thus, the stability of the plasmid could be called into question. To this end the bacterial burden was evaluated in the presence of kanamycin and most of the time points did not show major inconsistencies between the numbers of colonies on the kanamycin plates compared to the antibiotic free plates. Also, the curtailment of antigen presentation in the control mice occurs around 30 days of infection and at this time point the majority of the bacteria still maintain the plasmid.

The fourth possibility is that the relative amount of Ova declines despite the persistence of Ova. When the relative expression of Ova mRNA was measured, it was expressed at a similar ratio to the mRNA of the BCG 16S rRNA. Thus, the stability of the antigen itself seems adequate. However, when the overall level of Ova was measured in absolute terms, Ova mRNA level declined rapidly within the first month, which could perhaps be a major reason for curtailment in antigen-presentation. An important question that arises is why would the mRNA level of Ova decline during BCG-Ova infection? This could partly be due to the reduction in bacterial burden that occurs after the first few weeks

of infection. However, it is also possible that the bacteria go into some sort of a "non-replicative persistent" state. Indeed, it has been shown that Mycobacteria enter a state of non-replicative persistence in mice [136]. In fact it has been shown in vivo and in vitro that when placed under low nutrient stress [137;138] or low oxygen stress [139] that Mycobateria enter a dormancy-like state. When an activated T cell recognizes an infected macrophage, it releases cytokines such as IFN-γ and TNF-α and TNF-β that activate the macrophage and induce phagosome-lysosomal fusion and macrophage bactericidal activity [140]. This causes up-regulation of the TNF receptors on the macrophage and causes it to produce TNF-α. This autocrine system causes an increase in pH within the phagosome along with increased nitrous oxide production and free radical production [140].

From this information a speculative model is proposed in an attempt to explain what may be occurring in this infection model at later stages of infection. It is speculated that in the control mice, inflammatory mediators are thought to be applying stress to BCG within the hostile environment of the phagosome. In response to this stress BCG may be entering a state of non-replicative persistence. This causes the overall antigen to decline to low levels. When some of the inflammatory mediators are removed or the cells that provide those mediators are removed the stress on BCG is alleviated and thus the curtailment in antigen presentation does not occur as fast as what is seen in the control mice.

Along with the decline in antigen presentation the frequency of Ova-specific $CD8^+$ T cells seems to plateau rather than increase or decrease. Surprisingly, there is no major contraction of $CD8^+$ T cell response during BCG-Ova infection that is typical of acute or chronic viral infection models [55]. It is possible that either the response itself is qualitatively so different in that the primed cells get reduced stimulation and do not up-regulate the genes that would commit them for apoptosis. Additionally, it is possible that contraction of the

$CD8^+$ T cell response does happen, but that is offset by the continued, low-level, antigen-presentation which recruits a low number of antigen-specific $CD8^+$ T cells on a continual basis, giving the impression of reduced contraction. Indeed, the numbers of CD127 expressing Ova-specific $CD8^+$ T cells do not increase progressively during BCG-Ova infection. From the data it seems that this is due to the presence of peptide rather than inflammation because when the pathogen is eliminated using antibiotics, the CD127 expression beings to increase but it does not increase when additional inflammation is present. It has been shown that CD127 expression is crucial for the development of long-term resting memory cells [60]. Also, antigen persistence has been shown to be needed for maintenance of $CD8^+$ T cells in chronic LCMV models [106]. In addition to this, when fresh naïve OT-1 cells were introduced into BCG infected mice at later time points during the infection, they proliferated, albeit less than what is seen at the peak of bacterial burden, but nonetheless indicating that antigen is still being presented at these late stages of infection.

It was hypothesized that the chronic nature of the BCG infection may cause $CD8^+$ T cells to become functionally incompetent. This is because in some chronic viral infections the $CD8^+$ T cells become functionally exhausted due to hyper-activation of T cells [104;105]. However, surprisingly this did not appear to be the case in this BCG infection model. The $CD8^+$ T cells generated against BCG were able to produce IFN-γ upon stimulation and exhibited in vivo lytic activity. Even when challenged with a previously seen peptide, these cells were able to proliferate similar to memory cells generated by LM. In fact, the $CD8^+$ T cells induced by BCG-Ova have also been shown to mediate potent tumor control both locally and distally [95]. There are various reasons as to why in the case of BCG infection the $CD8^+$ T cells do not seem to succumb to exhaustion. Most viral infections in which $CD8^+$ T cell exhaustion occurs, have the viral proteins present in the cytosol and thus these peptides

are exposed to the classical MHC class I pathway and though it is not clear how efficient cross-priming is in comparison to the classical antigen processing pathway [141], it is speculated the classical pathway could be more efficient at T cell stimulation. Also, the levels of antigen produced are far greater in viral infections than in BCG infections. Thus, the $CD8^+$ T cells in chronic viral infections are chronically bombarded with antigen and become functionally exhausted overtime. Also, those cells that are functionally exhausted tend to possess an effector phenotype [142]. However, in the case of BCG-Ova infection, although the infection is chronic, antigen-presentation is curtailed during the chronic stage, antigenic levels would also be lesser, and the majority of the bacteria may go into a non-replicative stage [136], and consequently the $CD8^+$ T cells would receive reduced stimulation chronically. Not surprisingly, the majority of the $CD8^+$ T cells that persist during BCG-Ova infection do not display an effector phenotype.

5.0 – Concluding Remarks

The $CD8^+$ T cell response to BCG seems to be unique in that the magnitude of the response is minimal compared to LM and viral infections. The response is delayed and muted and at later stages of the infection the response becomes dampened or curtailed despite the presence of pathogen. Figure 32 outlines a proposed model based on the results obtained of what is thought to be occurring during a $CD8^+$ T cell response to BCG. The delay seemed to be dependent on the amount of antigen present initially in infection and not due to reduced inflammation. The $CD8^+$ T cells generated by BCG infection are fully functional despite reduced stimulation conditions. T cells and cytokines seem to regulate antigen presentation during BCG infection and the bacterial burden does not seem to influence this at later stages of infection. This hostile pressure from the T cells and cytokines is thought to force the

Figure 32: Model of the events that may be contributing to the $CD8^+$ T cell response to BCG. Low amounts of antigen results in weak stimulation, inducing a delayed response with reduced expansion and minimal contraction of $CD8^+$ T cells. When higher levels of antigen are present initially, stronger stimulation occurs, which results in a more rapid response with more expansion and contraction (A). T cells and cytokines regulate antigen presentation during BCG infection (B). When activated $CD8^+$ or $CD4^+$ T cells encounters an infected APC they produce various inflammatory cytokines such as IFN-γ and TNF. This induces phago-lysosome fusion within the macrophage lower the pH within the phagosome and it causes nitrogen and oxygen radicals to be produced. $CD8^+$ T cells also induce apoptosis of the infected macrophage via Fas/FasL interaction or lytic granules. This occurs in the first 3 weeks of the infection. This hostile pressure within the phagosome may force the bacterium to enter a state of non-replicative persistence, resulting in curtailment of antigen presentation. This occurs after 3 weeks of infection. When these stresses are removed (as is the case in the various knockout mice) the bacterium does not enter this quiescent state and continues to replicate and produce antigen and thus the curtailment of antigen presentation was rescued in these mice.

Figure 32

A Delayed response due to low antigen levels

Low BCG dose ($1x10^4$)

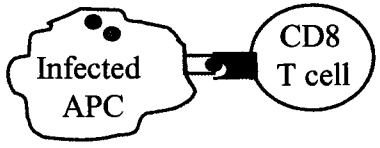

- Weak stimulation
- Delayed response
- Reduced expansion and contraction

High BCG dose ($1x10^6$)

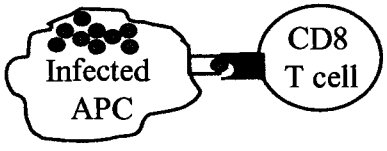

- Stronger stimulation
- Rapid response
- More expansion and contraction

B Lymphocytes and cytokines contribute to curtailment

~ 2-3 weeks of infection

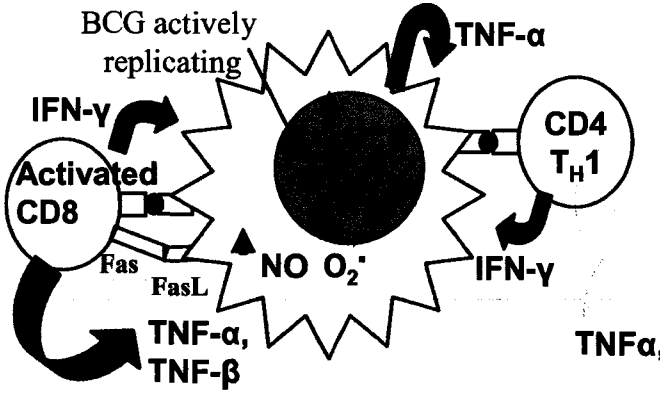

~4-6 weeks of infection

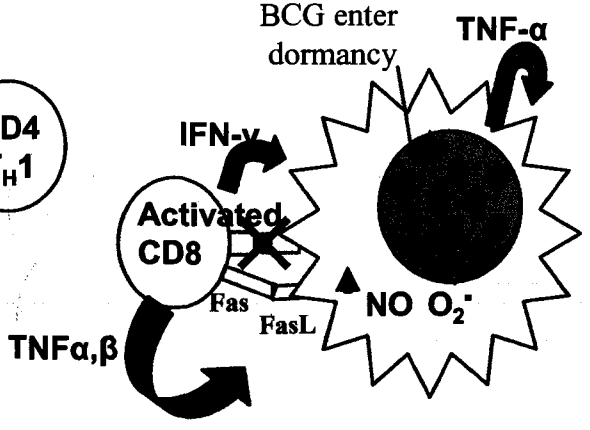

In knockout mice (Rag-$1^{-/-}$, TNF-Raβ$^{-/-}$, IFN-γ$^{-/-}$, iNOS-$2^{-/-}$)

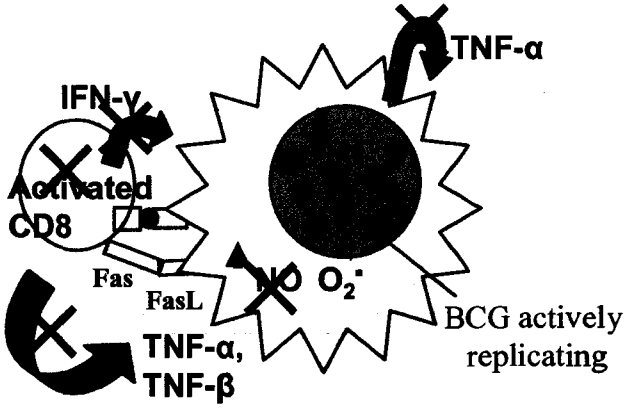

bacterium to enter a state of non-replicative persistence during which low levels of antigen presentation may still be occurring. This allows the pathogen to evade the immune system by remaining in this quiescent-like state. In fact many humans that contain latent *Mycobacterium tuberculosis* within granulomas in their lungs experience reactivation of the pathogen when the individual becomes immunocompromised [143]. The data shown here highlight the intricate networking between a host and an intracellular pathogen that has evolved over centuries. Understanding how the host immune system attempts to control and destroy intracellular pathogens is vital to the development of new strategies for vaccines to combat these pathogens.

Reference List

1. Tada,T. 1997. The immune system as a supersystem. *Annu.Rev.Immunol.* 15:1-13.

2. Underhill,D.M. and A.Ozinsky. 2002. Phagocytosis of microbes: complexity in action. *Annu.Rev.Immunol.* 20:825-852.

3. Hamerman,J.A., K.Ogasawara, and L.L.Lanier. 2005. NK cells in innate immunity. *Curr.Opin.Immunol.* 17:29-35.

4. Ljunggren,H.G. and K.Karre. 1990. In search of the 'missing self': MHC molecules and NK cell recognition. *Immunol.Today* 11:237-244.

5. Muller-Eberhard,H.J. 1986. The membrane attack complex of complement. *Annu.Rev.Immunol.* 4:503-528.

6. Larsen,G.L. and P.M.Henson. 1983. Mediators of inflammation. *Annu.Rev.Immunol.* 1:335-359.

7. Medzhitov,R. and C.A.Janeway, Jr. 1997. Innate immunity: impact on the adaptive immune response. *Curr.Opin.Immunol.* 9:4-9.

8. Sprent,J. and C.D.Surh. 2002. T cell memory. *Annu.Rev.Immunol.* 20:551-579.

9. Sprent,J. and C.D.Surh. 2001. Generation and maintenance of memory T cells. *Curr.Opin.Immunol.* 13:248-254.

10. Luu,R.A., K.Gurnani, R.Dudani, R.Kammara, H.van Faassen, J.C.Sirard, L.Krishnan, and S.Sad. 2006. Delayed Expansion and Contraction of CD8+ T Cell Response during Infection with Virulent Salmonella typhimurium. *J.Immunol.* 177:1516-1525.

11. Kaper,J.B., J.G.Morris, Jr., and M.M.Levine. 1995. Cholera. *Clin.Microbiol.Rev.* 8:48-86.

12. van Faassen,H., R.Dudani, L.Krishnan, and S.Sad. 2004. Prolonged antigen presentation, APC-, and CD8+ T cell turnover during mycobacterial infection: comparison with Listeria monocytogenes. *J.Immunol.* 172:3491-3500.

13. Sly,L.M., S.M.Hingley-Wilson, N.E.Reiner, and W.R.McMaster. 2003. Survival of Mycobacterium tuberculosis in host macrophages involves resistance to apoptosis dependent upon induction of antiapoptotic Bcl-2 family member Mcl-1. *J.Immunol.* 170:430-437.

14. Shimada,K., H.Takimoto, I.Yano, and Y.Kumazawa. 2006. Involvement of mannose receptor in glycopeptidolipid-mediated inhibition of phagosome-lysosome fusion. *Microbiol.Immunol.* 50:243-251.

15. Rooijakkers,S.H. and J.A.van Strijp. 2006. Bacterial complement evasion. *Mol.Immunol.*

16. Morrison,L.A., A.E.Lukacher, V.L.Braciale, D.P.Fan, and T.J.Braciale. 1986. Differences in antigen presentation to MHC class I-and class II-restricted influenza virus-specific cytolytic T lymphocyte clones. *J.Exp.Med.* 163:903-921.

17. Lankat-Buttgereit,B. and R.Tampe. 1999. The transporter associated with antigen processing TAP: structure and function. *FEBS Lett.* 464:108-112.

18. Uebel,S. and R.Tampe. 1999. Specificity of the proteasome and the TAP transporter. *Curr.Opin.Immunol.* 11:203-208.

19. Niedermann,G., E.Geier, M.Lucchiari-Hartz, N.Hitziger, A.Ramsperger, and K.Eichmann. 1999. The specificity of proteasomes: impact on MHC class I processing and presentation of antigens. *Immunol.Rev.* 172:29-48.

20. Germain,R.N. 1994. MHC-dependent antigen processing and peptide presentation: providing ligands for T lymphocyte activation. *Cell* 76:287-299.

21. Kovacsovics-Bankowski,M., K.Clark, B.Benacerraf, and K.L.Rock. 1993. Efficient major histocompatibility complex class I presentation of exogenous antigen upon phagocytosis by macrophages. *Proc.Natl.Acad.Sci.U.S.A* 90:4942-4946.

22. Nowak,A.K., R.A.Lake, A.L.Marzo, B.Scott, W.R.Heath, E.J.Collins, J.A.Frelinger, and B.W.Robinson. 2003. Induction of tumor cell apoptosis in vivo increases tumor antigen cross-presentation, cross-priming rather than cross-tolerizing host tumor-specific CD8 T cells. *J.Immunol.* 170:4905-4913.

23. den Haan,J.M. and M.J.Bevan. 2001. Antigen presentation to CD8+ T cells: cross-priming in infectious diseases. *Curr.Opin.Immunol.* 13:437-441.

24. den Haan,J.M. and M.J.Bevan. 2001. Antigen presentation to CD8+ T cells: cross-priming in infectious diseases. *Curr.Opin.Immunol.* 13:437-441.

25. Bevan,M.J. 1976. Cross-priming for a secondary cytotoxic response to minor H antigens with H-2 congenic cells which do not cross-react in the cytotoxic assay. *J.Exp.Med.* 143:1283-1288.

26. Shen,L. and K.L.Rock. 2006. Priming of T cells by exogenous antigen cross-presented on MHC class I molecules. *Curr.Opin.Immunol.* 18:85-91.

27. Shen,L., L.J.Sigal, M.Boes, and K.L.Rock. 2004. Important role of cathepsin S in generating peptides for TAP-independent MHC class I crosspresentation in vivo. *Immunity.* 21:155-165.

28. Pfeifer,J.D., M.J.Wick, R.L.Roberts, K.Findlay, S.J.Normark, and C.V.Harding. 1993. Phagocytic processing of bacterial antigens for class I MHC presentation to T cells. *Nature* 361:359-362.

29. Song,R. and C.V.Harding. 1996. Roles of proteasomes, transporter for antigen presentation (TAP), and beta 2-microglobulin in the processing of bacterial or particulate antigens via an alternate class I MHC processing pathway. *J.Immunol.* 156:4182-4190.

30. Winau,F., S.Weber, S.Sad, J.de Diego, S.L.Hoops, B.Breiden, K.Sandhoff, V.Brinkmann, S.H.Kaufmann, and U.E.Schaible. 2006. Apoptotic vesicles crossprime CD8 T cells and protect against tuberculosis. *Immunity.* 24:105-117.

31. Guermonprez,P., L.Saveanu, M.Kleijmeer, J.Davoust, P.Van Endert, and S.Amigorena. 2003. ER-phagosome fusion defines an MHC class I cross-presentation compartment in dendritic cells. *Nature* 425:397-402.

32. Touret,N., P.Paroutis, and S.Grinstein. 2005. The nature of the phagosomal membrane: endoplasmic reticulum versus plasmalemma. *J.Leukoc.Biol.* 77:878-885.

33. Gagnon,E., J.J.Bergeron, and M.Desjardins. 2005. ER-mediated phagocytosis: myth or reality? *J.Leukoc.Biol.* 77:843-845.

34. Touret,N., P.Paroutis, M.Terebiznik, R.E.Harrison, S.Trombetta, M.Pypaert, A.Chow, A.Jiang, J.Shaw, C.Yip, H.P.Moore, W.N.van der, D.Houben, P.J.Peters, C.de Chastellier, I.Mellman, and S.Grinstein. 2005. Quantitative and dynamic assessment of the contribution of the ER to phagosome formation. *Cell* 123:157-170.

35. Houde,M., S.Bertholet, E.Gagnon, S.Brunet, G.Goyette, A.Laplante, M.F.Princiotta, P.Thibault, D.Sacks, and M.Desjardins. 2003. Phagosomes are competent organelles for antigen cross-presentation. *Nature* 425:402-406.

36. Guermonprez,P., L.Saveanu, M.Kleijmeer, J.Davoust, P.Van Endert, and S.Amigorena. 2003. ER-phagosome fusion defines an MHC class I cross-presentation compartment in dendritic cells. *Nature* 425:397-402.

37. Houde,M., S.Bertholet, E.Gagnon, S.Brunet, G.Goyette, A.Laplante, M.F.Princiotta, P.Thibault, D.Sacks, and M.Desjardins. 2003. Phagosomes are competent organelles for antigen cross-presentation. *Nature* 425:402-406.

38. Ackerman,A.L., C.Kyritsis, R.Tampe, and P.Cresswell. 2003. Early phagosomes in dendritic cells form a cellular compartment sufficient for cross presentation of exogenous antigens. *Proc.Natl.Acad.Sci.U.S.A* 100:12889-12894.

39. Kovacsovics-Bankowski,M. and K.L.Rock. 1995. A phagosome-to-cytosol pathway for exogenous antigens presented on MHC class I molecules. *Science* 267:243-246.

40. Neijssen,J., C.Herberts, J.W.Drijfhout, E.Reits, L.Janssen, and J.Neefjes. 2005. Cross-presentation by intercellular peptide transfer through gap junctions. *Nature* 434:83-88.

41. Imai,J., H.Hasegawa, M.Maruya, S.Koyasu, and I.Yahara. 2005. Exogenous antigens are processed through the endoplasmic reticulum-associated degradation (ERAD) in cross-presentation by dendritic cells. *Int.Immunol.* 17:45-53.

42. Kaech,S.M. and R.Ahmed. 2001. Memory CD8+ T cell differentiation: initial antigen encounter triggers a developmental program in naive cells. *Nat.Immunol.* 2:415-422.

43. Oehen,S. and K.Brduscha-Riem. 1998. Differentiation of naive CTL to effector and memory CTL: correlation of effector function with phenotype and cell division. *J.Immunol.* 161:5338-5346.

44. Kagi,D., B.Ledermann, K.Burki, P.Seiler, B.Odermatt, K.J.Olsen, E.R.Podack, R.M.Zinkernagel, and H.Hengartner. 1994. Cytotoxicity mediated by T cells and natural killer cells is greatly impaired in perforin-deficient mice. *Nature* 369:31-37.

45. Nagata,S. and P.Golstein. 1995. The Fas death factor. *Science* 267:1449-1456.

46. Schuler,T., Z.Qin, S.Ibe, N.Noben-Trauth, and T.Blankenstein. 1999. T helper cell type 1-associated and cytotoxic T lymphocyte-mediated tumor immunity is impaired in interleukin 4-deficient mice. *J.Exp.Med.* 189:803-810.

47. Schluns,K.S., W.C.Kieper, S.C.Jameson, and L.Lefrancois. 2000. Interleukin-7 mediates the homeostasis of naive and memory CD8 T cells in vivo. *Nat.Immunol.* 1:426-432.

48. Tan,J.T., E.Dudl, E.LeRoy, R.Murray, J.Sprent, K.I.Weinberg, and C.D.Surh. 2001. IL-7 is critical for homeostatic proliferation and survival of naive T cells. *Proc.Natl.Acad.Sci.U.S.A* 98:8732-8737.

49. Schluns,K.S., K.Williams, A.Ma, X.X.Zheng, and L.Lefrancois. 2002. Cutting edge: requirement for IL-15 in the generation of primary and memory antigen-specific CD8 T cells. *J.Immunol.* 168:4827-4831.

50. Minami,Y., T.Kono, T.Miyazaki, and T.Taniguchi. 1993. The IL-2 receptor complex: its structure, function, and target genes. *Annu.Rev.Immunol.* 11:245-268.

51. Cerdan,C., Y.Martin, M.Courcoul, C.Mawas, F.Birg, and D.Olive. 1995. CD28 costimulation regulates long-term expression of the three genes (alpha, beta, gamma) encoding the high-affinity IL2 receptor. *Res.Immunol.* 146:164-168.

52. Testi,R., J.H.Phillips, and L.L.Lanier. 1989. T cell activation via Leu-23 (CD69). *J.Immunol.* 143:1123-1128.

53. Cosulich,M.E., A.Rubartelli, A.Risso, F.Cozzolino, and A.Bargellesi. 1987. Functional characterization of an antigen involved in an early step of T-cell activation. *Proc.Natl.Acad.Sci.U.S.A* 84:4205-4209.

54. Munoz-Fernandez,M.A., M.A.Fernandez, and M.Fresno. 1992. Synergism between tumor necrosis factor-alpha and interferon-gamma on macrophage activation for the killing of intracellular Trypanosoma cruzi through a nitric oxide-dependent mechanism. *Eur.J.Immunol.* 22:301-307.

55. Badovinac,V.P., B.B.Porter, and J.T.Harty. 2002. Programmed contraction of CD8(+) T cells after infection. *Nat.Immunol.* 3:619-626.

56. Ahmed,R. and D.Gray. 1996. Immunological memory and protective immunity: understanding their relation. *Science* 272:54-60.

57. Dutton,R.W., L.M.Bradley, and S.L.Swain. 1998. T cell memory. *Annu.Rev.Immunol.* 16:201-223.

58. Sprent,J. and C.D.Surh. 2001. Generation and maintenance of memory T cells. *Curr.Opin.Immunol.* 13:248-254.

59. Kaech,S.M., J.T.Tan, E.J.Wherry, B.T.Konieczny, C.D.Surh, and R.Ahmed. 2003. Selective expression of the interleukin 7 receptor identifies effector CD8 T cells that give rise to long-lived memory cells. *Nat.Immunol.* 4:1191-1198.

60. Buentke,E., A.Mathiot, M.Tolaini, J.Di Santo, R.Zamoyska, and B.Seddon. 2006. Do CD8 effector cells need IL-7R expression to become resting memory cells? *Blood.*

61. Sourdive,D.J., K.Murali-Krishna, J.D.Altman, A.J.Zajac, J.K.Whitmire, C.Pannetier, P.Kourilsky, B.Evavold, A.Sette, and R.Ahmed. 1998. Conserved T cell receptor repertoire in primary and memory CD8 T cell responses to an acute viral infection. *J.Exp.Med.* 188:71-82.

62. Murali-Krishna,K., J.D.Altman, M.Suresh, D.J.Sourdive, A.J.Zajac, J.D.Miller, J.Slansky, and R.Ahmed. 1998. Counting antigen-specific CD8 T cells: a reevaluation of bystander activation during viral infection. *Immunity.* 8:177-187.

63. Schuchat,A., B.Swaminathan, and C.V.Broome. 1991. Epidemiology of human listeriosis. *Clin.Microbiol.Rev.* 4:169-183.

64. Portnoy,D.A., P.S.Jacks, and D.J.Hinrichs. 1988. Role of hemolysin for the intracellular growth of Listeria monocytogenes. *J.Exp.Med.* 167:1459-1471.

65. Kocks,C., E.Gouin, M.Tabouret, P.Berche, H.Ohayon, and P.Cossart. 1992. L. monocytogenes-induced actin assembly requires the actA gene product, a surface protein. *Cell* 68:521-531.

66. Smith,G.A., J.A.Theriot, and D.A.Portnoy. 1996. The tandem repeat domain in the Listeria monocytogenes ActA protein controls the rate of actin-based motility, the percentage of moving bacteria, and the localization of vasodilator-stimulated phosphoprotein and profilin. *J.Cell Biol.* 135:647-660.

67. Portnoy,D.A., P.S.Jacks, and D.J.Hinrichs. 1988. Role of hemolysin for the intracellular growth of Listeria monocytogenes. *J.Exp.Med.* 167:1459-1471.

68. Mielke,M., S.Ehlers, and H.Hahn. 1988. The role of T cell subpopulations in cell mediated immunity to facultative intracellular bacteria. *Infection* 16 Suppl 2:S123-S127.

69. Naher,H., U.Sperling, and H.Hahn. 1985. H-2K-restricted granuloma formation by Ly-2+ T cells in antibacterial protection to facultative intracellular bacteria. *J.Immunol.* 134:569-572.

70. Bishop,D.K. and D.J.Hinrichs. 1987. Adoptive transfer of immunity to Listeria monocytogenes. The influence of in vitro stimulation on lymphocyte subset requirements. *J.Immunol.* 139:2005-2009.

71. Lukacs,K. and R.J.Kurlander. 1989. MHC-unrestricted transfer of antilisterial immunity by freshly isolated immune CD8 spleen cells. *J.Immunol.* 143:3731-3736.

72. Brunt,L.M., D.A.Portnoy, and E.R.Unanue. 1990. Presentation of Listeria monocytogenes to CD8+ T cells requires secretion of hemolysin and intracellular bacterial growth. *J.Immunol.* 145:3540-3546.

73. Kerksiek,K.M. and E.G.Pamer. 1999. T cell responses to bacterial infection. *Curr.Opin.Immunol.* 11:400-405.

74. Harty,J.T., A.R.Tvinnereim, and D.W.White. 2000. CD8+ T cell effector mechanisms in resistance to infection. *Annu.Rev.Immunol.* 18:275-308.

75. Wilson,M.E., H.V.Fineberg, and G.A.Colditz. 1995. Geographic latitude and the efficacy of bacillus Calmette-Guerin vaccine. *Clin.Infect.Dis.* 20:982-991.

76. Colditz,G.A., C.S.Berkey, F.Mosteller, T.F.Brewer, M.E.Wilson, E.Burdick, and H.V.Fineberg. 1995. The efficacy of bacillus Calmette-Guerin vaccination of newborns and infants in the prevention of tuberculosis: meta-analyses of the published literature. *Pediatrics* 96:29-35.

77. Colditz,G.A., T.F.Brewer, C.S.Berkey, M.E.Wilson, E.Burdick, H.V.Fineberg, and F.Mosteller. 1994. Efficacy of BCG vaccine in the prevention of tuberculosis. Meta-analysis of the published literature. *JAMA* 271:698-702.

78. Brewer,T.F. and G.A.Colditz. 1995. Bacille Calmette-Guerin vaccination for the prevention of tuberculosis in health care workers. *Clin.Infect.Dis.* 20:136-142.

79. Brewer,T.F. and G.A.Colditz. 1995. Relationship between bacille Calmette-Guerin (BCG) strains and the efficacy of BCG vaccine in the prevention of tuberculosis. *Clin.Infect.Dis.* 20:126-135.

80. Butler,D. 2000. New fronts in an old war. *Nature* 406:670-672.

81. PIERCE,C.H. and R.J.DUBOS. 1955. Morphological characteristics and behaviour in vivo of various substrains of BCG. *Tubercle.* 36:105-107.

82. Via,L.E., D.Deretic, R.J.Ulmer, N.S.Hibler, L.A.Huber, and V.Deretic. 1997. Arrest of mycobacterial phagosome maturation is caused by a block in vesicle fusion between stages controlled by rab5 and rab7. *J.Biol.Chem.* 272:13326-13331.

83. Jiao,X., R.Lo-Man, P.Guermonprez, L.Fiette, E.Deriaud, S.Burgaud, B.Gicquel, N.Winter, and C.Leclerc. 2002. Dendritic cells are host cells for mycobacteria in vivo that trigger innate and acquired immunity. *J.Immunol.* 168:1294-1301.

84. Gutierrez-Pabello,J.A., D.N.McMurray, and L.G.Adams. 2002. Upregulation of thymosin beta-10 by Mycobacterium bovis infection of bovine macrophages is associated with apoptosis. *Infect.Immun.* 70:2121-2127.

85. Keane,J., H.G.Remold, and H.Kornfeld. 2000. Virulent Mycobacterium tuberculosis strains evade apoptosis of infected alveolar macrophages. *J.Immunol.* 164:2016-2020.

86. Kremer,L., J.Estaquier, E.Brandt, J.C.Ameisen, and C.Locht. 1997. Mycobacterium bovis Bacillus Calmette Guerin infection prevents apoptosis of resting human monocytes. *Eur.J.Immunol.* 27:2450-2456.

87. Stover,C.K., l.C.de, V, T.R.Fuerst, J.E.Burlein, L.A.Benson, L.T.Bennett, G.P.Bansal, J.F.Young, M.H.Lee, G.F.Hatfull, and . 1991. New use of BCG for recombinant vaccines. *Nature* 351:456-460.

88. Stover,C.K., G.P.Bansal, M.S.Hanson, J.E.Burlein, S.R.Palaszynski, J.F.Young, S.Koenig, D.B.Young, A.Sadziene, and A.G.Barbour. 1993. Protective immunity elicited by recombinant bacille Calmette-Guerin (BCG) expressing outer surface protein A (OspA) lipoprotein: a candidate Lyme disease vaccine. *J.Exp.Med.* 178:197-209.

89. Orme,I.M., M.J.Ratcliffe, and F.M.Collins. 1984. Acquired immunity to heavy infection with Mycobacterium bovis bacillus Calmette-Guerin and its relationship to the development of nonspecific unresponsiveness in vitro. *Cell Immunol.* 88:285-296.

90. VanHeyningen,T.K., H.L.Collins, and D.G.Russell. 1997. IL-6 produced by macrophages infected with Mycobacterium species suppresses T cell responses. *J.Immunol.* 158:330-337.

91. Kremer,L., J.Estaquier, I.Wolowczuk, F.Biet, J.C.Ameisen, and C.Locht. 2000. Ineffective cellular immune response associated with T-cell apoptosis in susceptible Mycobacterium bovis BCG-infected mice. *Infect.Immun.* 68:4264-4273.

92. Hirsch,C.S., J.J.Ellner, R.Blinkhorn, and Z.Toossi. 1997. In vitro restoration of T cell responses in tuberculosis and augmentation of monocyte effector function against Mycobacterium tuberculosis by natural inhibitors of transforming growth factor beta. *Proc.Natl.Acad.Sci.U.S.A* 94:3926-3931.

93. Colizzi,V. 1984. In vivo and in vitro administration of interleukin 2-containing preparation reverses T-cell unresponsiveness in Mycobacterium bovis BCG-infected mice. *Infect.Immun.* 45:25-28.

94. Das,G., H.Vohra, B.Saha, J.N.Agrewala, and G.C.Mishra. 1999. Apoptosis of Th1-like cells in experimental tuberculosis (TB). *Clin.Exp.Immunol.* 115:324-328.

95. Dudani,R., Y.Chapdelaine, H.H.Faassen, D.K.Smith, H.Shen, L.Krishnan, and S.Sad. 2002. Multiple mechanisms compensate to enhance tumor-protective CD8(+) T cell response in the long-term despite poor CD8(+) T cell priming initially: comparison between an acute versus a chronic intracellular bacterium expressing a model antigen. *J.Immunol.* 168:5737-5745.

96. Pedras-Vasconcelos,J.A., Y.Chapdelaine, R.Dudani, H.van Faassen, D.K.Smith, and S.Sad. 2002. Mycobacterium bovis BCG-infected mice are more susceptible to staphylococcal enterotoxin B-mediated toxic shock than uninfected mice despite reduced in vitro splenocyte responses to superantigens. *Infect.Immun.* 70:4148-4157.

97. Sprott,G.D., C.J.Dicaire, K.Gurnani, S.Sad, and L.Krishnan. 2004. Activation of dendritic cells by liposomes prepared from phosphatidylinositol mannosides from Mycobacterium bovis bacillus Calmette-Guerin and adjuvant activity in vivo. *Infect.Immun.* 72:5235-5246.

98. Sprott,G.D., S.Sad, L.P.Fleming, C.J.Dicaire, G.B.Patel, and L.Krishnan. 2003. Archaeosomes varying in lipid composition differ in receptor-mediated endocytosis and differentially adjuvant immune responses to entrapped antigen. *Archaea.* 1:151-164.

99. Krishnan,L., S.Sad, G.B.Patel, and G.D.Sprott. 2003. Archaeosomes induce enhanced cytotoxic T lymphocyte responses to entrapped soluble protein in the absence of interleukin 12 and protect against tumor challenge. *Cancer Res.* 63:2526-2534.

100. Gurnani,K., J.Kennedy, S.Sad, G.D.Sprott, and L.Krishnan. 2004. Phosphatidylserine receptor-mediated recognition of archaeosome adjuvant promotes endocytosis and MHC class I cross-presentation of the entrapped antigen by phagosome-to-cytosol transport and classical processing. *J.Immunol.* 173:566-578.

101. Tough,D.F. and J.Sprent. 1994. Turnover of naive- and memory-phenotype T cells. *J.Exp.Med.* 179:1127-1135.

102. Barber,D.L., E.J.Wherry, and R.Ahmed. 2003. Cutting edge: rapid in vivo killing by memory CD8 T cells. *J.Immunol.* 171:27-31.

103. Lyons,A.B. and C.R.Parish. 1994. Determination of lymphocyte division by flow cytometry. *J.Immunol.Methods* 171:131-137.

104. Moskophidis,D., F.Lechner, H.Pircher, and R.M.Zinkernagel. 1993. Virus persistence in acutely infected immunocompetent mice by exhaustion of antiviral cytotoxic effector T cells. *Nature* 362:758-761.

105. Zajac,A.J., J.N.Blattman, K.Murali-Krishna, D.J.Sourdive, M.Suresh, J.D.Altman, and R.Ahmed. 1998. Viral immune evasion due to persistence of activated T cells without effector function. *J.Exp.Med.* 188:2205-2213.

106. Wherry,E.J., D.L.Barber, S.M.Kaech, J.N.Blattman, and R.Ahmed. 2004. Antigen-independent memory CD8 T cells do not develop during chronic viral infection. *Proc.Natl.Acad.Sci.U.S.A* 101:16004-16009.

107. Kundig,T.M., M.F.Bachmann, S.Oehen, U.W.Hoffmann, J.J.Simard, C.P.Kalberer, H.Pircher, P.S.Ohashi, H.Hengartner, and R.M.Zinkernagel. 1996. On the role of antigen in maintaining cytotoxic T-cell memory. *Proc.Natl.Acad.Sci.U.S.A* 93:9716-9723.

108. Oehen,S., H.Waldner, T.M.Kundig, H.Hengartner, and R.M.Zinkernagel. 1992. Antivirally protective cytotoxic T cell memory to lymphocytic choriomeningitis virus is governed by persisting antigen. *J.Exp.Med.* 176:1273-1281.

109. Cerwenka,A., T.M.Morgan, and R.W.Dutton. 1999. Naive, effector, and memory CD8 T cells in protection against pulmonary influenza virus infection: homing properties rather than initial frequencies are crucial. *J.Immunol.* 163:5535-5543.

110. Sprent,J. and D.F.Tough. 2001. T cell death and memory. *Science* 293:245-248.

111. Kaech,S.M., E.J.Wherry, and R.Ahmed. 2002. Effector and memory T-cell differentiation: implications for vaccine development. *Nat.Rev.Immunol.* 2:251-262.

112. Sallusto,F., D.Lenig, R.Forster, M.Lipp, and A.Lanzavecchia. 1999. Two subsets of memory T lymphocytes with distinct homing potentials and effector functions. *Nature* 401:708-712.

113. Wherry,E.J., V.Teichgraber, T.C.Becker, D.Masopust, S.M.Kaech, R.Antia, U.H.von Andrian, and R.Ahmed. 2003. Lineage relationship and protective immunity of memory CD8 T cell subsets. *Nat.Immunol.* 4:225-234.

114. Lanzavecchia,A. and F.Sallusto. 2000. Dynamics of T lymphocyte responses: intermediates, effectors, and memory cells. *Science* 290:92-97.

115. Opferman,J.T., B.T.Ober, and P.G.Ashton-Rickardt. 1999. Linear differentiation of cytotoxic effectors into memory T lymphocytes. *Science* 283:1745-1748.

116. Vidric,M., A.T.Bladt, U.Dianzani, and T.H.Watts. 2006. Role for inducible costimulator in control of Salmonella enterica serovar Typhimurium infection in mice. *Infect.Immun.* 74:1050-1061.

117. van Faassen,H., M.Saldanha, D.Gilbertson, R.Dudani, L.Krishnan, and S.Sad. 2005. Reducing the stimulation of CD8+ T cells during infection with intracellular bacteria promotes differentiation primarily into a central (CD62LhighCD44high) subset. *J.Immunol.* 174:5341-5350.

118. Ferrari,G., H.Langen, M.Naito, and J.Pieters. 1999. A coat protein on phagosomes involved in the intracellular survival of mycobacteria. *Cell* 97:435-447.

119. Walburger,A., A.Koul, G.Ferrari, L.Nguyen, C.Prescianotto-Baschong, K.Huygen, B.Klebl, C.Thompson, G.Bacher, and J.Pieters. 2004. Protein kinase G from pathogenic mycobacteria promotes survival within macrophages. *Science* 304:1800-1804.

120. Miller,B.H., R.A.Fratti, J.F.Poschet, G.S.Timmins, S.S.Master, M.Burgos, M.A.Marletta, and V.Deretic. 2004. Mycobacteria inhibit nitric oxide synthase recruitment to phagosomes during macrophage infection. *Infect.Immun.* 72:2872-2878.

121. Akaishi,H., K.Takeda, T.Kaisho, R.Shineha, S.Satomi, J.Takeda, and S.Akira. 1998. Defective IL-2-mediated IL-2 receptor alpha chain expression in Stat3-deficient T lymphocytes. *Int.Immunol.* 10:1747-1751.

122. Nakajima,H., X.W.Liu, A.Wynshaw-Boris, L.A.Rosenthal, K.Imada, D.S.Finbloom, L.Hennighausen, and W.J.Leonard. 1997. An indirect effect of Stat5a in IL-2-induced proliferation: a critical role for Stat5a in IL-2-mediated IL-2 receptor alpha chain induction. *Immunity.* 7:691-701.

123. Cousens,L.P., J.S.Orange, and C.A.Biron. 1995. Endogenous IL-2 contributes to T cell expansion and IFN-gamma production during lymphocytic choriomeningitis virus infection. *J.Immunol.* 155:5690-5699.

124. Ellery,J.M. and P.J.Nicholls. 2002. Possible mechanism for the alpha subunit of the interleukin-2 receptor (CD25) to influence interleukin-2 receptor signal transduction. *Immunol.Cell Biol.* 80:351-357.

125. Lanzavecchia,A. and F.Sallusto. 2002. Progressive differentiation and selection of the fittest in the immune response. *Nat.Rev.Immunol.* 2:982-987.

126. Manjunath,N., P.Shankar, J.Wan, W.Weninger, M.A.Crowley, K.Hieshima, T.A.Springer, X.Fan, H.Shen, J.Lieberman, and U.H.von Andrian. 2001. Effector

differentiation is not prerequisite for generation of memory cytotoxic T lymphocytes. *J.Clin.Invest* 108:871-878.

127. Sallusto,F. and A.Lanzavecchia. 2001. Exploring pathways for memory T cell generation. *J.Clin.Invest* 108:805-806.

128. Lavoie,P.M., A.R.Dumont, H.McGrath, A.E.Kernaleguen, and R.P.Sekaly. 2005. Delayed expansion of a restricted T cell repertoire by low-density TCR ligands. *Int.Immunol.* 17:931-941.

129. Hemmer,B., I.Stefanova, M.Vergelli, R.N.Germain, and R.Martin. 1998. Relationships among TCR ligand potency, thresholds for effector function elicitation, and the quality of early signaling events in human T cells. *J.Immunol.* 160:5807-5814.

130. De Creus,A., K.Van Beneden, T.Taghon, F.Stolz, V.Debacker, J.Plum, and G.Leclercq. 2000. Langerhans cells that have matured in vivo in the absence of T cells are fully capable of inducing a helper CD4 as well as a cytotoxic CD8 response. *J.Immunol.* 165:645-653.

131. Dieli,F., J.Ivanyi, P.Marsh, A.Williams, I.Naylor, G.Sireci, N.Caccamo, C.Di Sano, and A.Salerno. 2003. Characterization of lung gamma delta T cells following intranasal infection with Mycobacterium bovis bacillus Calmette-Guerin. *J.Immunol.* 170:463-469.

132. Sugita,M., D.B.Moody, R.M.Jackman, E.P.Grant, J.P.Rosat, S.M.Behar, P.J.Peters, S.A.Porcelli, and M.B.Brenner. 1998. CD1--a new paradigm for antigen presentation and T cell activation. *Clin.Immunol.Immunopathol.* 87:8-14.

133. Boom,W.H. 1999. Gammadelta T cells and Mycobacterium tuberculosis. *Microbes.Infect.* 1:187-195.

134. Mombaerts,P. 1995. Lymphocyte development and function in T-cell receptor and RAG-1 mutant mice. *Int.Rev.Immunol.* 13:43-63.

135. Wong,P. and E.G.Pamer. 2003. Feedback regulation of pathogen-specific T cell priming. *Immunity.* 18:499-511.

136. Shi,L., Y.J.Jung, S.Tyagi, M.L.Gennaro, and R.J.North. 2003. Expression of Th1-mediated immunity in mouse lungs induces a Mycobacterium tuberculosis transcription pattern characteristic of nonreplicating persistence. *Proc.Natl.Acad.Sci.U.S.A* 100:241-246.

137. Hampshire,T., S.Soneji, J.Bacon, B.W.James, J.Hinds, K.Laing, R.A.Stabler, P.D.Marsh, and P.D.Butcher. 2004. Stationary phase gene expression of Mycobacterium tuberculosis following a progressive nutrient depletion: a model for persistent organisms? *Tuberculosis.(Edinb.)* 84:228-238.

138. Archuleta,R.J., H.P.Yvonne, and T.P.Primm. 2005. Mycobacterium avium enters a state of metabolic dormancy in response to starvation. *Tuberculosis.(Edinb.)* 85:147-158.

139. Wayne,L.G. and C.D.Sohaskey. 2001. Nonreplicating persistence of mycobacterium tuberculosis. *Annu.Rev.Microbiol.* 55:139-163.

140. Sato,K., T.Akaki, and H.Tomioka. 1998. Differential potentiation of anti-mycobacterial activity and reactive nitrogen intermediate-producing ability of murine peritoneal macrophages activated by interferon-gamma (IFN-gamma) and tumour necrosis factor-alpha (TNF-alpha). *Clin.Exp.Immunol.* 112:63-68.

141. Freigang,S., D.Egger, K.Bienz, H.Hengartner, and R.M.Zinkernagel. 2003. Endogenous neosynthesis vs. cross-presentation of viral antigens for cytotoxic T cell priming. *Proc.Natl.Acad.Sci.U.S.A* 100:13477-13482.

142. Wherry,E.J. and R.Ahmed. 2004. Memory CD8 T-cell differentiation during viral infection. *J.Virol.* 78:5535-5545.

143. Chan,J. and J.Flynn. 2004. The immunological aspects of latency in tuberculosis. *Clin.Immunol.* 110:2-12.

Appendix I

Awards, Achievements, and Publications

Portions of the data from this thesis were presented by me at the University of Ottawa BMI graduate student poster day for which I was awarded 2nd prize for my poster. Portions of the data from this thesis were also presented by me at the University of Ottawa BMI graduate student research symposium day for which I was awarded 1st prize for my presentation. I have also been awarded the University of Ottawa's Faculty of Medicine Award for Academic Excellence in Graduate Studies.

This data was presented by me at the 19th Annual Canadian Society for Immunology conference held in Halifax, Nova Scotia, Canada this summer. Some of the data has been published in the Journal of Immunology and two manuscripts are currently in the process of being written. These will be published under my married name, Marsha Russell. The titles for these papers are listed below.

1. van Faassen H, Saldanha M, Gilbertson D, Dudani R, Krishnan L, Sad S. 2005 Reducing the stimulation of CD8+ T cells during infection with intracellular bacteria promotes differentiation primarily into a central (CD62LhighCD44high) subset. J Immunol. 174(9):5341-50.
2. Russell, M.S, Iskandar M., Dudani R., Nash, J., Mykytczuk, O., Krishnan L. and Sad S. (2006). Dose of an attenuated intracellular bacterium defines the expansion and contraction of CD8+ T cell response. (Manuscript in preparation).
3. Russell, M.S, Dudani R., Krishnan and Sad S. (2006). Multiple mechanisms curtail antigen-presentation during the chronic stage of infection with an attenuated intracellular bacterium. (Manuscript in preparation).

Marsha Saldanha BSc. MSc candidate.

190 Elgin St, Unit 206 Arnprior, On. K7S 1P1 (613) 622-0521 marsha.saldanha@nrc.ca

Skills:

General Skills:

- Extensive lab experience and aseptic technique; WHIMIS Trained; CCAC Certified 2004; NRC-Radioisotope Certified Oct 2006
- Experience in Molecular Biology, Immunology, Microbiology, Plant Physiology, Animal based *in vivo* health
- Able to multi-task and work independently and in a team efficiently.

Animal Skills:

- Lateral tail vein, Intraperitoneal, and subcutaneous injections. Perfusions in mice.
- Mice: C57BL/6, 129Xsv/J, BALB/C, 129XsvJxC57BL/6 F1 hybrid, nude

Immunology Skills:

- Cell culture EL4, EG7, B16melanoma; ELISA; ELISPOT; ^{51}Cr-release and *in vivo* CTL assays; Flow cytometry; intracellular cytokine and BrdU staining, CD8 purification with beads and columns; Cell surface and tetramer staining; CFSE and PKH26 labeling
- lymphocyte extraction from blood, spleen, lungs, liver and brain.

Molecular Biology Skills

- Cloning in *E. coli* DH5α, PCR, quantitative RT-PCR; Gel Electrophoresis, Southern Blot;

  RNA extraction from plants and bacteria within infected organs and cell cultures; Nanodrop; Denaturing agarose gels and agilent gels
- Transductions, transformations

Microbiology Skills:

- Experience working with Level II pathogens *M. bovis* BCG and *S. typhimurium*
- Other bacteria: *Escherichia coli* DH5α; *S. meliloti*
- triparental mating

Analytical Chemistry

- Atomic absorption spectroscopy

Publications and conferences:

Russell, M. S. et al. **Dose of an attenuated intracellular bacterium defines the expansion and contraction of CD8+ T cell response**. (Manuscript in preparation)

Russell, M. S. et al. **Multiple mechanisms curtail antigen-presentation during the chronic stage of infection with an attenuated intracellular bacterium**. (Manuscript in preparation)

Wang C. et al. **Roles of poly-3-hydroxybutyrate (PHB) and glycogen in symbiosis of *Sinorhizobium meliloti* with *Medicago sp***. Microbiology [in print]

Griffith M. et al. **Thellungiella: An Arabidopsis-related model plant adapted to cold temperatures.** PC&E [in print].

19th Annual Canadian Society for Immunology Conference June 2006. Oral and Poster presentation. Saldanha, M., Dudani, R., Krishnan, L., and Sad, S. **T cells and cytokines regulate antigen presentation during infection with a chronic intracellular bacterium**.

Van Faassen H. et al. **Reducing the stimulation of CD8$^+$ T cells during infection with intracellular bacteria promotes differentiation primarily into a central (CD62LhighCD44high) subset.** J Immunol. 2005 May 1;174(9):5341-50

Awards and Grants

- University of Ottawa Faculty of Medicine-Award for Academic Excellence Dec06 $500

- Ontario Graduate Scholarship in Science and Technology Jan05-Sept06 $15 000/yr
- NRC-Graduate Student Supplement Scholarship Sept 2004 to Sept 2006 $5 000/yr
- University of Ottawa BMI Department Graduate Student Poster Day 2nd Place 2004 and Graduate Symposium 1st Place 2005
- Undergraduate NSERC grant in Jan 2003 and May 2003
- Dean's Honours list April 2002 to December 2002

Work Experience:

National Research Council-IBS/U of Ottawa Sept 2006 to present

Research Technician

- Worked on independent and team projects pertaining to vaccine development for intracellular pathogens and cancers. Provided technical guidance and training to students. Maintained inventories and general upkeep of laboratory
- Gained experience in various molecular biology and immunology techniques and in vivo animal based research

University Of Waterloo: Dr. Charles Jan 2003 to Sept 2003

Research Assistant

- Worked on an independent project to develop and study glycogen synthase mutants of *S. meliloti.* Work Report: Construction of Glycogen Synthase Mutants of S. *meliloti*
- Gained experience in various molecular and microbiology techniques

University of Waterloo: Dr. Griffith April 2002 to Sept 2002

Research Assistant

- Worked on an independent project on freezing tolerance of *T. salsuginea* and microbial isolation of its rhizosphere. Work Report: Physiological Adaptations of Crucifer Plant
- Gained experience in various freezing assays used in antifreeze protein studies; RNA extraction and soil extraction of ACC utilizing bacteria from rhizosphere of *T. salsuginea*

Natural Resources Canada-Mining and Minerals Branch Sept 2001 to Dec 2001

Assistant Laboratory Technician

- Performed sample preparation and analysis using AAS and created and verified methods for flame AAS to meet ISO standards. Quantified at ppm and ppb levels
- Gained knowledge of various analytical procedures and techniques

Education

University of Ottawa Supervisor: Dr Subash Sad

Institute For Biological Sciences - National Research Council Canada

Candidate for Masters of Science Degree in Immunology

Thesis: Influence of the potency of antigen-presentation on $CD8^+$ T cell differentiation and memory

Courses: Introduction to Immunology, and Advanced Topics in Immunology

University of Waterloo

Graduated with Bachelor of Science Degree in Honours Biology, Co-operative Education Program (Dean's Honours List)

Specialization in Molecular biology and Biotechnology

- Relevant courses: molecular biology techniques, molecular biotechnology, genetics, microbial genetics, cell and molecular biology, Applied microbiology, virology, and immunology

Senior Honours Research Project: The Characterization of Glycogen Synthase and *phbC* Mutants of *Sinorhizobium meliloti*

Computer Skills:

- Microsoft Office; Adobe Photoshop; DNA Star and primer design; NCBI Database; FACS Diva Software; iCycler, ABI Prism 7000; Beacon Designer 4.0, and Primer Express 2.0